

Chapter 4

Table of Contents

| | | |
|------------|--|----------|
| 4.0 | THERMAL EVALUATION | 4.1-1 |
| 4.1 | Discussion | 4.1-1 |
| 4.2 | Summary of Thermal Properties of Materials | 4.2-1 |
| 4.3 | Technical Specifications for Components..... | 4.3-1 |
| 4.4 | Thermal Evaluation for Normal Conditions of Storage | 4.4-1 |
| 4.4.1 | Thermal Models | 4.4.1-1 |
| 4.4.1.1 | Two-Dimensional Axisymmetric Air Flow and Concrete Cask Models | 4.4.1-3 |
| 4.4.1.2 | Three-Dimensional Canister Models | 4.4.1-13 |
| 4.4.1.3 | Three-Dimensional Transfer Cask and Canister Models | 4.4.1-26 |
| 4.4.1.4 | Three-Dimensional Periodic Canister Internal Models..... | 4.4.1-31 |
| 4.4.1.5 | Two-Dimensional Fuel Models..... | 4.4.1-35 |
| 4.4.1.6 | Two-Dimensional Fuel Tube Models | 4.4.1-38 |
| 4.4.1.7 | Two-Dimensional Forced Air Flow Model for Transfer Cask Cooling | 4.4.1-44 |
| 4.4.2 | Test Model..... | 4.4.2-1 |
| 4.4.3 | Maximum Temperatures for PWR and BWR Fuel..... | 4.4.3-1 |
| 4.4.3.1 | Maximum Temperatures at Reduced Total Heat Loads..... | 4.4.3-2 |
| 4.4.4 | Minimum Temperatures | 4.4.4-1 |
| 4.4.5 | Maximum Internal Pressures..... | 4.4.5-1 |
| 4.4.5.1 | Maximum Internal Pressure for PWR Fuel Canister..... | 4.4.5-1 |
| 4.4.5.2 | Maximum Internal Pressure for BWR Fuel Canister | 4.4.5-3 |
| 4.4.6 | Maximum Thermal Stresses..... | 4.4.6-1 |
| 4.4.7 | Maximum Allowable Cladding Temperature and Canister Heat Load..... | 4.4.7-1 |
| 4.4.7.1 | Maximum Allowable Cladding Temperature | 4.4.7-2 |
| 4.4.7.2 | Maximum Allowable Canister Heat Load..... | 4.4.7-5 |
| 4.4.8 | Evaluation of System Performance for Normal Conditions of Storage | 4.4.8-1 |

Table of Contents (Continued)

| | | |
|---------|--|--------|
| 4.5 | Thermal Evaluation for Site Specific Spent Fuel..... | 4.5-1 |
| 4.5.1 | Maine Yankee Site Specific Spent Fuel..... | 4.5-1 |
| 4.5.1.1 | Thermal Evaluation for Maine Yankee Site Specific Spent Fuel | 4.5-3 |
| 4.5.1.2 | Maximum Allowable Heat Loads for Maine Yankee Site Specific Spent Fuel..... | 4.5-17 |
| 4.6 | References | 4.6-1 |

List of Figures

| | | |
|------------------|--|----------|
| Figure 4.3-1 | PWR Heat Transfer Disk Model for Normal Handling Condition | 4.3-2 |
| Figure 4.3-2 | BWR Heat Transfer Disk Model for Normal Handling Condition | 4.3-3 |
| Figure 4.4.1.1-1 | Two-Dimensional Axisymmetric Air Flow and Concrete Cask Model: PWR..... | 4.4.1-9 |
| Figure 4.4.1.1-2 | Two-Dimensional Axisymmetric Air Flow and Concrete Cask Finite Element Model: PWR..... | 4.4.1-10 |
| Figure 4.4.1.1-3 | Axial Power Distribution for PWR Fuel..... | 4.4.1-11 |
| Figure 4.4.1.1-4 | Axial Power Distribution for BWR Fuel..... | 4.4.1-12 |
| Figure 4.4.1.2-1 | Three-Dimensional Canister Model for PWR Fuel..... | 4.4.1-18 |
| Figure 4.4.1.2-2 | Three-Dimensional Canister Model for PWR Fuel - Cross Section..... | 4.4.1-19 |
| Figure 4.4.1.2-3 | Three-Dimensional Canister Model for BWR Fuel | 4.4.1-20 |
| Figure 4.4.1.2-4 | Three-Dimensional Canister Model for BWR Fuel - Cross Section..... | 4.4.1-21 |
| Figure 4.4.1.3-1 | Three-Dimensional Standard Transfer Cask and Canister Model - PWR | 4.4.1-28 |
| Figure 4.4.1.3-2 | Three-Dimensional Standard Transfer Cask and Canister Model – BWR | 4.4.1-29 |
| Figure 4.4.1.3-3 | Cross-section of the 100-Ton Transfer Cask and Canister Thermal Model – Cask in Horizontal Position | 4.4.1-30 |
| Figure 4.4.1.4-1 | Three-Dimensional Periodic Canister Internal Model - PWR | 4.4.1-33 |
| Figure 4.4.1.4-2 | Three-Dimensional Periodic Canister Internal Model - BWR | 4.4.1-34 |
| Figure 4.4.1.5-1 | Two-Dimensional PWR (17 × 17) Fuel Model..... | 4.4.1-37 |
| Figure 4.4.1.6-1 | Two-Dimensional Fuel Tube Model: PWR Fuel | 4.4.1-41 |
| Figure 4.4.1.6-2 | Two-Dimensional Fuel Tube Model: BWR Fuel Tube with Neutron Absorber..... | 4.4.1-42 |
| Figure 4.4.1.6-3 | Two-Dimensional Fuel Tube Model: BWR Fuel Tube without Neutron Absorber..... | 4.4.1-43 |
| Figure 4.4.1.7-1 | Two-Dimensional Axisymmetric Finite Element Model for Transfer Cask Forced Air Cooling | 4.4.1-45 |
| Figure 4.4.1.7-2 | Two-Dimensional Axisymmetric Outlet Air Flow Model for Transfer Cask Cooling | 4.4.1-46 |

List of Figures (continued)

| | | |
|------------------|--|----------|
| Figure 4.4.1.7-3 | Two-Dimensional Axisymmetric Inlet Air Flow Model for Transfer Cask Cooling | 4.4.1-47 |
| Figure 4.4.1.7-4 | Non-Uniform Heat Load from Canister Contents | 4.4.1-48 |
| Figure 4.4.1.7-5 | Maximum Canister Temperature Versus Air Volume Flow Rate | 4.4.1-49 |
| Figure 4.4.3-1 | Temperature Distribution (°F) for the Normal Storage Condition: PWR Fuel | 4.4.3-6 |
| Figure 4.4.3-2 | Air Flow Pattern in the Concrete Cask in the Normal Storage Condition: PWR Fuel | 4.4.3-7 |
| Figure 4.4.3-3 | Air Temperature (°F) Distribution in the Concrete Cask During the Normal Storage Condition: PWR Fuel | 4.4.3-8 |
| Figure 4.4.3-4 | Concrete Temperature (°F) Distribution During the Normal Storage Condition: PWR Fuel | 4.4.3-9 |
| Figure 4.4.3-5 | History of Maximum Component Temperature (°F) for Transfer Conditions for PWR Fuel with Design Basis 23 kW Uniformly Distributed Heat Load | 4.4.3-10 |
| Figure 4.4.3-6 | History of Maximum Component Temperature (°F) for Transfer Conditions for BWR Fuel with Design Basis 23 kW Uniformly Distributed Heat Load | 4.4.3-11 |
| Figure 4.4.3-7 | Basket Location for the Thermal Analysis of PWR Reduced Heat Load Cases | 4.4.3-12 |
| Figure 4.4.3-8 | BWR Fuel Basket Location Numbers | 4.4.3-13 |
| Figure 4.4.7-1 | PWR Fuel Dry Storage Temperature versus Cladding Stress | 4.4.7-6 |
| Figure 4.4.7-2 | BWR Fuel Dry Storage Temperature versus Cladding Stress | 4.4.7-6 |
| Figure 4.4.7-3 | PWR and BWR Fuel Cladding Dry Storage Temperature versus Basket Heat Load | 4.4.7-7 |
| Figure 4.5.1.1-1 | Quarter Symmetry Model for Maine Yankee Consolidated Fuel | 4.5-12 |
| Figure 4.5.1.1-2 | Maine Yankee Three-Dimensional Periodic Canister Internal Model | 4.5-13 |
| Figure 4.5.1.1-3 | Evaluated Locations for the Maine Yankee Consolidated Fuel Lattice in the PWR Fuel Basket | 4.5-14 |
| Figure 4.5.1.1-4 | Active Fuel Region in the Three-Dimensional Canister Model | 4.5-15 |

List of Figures (continued)

| | | |
|------------------|--|--------|
| Figure 4.5.1.1-5 | Fuel Debris and Damaged Fuel Regions in the Three-Dimensional Canister Model | 4.5-16 |
| Figure 4.5.1.2-1 | Canister Basket Preferential Loading Plan..... | 4.5-22 |
| Figure 4.5.1.2-2 | Maximum Allowable Cladding Temperature at Initial Storage versus Cladding Stress (50,000 MWD/MTU)..... | 4.5-23 |

List of Tables

| | | |
|-----------------|---|----------|
| Table 4.1-1 | Summary of Thermal Design Conditions for Storage..... | 4.1-4 |
| Table 4.1-2 | Summary of Thermal Design Conditions for Transfer..... | 4.1-5 |
| Table 4.1-3 | Maximum Allowable Material Temperatures | 4.1-6 |
| Table 4.1-4 | Summary of Thermal Evaluation Results for the Universal Storage System: PWR Fuel | 4.1-7 |
| Table 4.1-5 | Summary of Thermal Evaluation Results for the Universal Storage System: BWR Fuel | 4.1-8 |
| Table 4.2-1 | Thermal Properties of Solid Neutron Shield (NS-4-FR and NS-3)..... | 4.2-2 |
| Table 4.2-2 | Thermal Properties of Stainless Steel..... | 4.2-2 |
| Table 4.2-3 | Thermal Properties of Carbon Steel | 4.2-3 |
| Table 4.2-4 | Thermal Properties of Chemical Copper Lead..... | 4.2-3 |
| Table 4.2-5 | Thermal Properties of Type 6061-T651 Aluminum Alloy..... | 4.2-3 |
| Table 4.2-6 | Thermal Properties of Helium..... | 4.2-4 |
| Table 4.2-7 | Thermal Properties of Dry Air | 4.2-4 |
| Table 4.2-8 | Thermal Properties of Zircaloy and Zircaloy-4 Cladding | 4.2-5 |
| Table 4.2-9 | Thermal Properties of Fuel (UO ₂)..... | 4.2-5 |
| Table 4.2-10 | Thermal Properties of BORAL Composite Sheet | 4.2-6 |
| Table 4.2-11 | Thermal Properties of Concrete | 4.2-6 |
| Table 4.2-12 | Thermal Properties of Water | 4.2-7 |
| Table 4.2-13 | Thermal Properties of METAMIC | 4.2-7 |
| Table 4.4.1.2-1 | Effective Thermal Conductivities for PWR Fuel Assemblies | 4.4.1-22 |
| Table 4.4.1.2-2 | Effective Thermal Conductivities for BWR Fuel Assemblies | 4.4.1-23 |
| Table 4.4.1.2-3 | Effective Thermal Conductivities for PWR Fuel Tubes | 4.4.1-24 |
| Table 4.4.1.2-4 | Effective Thermal Conductivities for BWR Fuel Tubes..... | 4.4.1-25 |
| Table 4.4.3-1 | Maximum Component Temperatures for the Normal Storage Condition - PWR..... | 4.4.3-14 |
| Table 4.4.3-2 | Maximum Component Temperatures for the Normal Storage Condition - BWR | 4.4.3-15 |

List of Tables (continued)

| | | |
|----------------|---|----------|
| Table 4.4.3-3 | Maximum Component Temperatures for the Transfer Condition – PWR Fuel with Design Basis 23 kW Uniformly Distributed Heat Load..... | 4.4.3-16 |
| Table 4.4.3-4 | Maximum Component Temperatures for the Transfer Condition – BWR Fuel with Design Basis 23 kW Uniformly Distributed Heat Load..... | 4.4.3-16 |
| Table 4.4.3-5 | Maximum Limiting Component Temperatures in Transient Operations for the Reduced Heat Load Cases for PWR Fuel | 4.4.3-17 |
| Table 4.4.3-6 | Maximum Limiting Component Temperatures in Transient Operations for the Reduced Heat Load Cases for PWR Fuel after In-Pool Cooling..... | 4.4.3-18 |
| Table 4.4.3-7 | Maximum Limiting Component Temperatures in Transient Operations for the Reduced Heat Load Cases for PWR Fuel after Forced-Air Cooling | 4.4.3-18 |
| Table 4.4.3-8 | Maximum Limiting Component Temperatures in Transient Operations for BWR Fuel | 4.4.3-19 |
| Table 4.4.3-9 | Maximum Limiting Component Temperatures in Transient Operations after Vacuum for BWR Fuel after In-Pool Cooling..... | 4.4.3-20 |
| Table 4.4.3-10 | Maximum Limiting Component Temperatures in Transient Operations after Vacuum for BWR Fuel after Forced-Air Cooling. | 4.4.3-20 |
| Table 4.4.3-11 | Maximum Limiting Component Temperatures in Transient Operations after Helium for BWR Fuel after In-Pool Cooling | 4.4.3-21 |
| Table 4.4.3-12 | Maximum Limiting Component Temperatures in Transient Operations after Helium for BWR Fuel after Forced-Air Cooling .. | 4.4.3-21 |
| Table 4.4.5-1 | PWR Per Assembly Fuel Generated Gas Inventory | 4.4.5-4 |
| Table 4.4.5-2 | PWR Canister Free Volume (No Fuel or Inserts) | 4.4.5-4 |
| Table 4.4.5-3 | PWR Maximum Normal Condition Pressure Summary | 4.4.5-4 |
| Table 4.4.5-4 | BWR Per Assembly Fuel Generated Gas Inventory..... | 4.4.5-5 |
| Table 4.4.5-5 | BWR Canister Free Volume (No Fuel or Inserts) | 4.4.5-5 |
| Table 4.4.5-6 | BWR Maximum Normal Condition Pressure Summary | 4.4.5-5 |

List of Tables (continued)

| | | |
|-----------------|--|----------|
| Table 4.4.7-1 | PWR Cladding Stress Level Comparison Chart | 4.4.7-8 |
| Table 4.4.7-2 | BWR Cladding Stress Level Comparison Chart | 4.4.7-8 |
| Table 4.4.7-3 | Cladding Stress as a Function of Fuel Assembly Average Burnup and Temperature..... | 4.4.7-9 |
| Table 4.4.7-4 | Maximum Allowable Initial Storage Temperature (°C) As a Function of Initial Cladding Stress and Initial Cool Time | 4.4.7-9 |
| Table 4.4.7-5 | Maximum Allowable Cladding Temperature for PWR and BWR Fuel Assemblies | 4.4.7-10 |
| Table 4.4.7-6 | Cladding Maximum Temperature as a Function of Basket Heat Load (PWR)..... | 4.4.7-10 |
| Table 4.4.7-7 | Cladding Maximum Temperature as a Function of Basket Heat Load (BWR) | 4.4.7-10 |
| Table 4.4.7-8 | Maximum Allowable Decay Heat for UMS® PWR and BWR Systems | 4.4.7-11 |
| Table 4.4.7-9 | Temperature Bias Applied to Maximum Allowable Decay Heats ... | 4.4.7-11 |
| Table 4.5.1.2-1 | Cladding Stress for 50,000 MWD/MTU Burnup Fuel..... | 4.5-24 |
| Table 4.5.1.2-2 | Maximum Allowable Cladding Temperature for 50,000 MWD/MTU Burnup Fuel..... | 4.5-24 |
| Table 4.5.1.2-3 | Maximum Allowable Canister Heat Load for 50,000 MWD/MTU Burnup Fuel..... | 4.5-24 |
| Table 4.5.1.2-4 | Heat Load for Interior Assemblies for the Configuration with 0.958 kW Assemblies in Peripheral Locations | 4.5-25 |
| Table 4.5.1.2-5 | Heat Load Limit for Interior Assemblies for the Configuration with 1.05 kW Assemblies in Peripheral Locations | 4.5-25 |

4.0 THERMAL EVALUATION

This section presents the thermal design and analyses of the Universal Storage System for normal conditions of storage of spent nuclear fuel. The analyses include consideration of design basis PWR and BWR fuel. Results of the analyses demonstrate that with the design basis contents, the Universal Storage System meets the thermal performance requirements of 10 CFR 72 [1].

4.1 Discussion

The Universal Storage System consists of a Transportable Storage Canister, Vertical Concrete Cask, and a transfer cask. In long-term storage, the canister is installed in the concrete cask, which provides passive radiation shielding and natural convection cooling. The fuel is loaded in a basket structure positioned within the canister. The transfer cask is used for the handling of the canister. The thermal performance of the concrete cask containing the design basis fuel (during storage) and the performance of the transfer cask containing design basis fuel (during handling) are evaluated herein.

The significant thermal design feature of the Vertical Concrete Cask is the passive convective air flow up along the side of the canister. Cool (ambient) air enters at the bottom of the concrete cask through four inlet vents. Heated air exits through the four outlets at the top of the cask. Radiant heat transfer occurs from the canister shell to the concrete cask liner, which also transmits heat to the adjoining air flow. Conduction does not play a substantial role in heat removal from the canister surface. Natural circulation of air inside the Vertical Concrete Cask, in conjunction with radiation from the canister surface, maintains the fuel cladding temperature and all of the concrete cask component temperatures below their design limits.

The UMS[®] Storage System design basis heat load is 23.0 kW for up to 24 PWR or up to 56 BWR fuel assemblies. As shown in Section 4.4.7, the thermal analysis considers a range of fuel assembly burnup and cooling times for both fuel types to establish the allowable cladding temperatures. These limits are used to establish the UMS[®] Storage System allowable decay heat loads for fuel having cooling times of 5 years, or longer.

The thermal evaluation considers normal, off-normal, and accident conditions of storage. Each of these conditions can be described in terms of the environmental temperature, use of solar insolation, and the condition of the air inlets and outlets, as shown in Table 4.1-1. The design conditions for transfer are defined in Table 4.1-2. The transfer conditions consider the transient effect for PWR and BWR fuel, starting from the removal of the transfer cask/canister from the spent fuel pool. The canister is considered under normal operation to be inside the transfer cask and initially filled with water. The canister is vacuum dried, back-filled with helium and then transferred into the Vertical Concrete Cask. As shown in Section 4.4.3, the time duration of the spent fuel in the water and vacuum conditions is administratively controlled to prevent general boiling of the water and to ensure that the allowable temperatures of the limiting components (fuel cladding, structural disks and heat transfer disks) are not exceeded.

This evaluation applies different component temperature limits and different material stress limits for long-term conditions and short-term conditions. Normal storage is considered to be a long-term condition. Off-normal and accident events, as well as the transfer condition that temporarily occurs during the preparation of the canister while it is in the transfer cask, are considered as short-term conditions. Thermal evaluations are performed for the design basis PWR and BWR fuels for all design conditions. The maximum allowable material temperatures for long-term and short-term conditions are provided in Table 4.1-3.

During normal conditions of storage and hypothetical accident conditions, the concrete cask must reject the fuel decay heat to the environment without exceeding the operational temperature ranges of the components important to safety. In addition, to maintain fuel rod integrity for normal conditions of storage the fuel must be maintained at a sufficiently low temperature in an inert atmosphere to preclude thermally induced fuel rod cladding deterioration. To preclude fuel degradation, the maximum allowable cladding temperatures under normal conditions of storage for 5-year cooled PWR fuel and BWR fuel are determined to be 716°F (380°C). For either of these fuel types, the maximum cladding temperature under off-normal, transfer and accident conditions must remain below 1,058°F (570°C). Finally, for the structural components of the storage system, the thermally induced stresses, in combination with pressure and mechanical load stresses, must be below material allowable stress levels.

Thermal evaluations for normal conditions of storage and transfer (canister handling) condition operations are presented in Section 4.4. The finite element method is used to calculate the temperatures for the various components of the concrete cask, canister, basket, fuel cladding and transfer cask. Thermal models used in evaluation of normal and transfer conditions are described in Section 4.4.1.

The transfer cask is provided in either a standard, advanced configuration standard, or 100-ton configuration. The 100-ton transfer cask weighs less than the standard transfer casks and is designed to accommodate sites having a 100-ton cask handling crane weight limit. Canister handling, fuel loading and canister closing are operationally identical for either transfer cask configuration.

The evaluation for the 100-ton transfer cask is bounded by the evaluation using the models presented in this section. The overall wall thickness for the 100-ton transfer cask is less than that for the standard/advanced configuration standard transfer casks. The water-neutron shield for the 100-ton transfer cask has better heat transfer capability (conduction and convection) than the NS-4-FR used for the standard transfer cask.

A summary of the thermal evaluation results for the Universal Storage System are provided in Tables 4.1-4 and 4.1-5 for the PWR and BWR cases, respectively. Evaluation results for accident conditions of "All air inlets and outlets blocked" and "Fire" are presented in Chapter 11. The results demonstrate that the calculated temperatures are below the allowable component temperatures for all normal (long-term) storage conditions and for short-term events. The thermally induced stresses, combined with pressure and mechanical load stresses, are also within the allowable levels, as demonstrated in Chapter 3.

Table 4.1-1 Summary of Thermal Design Conditions for Storage

| Condition ¹ | | Environmental Temperature (°F) | Solar Insolation ² | Condition of Concrete Cask Inlets and Outlets |
|---|-----------------------|--------------------------------|-------------------------------|---|
| Normal | | 76 | Yes | All inlets and outlets open |
| Off-Normal - Half Air Inlets Blocked | | 76 | Yes | Half inlets blocked and all outlets open |
| Off-Normal - Severe Heat | | 106 | Yes | All inlets and outlets open |
| Off-Normal - Severe Cold | | -40 | No | All inlets and outlets open |
| Accident - Extreme Heat | | 133 | Yes | All inlets and outlets open |
| Accident - All Air Inlets and Outlets Blocked ³ | | 76 | Yes | All inlets and outlets blocked |
| Accident - Fire ⁴ | During Fire | 1475 | Yes | All inlets and outlets open |
| | Before and After Fire | 76 | Yes | All inlets and outlets open |

1. Off-normal and accident condition analyses are presented in Chapter 11.
2. Solar Insolation per 10 CFR 71:
Curved Surface: 400 g cal/cm² (1475 Btu/ft²) for a 12-hour period.
Flat Horizontal Surface: 800 g cal/cm² (2950 Btu/ft²) for a 12-hour period.
3. This condition bounds the case in which all inlets are blocked, with all outlets open.
4. The evaluated fire accident is the described in Section 11.2.6.

Table 4.1-2 Summary of Thermal Design Conditions for Transfer

| Condition ^{1,2} | Maximum Duration (Hours) ³ | |
|---|---------------------------------------|-----|
| | PWR | BWR |
| Canister Filled with Water ⁴ | 17 | 17 |
| Vacuum Drying | 32 | 25 |
| Canister Filled with Helium | No Limit | 16 |

- (1) The canister is inside the transfer cask, with an ambient temperature of 76°F.
- (2) See Section 8.4 for description of limiting conditions.
- (3) Maximum durations based on 23 kW heat load.
- (4) The initial water temperature is considered to be 100°F.

Table 4.1-3 Maximum Allowable Material Temperatures

| Material | Temperature Limits (°F) | | Reference |
|--|------------------------------|------------|----------------------------------|
| | Long Term | Short Term | |
| Concrete | 150(B)/300(L) ⁽¹⁾ | 350 | ACI-349 [4] |
| Fuel Clad | | | |
| PWR Fuel (5-year cooled) | 716 ⁽²⁾ | 1,058 | PNL-6189 [5] and PNL-4835 [2] |
| BWR Fuel (5-year cooled) | 716 ⁽²⁾ | 1,058 | |
| Aluminum 6061-T651 | 650 | 750 | MIL-HDBK-5G [7] |
| NS-4-FR | 300 | 300 | GESC [8] |
| Chemical Copper Lead | 600 | 600 | Baumeister [9] |
| SA693 17-4PH Type 630 Stainless Steel | 650 | 800 | ASME Code [13] ARMCO [11] |
| SA240 Type 304 Stainless Steel | 800 | 800 | ASME Code [13] |
| SA240 Type 304L Stainless Steel | 800 | 800 | ASME Code [13] |
| ASTM A533 Type B Carbon Steel | 700 | 700 | ASME Code [13] |
| ASME SA588 Carbon Steel | 700 | 700 | ASME Code Case N-71-17 [12] |
| ASTM A36 Carbon Steel | 700 | 700 | ASME Code Case N-71-17 [12] |

- (1) B and L refer to bulk temperatures and local temperatures, respectively. The local temperature allowable applies to a restricted region where the bulk temperature allowable may be exceeded.
- (2) In accordance with PNL-6189, the temperature limit of 380°C (716°F) is used for the evaluation of fuel considered in the design basis heat load (23 kW). For temperature limits corresponding to different burnup and cooling times, refer to Table 4.4.7-5.

Table 4.1-4 Summary of Thermal Evaluation Results for the Universal Storage System:
PWR Fuel

| Long-Term Condition: | | | | | | |
|---|----------|-------|---------------------|------------------------------|-------------------------|-----------|
| Maximum Temperatures (°F) | | | | | | |
| Design Condition | Concrete | | Heat Transfer Disks | Support Disks ⁽¹⁾ | Canister ⁽²⁾ | Fuel Clad |
| Normal (76°F Ambient) | Bulk | Local | | | | |
| | 135 | 186 | 599 | 601 | 351 | 648 |
| Allowable | 150 | 300 | 650 | 650 | 800 | 716 |
| Short-Term Condition: | | | | | | |
| Maximum Temperatures (°F) | | | | | | |
| Design Condition | Concrete | | Heat Transfer Disks | Support Disks ⁽¹⁾ | Canister ⁽²⁾ | Fuel Clad |
| Off-Normal - Half Inlets Blocked (76°F Ambient) | 191 | | 600 | 603 | 350 | 649 |
| Off-Normal - Severe Heat (106°F Ambient) | 228 | | 626 | 628 | 381 | 672 |
| Off-Normal - Severe Cold (-40°F Ambient) | 17 | | 502 | 505 | 226 | 561 |
| Accident - Extreme Heat (133°F Ambient) | 262 | | 648 | 650 | 408 | 693 |
| Accident - Fire | 244 | | 639 | 641 | 391 | 688 |
| Transfer - Vacuum Drying | N/A | | 702 | 705 | 333 | 822 |
| Transfer - Backfilled with Helium | N/A | | 732 | 734 | 481 | 822 |
| Allowable | 350 | | 750 | 800 | 800 | 1058 |

1. SA 693, 17-4PH Type 630 SS.
2. SA240, Type 304L SS (including canister shell, lid and bottom plate).

Table 4.1-5 Summary of Thermal Evaluation Results for the Universal Storage System:
BWR Fuel

| Long-Term Condition: | | | | | | |
|---|-------------|--------------|---------------------|------------------------------|-------------------------|-----------|
| Maximum Temperatures (°F) | | | | | | |
| Design Condition | Concrete | | Heat Transfer Disks | Support Disks ⁽¹⁾ | Canister ⁽²⁾ | Fuel Clad |
| Normal (76°F Ambient) | Bulk 136 | Local 192 | 612 | 614 | 376 | 642 |
| Allowable | 150 | 300 | 650 | 700 | 800 | 716 |
| Short-Term Condition: | | | | | | |
| Maximum Temperatures (°F) | | | | | | |
| Design Condition | Concrete | | Heat Transfer Disks | Support Disks ⁽¹⁾ | Canister ⁽²⁾ | Fuel Clad |
| Off-Normal - Half Inlets Blocked (76°F Ambient) | 195 | | 612 | 614 | 373 | 642 |
| Off-Normal - Severe Heat (106°F Ambient) | 231 | | 638 | 640 | 405 | 667 |
| Off-Normal - Severe Cold (-40°F Ambient) | 20 | | 504 | 505 | 252 | 540 |
| Accident - Extreme Heat (133°F Ambient) | 266 | | 662 | 664 | 432 | 690 |
| Accident - Fire | 244 | | 652 | 654 | 416 | 682 |
| Transfer - Vacuum Drying | N/A | | 653 | 659 | 267 | 733 |
| Transfer - Backfilled with Helium | N/A | | 683 | 686 | 462 | 728 |
| Allowable | 350 | | 750 | 700 | 800 | 1058 |

1. SA 533, Type B, CS.
2. SA240, Type 304L SS (including canister shell, lid and bottom plate).

4.2 Summary of Thermal Properties of Materials

The material thermal properties used in the thermal analyses are shown in Tables 4.2-1 through 4.2-12. Derivation of effective conductivities is described in Section 4.4.1. Tables 4.2-1 through 4.2-12 include only the materials that form the heat transfer pathways employed in the thermal analysis models. Materials for small components, which are not directly modeled are not included in the property tabulation.

Table 4.2-1 Thermal Properties of Solid Neutron Shield (NS-4-FR and NS-3)

| Property (units) [8] | NS-4-FR | NS-3 |
|---|---------|--------|
| Conductivity (Btu/hr-in-°F) | 0.0311 | 0.0407 |
| Density (borated) (lbm/in ³) | 0.0589 | 0.0621 |
| Density (nonborated) (lbm/in ³) | 0.0607 | 0.0640 |
| Specific Heat (Btu/lbm-°F) | 0.319 | 0.149 |

Table 4.2-2 Thermal Properties of Stainless Steel

Type 304 and 304L

| Property (units) | Value at Temperature | | | | |
|------------------------------------|----------------------|--------|--------|--------|--------|
| | 100°F | 200°F | 400°F | 550°F | 750°F |
| Conductivity (Btu/hr-in-°F) [13] | 0.7250 | 0.7750 | 0.8667 | 0.9250 | 1.0000 |
| Density (lb/in ³) [14] | 0.2896 | 0.2888 | 0.2872 | 0.2857 | 0.2839 |
| Specific Heat (Btu/lbm-°F) [14] | 0.1156 | 0.1202 | 0.1274 | 0.1314 | 0.1355 |
| Emissivity [14] | ← 0.36 → | | | | |

17-4PH, Type 630

| Property (units) | Value at Temperature | | | |
|------------------------------------|----------------------|-------|-------|-------|
| | 70°F | 200°F | 400°F | 650°F |
| Conductivity (Btu/hr-in-°F) [13] | 0.824 | 0.883 | 0.975 | 1.083 |
| Density (lb/in ³) [13] | ← 0.291 → | | | |
| Specific Heat (Btu/lbm-°F) [11] | ← 0.11 → | | | |
| Emissivity [15] | ← 0.58 → | | | |

Table 4.2-3 Thermal Properties of Carbon Steel

| Material ¹ Property (units) | Value at Temperature | | | | | |
|--|----------------------|-------|-------|-------|-------|-------|
| | 100°F | 200°F | 400°F | 500°F | 700°F | 800°F |
| Conductivity (Btu/hr-in-°F) [13] | 1.992 | 2.033 | 2.017 | 1.975 | 1.867 | 1.808 |
| Density (lb/in ³) [16] | ←————— 0.284 —————→ | | | | | |
| Specific Heat (Btu/lbm-°F) [17] | ←————— 0.113 —————→ | | | | | |
| Emissivity [9] | ←————— 0.80 —————→ | | | | | |

1. A-36, SA-533, A-588 and SA-350.

Table 4.2-4 Thermal Properties of Chemical Copper Lead

| Property (units) | Value at Temperature | | | |
|------------------------------------|---------------------------|--------|--------|--------|
| | 209°F | 400°F | 581°F | 630°F |
| Conductivity (Btu/hr-in-°F) [18] | 1.6308 | 1.5260 | 1.2095 | 1.0079 |
| Density (lb/in ³) [18] | ←————— 0.411 —————→ | | | |
| Specific Heat (Btu/lbm-°F) [18] | ←————— 0.03 —————→ | | | |
| Emissivity [9] | ←————— 0.28 (75°F) —————→ | | | |

Table 4.2-5 Thermal Properties of Type 6061-T651 Aluminum Alloy

| Property (units) | Value at Temperature | | | | | |
|------------------------------------|----------------------|-------|-------|-------|-------|-------|
| | 200°F | 300°F | 400°F | 500°F | 600°F | 750°F |
| Conductivity (Btu/hr-in-°F) [7,13] | 8.25 | 8.38 | 8.49 | 8.49 | 8.49 | 8.49 |
| Specific Heat (Btu/hr-in-°F) [13] | ←————— 0.23 —————→ | | | | | |
| Emissivity [15] | ←————— 0.22 —————→ | | | | | |

Table 4.2-6 Thermal Properties of Helium

| Property (units) | Value at Temperature | | | |
|----------------------------------|----------------------|---------|---------|---------|
| | 80°F | 260°F | 440°F | 800°F |
| Conductivity (Btu/hr-in-°F) [20] | 0.00751 | 0.00915 | 0.01068 | 0.01355 |

| Property (units) | Value at Temperature | | | |
|------------------------------------|----------------------|----------|----------|----------|
| | 200°F | 400°F | 600°F | 800°F |
| Density (lb/in ³) [19] | 4.83E-06 | 3.70E-06 | 3.01E-06 | 2.52E-06 |
| Specific Heat (Btu/lbm-°F) [19] | 1.24 | | | |

Table 4.2-7 Thermal Properties of Dry Air

| Property (units) | Value at Temperature | | | |
|------------------------------------|----------------------|----------|----------|----------|
| | 100°F | 300°F | 500°F | 700°F |
| Conductivity (Btu/hr-in-°F) [19] | 0.00128 | 0.00161 | 0.00193 | 0.00223 |
| Density (lb/in ³) [19] | 4.11E-05 | 3.01E-05 | 2.38E-05 | 1.97E-05 |
| Specific Heat (Btu/lbm-°F) [19] | 0.240 | 0.244 | 0.247 | 0.253 |

Table 4.2-8 Thermal Properties of Zircaloy and Zircaloy-4 Cladding

| Property (units) | Value at Temperature | | | |
|------------------------------------|----------------------|-------|-------|-------|
| | 392°F | 572°F | 752°F | 932°F |
| Conductivity (Btu/hr-in-°F) [22] | 0.69 | 0.73 | 0.80 | 0.87 |
| Density (lb/in ³) [23] | 0.237 | | | |
| Specific Heat (Btu/lbm-°F) [22] | 0.072 | 0.074 | 0.076 | 0.079 |
| Emissivity [22] | 0.75 | | | |

Table 4.2-9 Thermal Properties of Fuel (UO₂)

| Property (units) | Value at Temperature | | | | |
|-------------------------------------|----------------------|-------|-------|-------|-------|
| | 100°F | 257°F | 482°F | 707°F | 932°F |
| Conductivity (Btu/hr-in-°F) [22] | 0.38 | 0.347 | 0.277 | 0.236 | 0.212 |
| Specific Heat (Btu/lbm-°F) [22] | 0.057 | 0.062 | 0.067 | 0.071 | 0.073 |
| Density (lbm/in ³) [23] | 0.396 | | | | |
| Emissivity [22] | 0.85 | | | | |

Table 4.2-10 Thermal Properties of BORAL Composite Sheet

| Property (units) | Value at Temperature | |
|--------------------------------|----------------------|-------|
| | 100°F | 500°F |
| Conductivity (Btu/hr-in-°F) | | |
| Aluminum Clad [24] | 7.805 | 8.976 |
| Core Matrix | | |
| PWR (calculated) | 3.45 | 3.05 |
| BWR (calculated) | 6.60 | 7.23 |
| Emissivity ⁽¹⁾ [25] | 0.15 | |

⁽¹⁾ The emissivity of the aluminum clad of the BORAL sheet ranges from 0.10 to 0.19. An averaged value of 0.15 is used.

Table 4.2-11 Thermal Properties of Concrete

| Property (units) | Value at Temperature | | |
|-------------------------------------|----------------------|-------|-------|
| | 100°F | 200°F | 300°F |
| Conductivity (Btu/hr-in-°F) [26] | 0.091 | 0.089 | 0.086 |
| Density (lbm/in ³) [27] | 140 | | |
| Specific Heat (Btu/lbm-°F) [17] | 0.20 | | |
| Emissivity ⁽¹⁾ [17,28] | 0.90 | | |
| Absorptivity [29] | 0.60 | | |

⁽¹⁾ Emissivity = 0.93 for masonry, 0.94 for rough concrete; 0.9 is used.

Table 4.2-12 Thermal Properties of Water

| Property (units) | Value at Temperature | | |
|-------------------------------------|----------------------|-------|-------|
| | 70°F | 200°F | 300°F |
| Conductivity (Btu/hr-in-°F) [32] | 0.029 | 0.033 | 0.033 |
| Specific Heat (Btu/lbm-°F) [32] | 0.998 | 1.00 | 1.03 |
| Density (lbm/in ³) [32] | 0.036 | 0.035 | 0.033 |

Table 4.2-13 Thermal Properties of METAMIC

| Property (units) | Value at Temperature | | |
|-------------------------------------|----------------------|--------|--------|
| | 77°F | 212°F | 482°F |
| Conductivity (Btu/hr-in-°F) [39] | 4.54 | 4.42 | 4.64 |
| Specific Heat (Btu/lbm-°F) [39] | 0.2207 | 0.2412 | 0.2938 |
| Density (lbm/in ³) [39] | 0.094 | | |

THIS PAGE INTENTIONALLY LEFT BLANK

4.3 Technical Specifications for Components

Five major components of the Universal Storage System must be maintained within their safe operating temperature ranges: the concrete, the lead gamma shield, the NS-4-FR solid neutron shield in the transfer cask, the aluminum heat transfer disks and steel (17-4PH and ASTM A533) support disks in the basket structure inside the canister. The safe operating ranges for these components are from a minimum temperature of -40°F to the maximum temperatures as shown in Table 4.1-3.

The criterion for the safe operating range of the lead gamma shield is the prevention of the lead from reaching its melting point of 620°F [9]. The maximum operating temperature limit of the NS-4-FR solid neutron shield material, determined by the manufacturer, is to ensure sufficient neutron shielding capacity.

The primary consideration in establishing the safe operating range of the aluminum heat transfer disks and steel support disks is maintaining the integrity of the aluminum and steel.

The temperature limit for the aluminum heat transfer disks is 650°F and 750°F for the long-term and short-term conditions, respectively, based on data from MIL-HDBK-5G. Note that the heat transfer disk is not a structural component. During the transfer operation (limiting condition for short-term condition), the heat transfer disk is subjected to a maximum loading of 1.1 g (normal handling). An evaluation is performed for the heat transfer disks for both PWR and BWR configurations to the stresses for this condition. Two quarter-symmetry models were generated using ANSYS SHELL63 elements for the evaluation, as shown in Figures 4.3-1 and 4.3-2. The disks are supported at the basket tie-rod locations in the canister axial direction. Symmetry boundary conditions are applied at the planes of symmetry. An inertia load of 1.1 g is applied to the disk in the out-of-plane direction.

The analysis results indicate that the stress is less than 0.13 ksi at the central region of the basket where maximum temperature occurs for both the PWR and BWR configuration. The corresponding margin of safety is + 9.8 based on the yield stress of 1.4 ksi at 750°F. Therefore, the aluminum heat transfer disk will maintain its integrity as long as it does not exceed the temperature limits.

Figure 4.3-1 PWR Heat Transfer Disk Model for Normal Handling Condition

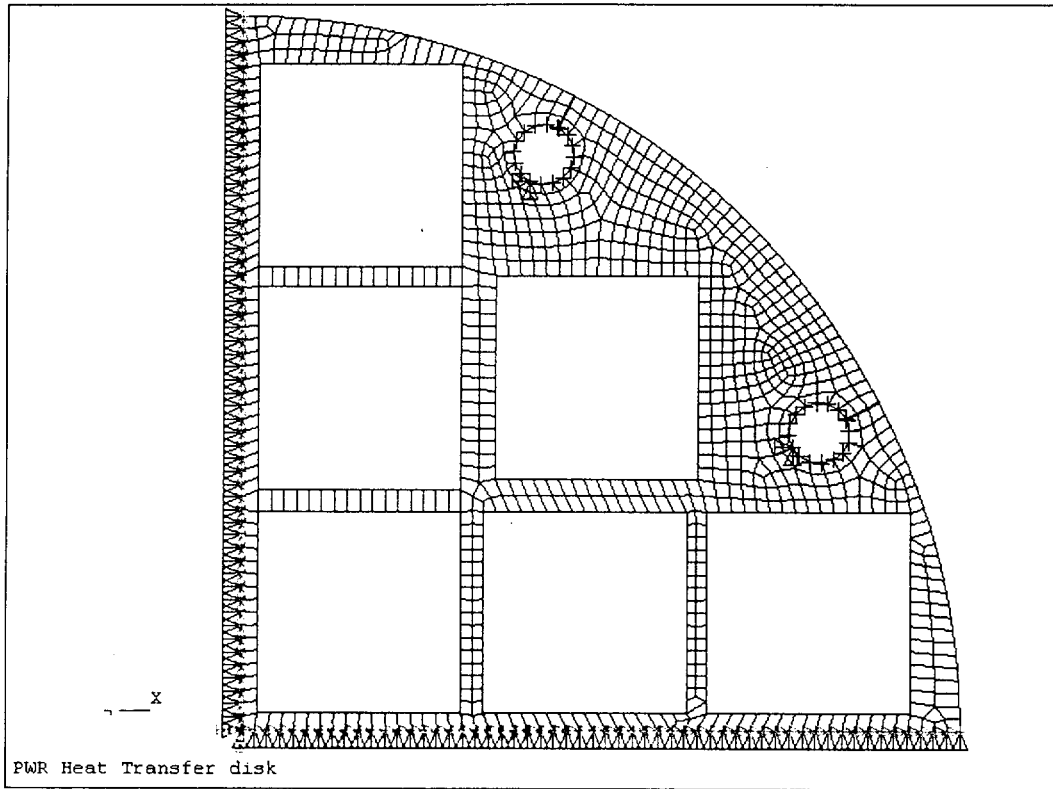
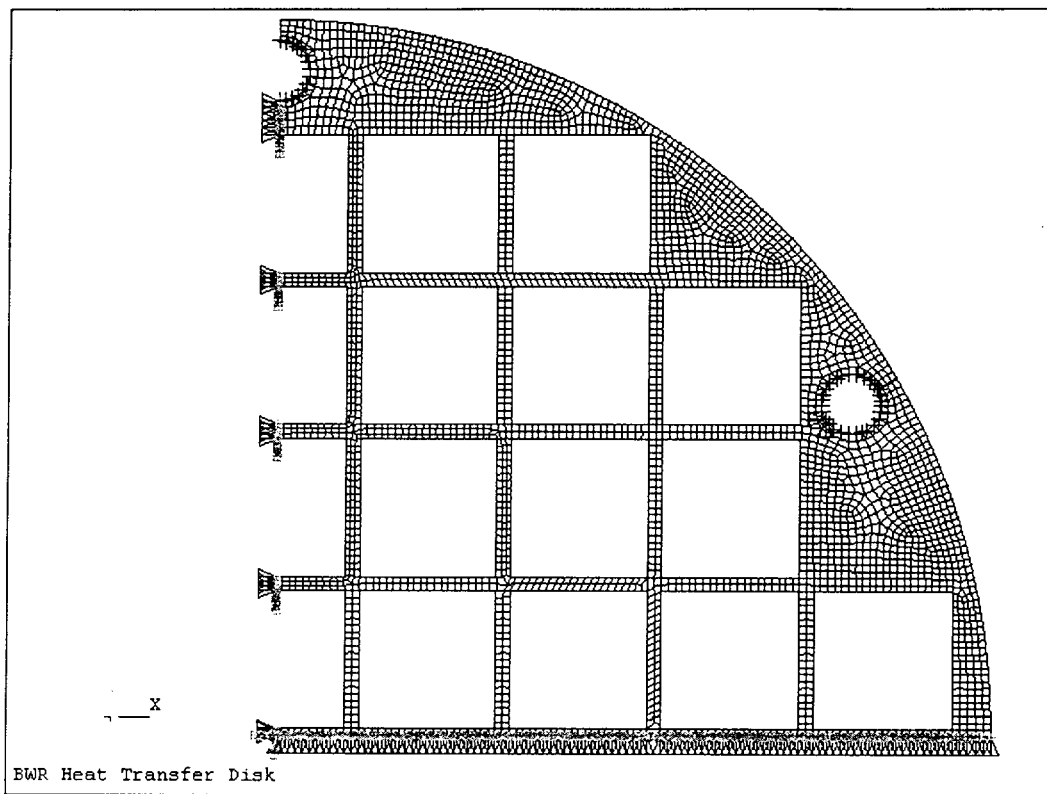


Figure 4.3-2 BWR Heat Transfer Disk Model for Normal Handling Condition



THIS PAGE INTENTIONALLY LEFT BLANK

4.4 Thermal Evaluation for Normal Conditions of Storage

The finite element method is used to evaluate the thermal performance of the Universal Storage System for normal conditions of storage. The general-purpose finite element analysis program ANSYS Revisions 5.2 and 5.5 [6] is used to perform the finite element evaluations.

THIS PAGE INTENTIONALLY LEFT BLANK

4.4.1 Thermal Models

Finite element models are utilized for the thermal evaluation of the Universal Storage System, as shown below. These models are used separately to evaluate the system for the storage of PWR or BWR fuel.

1. Two-Dimensional Axisymmetric Air Flow and Concrete Cask Models
2. Three-Dimensional Canister Models
3. Three-Dimensional Transfer Cask and Canister Models
4. Three-Dimensional Periodic Canister Internal Models
5. Two-Dimensional Fuel Models
6. Two-Dimensional Fuel Tube Models
7. Two-Dimensional Forced Air Flow Model for Transfer Cask Cooling

The two-dimensional axisymmetric air flow and concrete cask model includes the concrete cask, air in the air inlets, annulus and the air outlets, the canister and the canister internals, which are modeled as homogeneous regions with effective thermal conductivities. The effective thermal conductivities for the canister internals in the radial direction are determined using the three-dimensional periodic canister internal models. The effective conductivities in the canister axial direction are calculated using classical methods. The two-dimensional axisymmetric air flow and concrete cask model is used to perform computational fluid dynamic analyses to determine the mass flow rate, velocity and temperature of the air flow, as well as the temperature distribution of the concrete, concrete cask steel liner and the canister. Two models are generated for the evaluations of the PWR and the BWR systems, respectively. These models are essentially identical, but have slight differences in dimensions and the effective properties of the canister internals.

The three-dimensional canister model comprises the fuel assemblies, fuel tubes, stainless steel or carbon steel support disks, aluminum heat transfer disks, top and bottom weldments, the canister shell, lids and bottom plate. The canister model is employed to evaluate the temperature distribution of the fuel cladding and basket components. The fuel assemblies and the fuel tubes in the three-dimensional canister model are modeled using effective conductivities. The effective conductivities for the fuel assemblies are determined using the two-dimensional fuel models. The effective conductivities for the fuel tubes are determined using the two-dimensional fuel tube

models. Two three-dimensional canister models are generated for the PWR and BWR canisters, respectively.

The three-dimensional transfer cask model includes the transfer cask and the canister with its internals. This model is used to perform transient and steady state analyses for the transfer condition, starting from removing the transfer cask/canister from the spent fuel pool, vacuum drying and finally back-filling the canister with helium. Separate transfer cask models are required for PWR and BWR systems.

The three-dimensional canister internal model consists of a periodic section of the canister internals. For the PWR canister, the model contains one support disk with two heat transfer disks (half thickness) on its top and bottom, fuel assemblies, fuel tubes and the media in the canister. For the BWR canister, two models are required. The first model, for the central region of the BWR canister, contains one heat transfer disk with two support disks (half thickness) on its top and bottom, fuel assemblies, fuel tubes and the media in the canister. The other model, for the region without heat transfer disks, contains two support disks (half thickness), fuel assemblies, fuel tubes and the media in the canister. The purpose of the three-dimensional periodic canister internal model is to determine the effective thermal conductivity of the canister internals in the canister radial direction. The effective conductivities are used in the two-dimensional axisymmetric air flow and concrete cask models. The media in the canister is considered to be helium. The fuel assemblies and fuel tubes in this model are modeled as homogeneous regions with effective thermal properties, which are determined by the two-dimensional fuel models and the two-dimensional fuel tube models.

The two-dimensional fuel model includes the fuel pellets, cladding and the media occupying the space between fuel rods. The media is considered to be helium for storage conditions and water, vacuum or helium for transfer conditions. The model is used to determine the effective thermal conductivities of the fuel assembly. In order to account for various types of fuel assemblies, a total of seven fuel models are generated: Four models for the 14×14, 15×15, 16×16 and 17×17 PWR fuel assemblies and three models for the 7×7, 8×8 and 9×9 BWR fuel assemblies. The effective properties are used in the three-dimensional canister models, the three-dimensional periodic canister internal models and the three-dimensional transfer cask and canister model.

The two-dimensional fuel tube model is used to determine the effective conductivities of the fuel tube wall and neutron absorber (BORAL or METAMIC). Only BORAL is considered in the model, since the thermal properties of METAMIC are essentially identical to the properties of BORAL. The effective conductivities are used in the three-dimensional canister models, the three-dimensional periodic canister internal models and the three-dimensional transfer cask and canister model.

The two-dimensional axisymmetric air flow model is used to determine the air flow rate needed for the forced air cooling of the canister inside the transfer cask.

Detailed description of the finite element models are presented in Sections 4.4.1.1 through 4.4.1.7.

4.4.1.1 Two-Dimensional Axisymmetric Air Flow and Concrete Cask Models

This section describes the finite element models used to evaluate the thermal performance of the vertical concrete cask for the PWR and BWR configurations. The model includes the concrete cask, the air in the air inlets, the annulus and the air outlets, the canister and the canister internals, which are modeled as homogeneous regions with effective thermal conductivities. Two separate two-dimensional axisymmetric models are used for the PWR and BWR configurations, respectively. The PWR model is shown in Figures 4.4.1.1-1 and 4.4.1.1-2. The BWR model is essentially identical to the PWR model, but it incorporates different effective thermal properties of the canister internals, and slight differences in dimensions.

The fuel canister is cooled by (1) natural/free convection of air through the lower vents (the air inlets), the vertical air annulus, and the upper vents (the air outlets); and (2) radiation heat transfer between the surfaces of the canister shell and the steel liner. The heat transferred to the liner is rejected by air convection in the annulus and by conduction through the concrete. The heat flow through the concrete is dissipated to the surroundings by natural convection and radiation heat transfer. The temperature in the concrete region is controlled by radiation heat transfer between the vertical annulus surfaces (the canister shell outer surface and the steel liner inner surface), natural convection of air in the annulus, and boundary conditions applicable to the concrete cask outer surfaces—e.g., natural convection and radiation heat transfer between the outer surfaces and the environment, including consideration of incident solar energy. These heat transfer modes are combined in the air flow and concrete cask model. The entire thermal system,

including mass, momentum, and energy, is analyzed using the two-dimensional axisymmetric air flow and concrete cask models. The temperature distributions of the concrete cask, the air region and the canister are determined by these models. Detailed thermal evaluations for the canister internals (fuel cladding, basket, etc.) are performed using the three-dimensional canister models as described in Section 4.4.1.2.

The concrete cask has four air inlets at the bottom and four air outlets at the top that extend through the concrete. Since the configuration is symmetrical, it can be simplified into a two-dimensional axisymmetric model by using equivalent dimensions for the air inlets and outlets, which are assumed to extend around the concrete cask periphery. The canister internals are modeled as three homogeneous regions using effective thermal conductivities - the active fuel region and the regions above and below the active fuel region. The two-dimensional axisymmetric model is shown schematically in Figure 4.4.1.1-1. Determination of the effective properties is described in Section 4.4.1.4.

ANSYS FLOTRAN FLUID141 fluid thermal elements are used to construct the two-dimensional axisymmetric finite element models, as shown in Figure 4.4.1.1-2. In the air region (including the air inlet, outlet and annulus regions), only quadrilateral elements are used and the element sizes are nonuniform with much smaller element sizes close to the walls. In other regions, to simulate conduction, a mix of quadrilateral elements and triangular elements are used. Radiation heat transfer that occurs in the following regions is included in the model:

1. From the concrete outer surfaces to the ambient
2. Across the vertical air annulus (from the canister shell to the concrete cask liner)
3. From the top of the active fuel region to the bottom of the canister shield lid
4. From the bottom of the active fuel region to the top of the canister bottom plate
5. From the canister structural lid to the shield plug
6. From the shield plug to the concrete cask lid

Loads and Boundary Conditions

1. Heat generation in the active fuel region.

The distribution of the heat generation is based on the axial power distribution shown in Figure 4.4.1.1-3 and 4.4.1.1-4 for PWR and BWR fuels, respectively (see description in Chapter 5, Section 5.2.6, for the design-basis fuel).

2. Solar insolation to the outer surfaces of the concrete cask.

The solar insolation to the concrete cask outer surfaces is considered in the model. The incident solar energy is applied based on 24-hour averages as shown below.

$$\text{Side surface: } \frac{1475\text{Btu} / \text{ft}^2}{24\text{hrs}} = 61.46\text{Btu} / \text{hr} \cdot \text{ft}^2$$

$$\text{Top surface: } \frac{2950\text{Btu} / \text{ft}^2}{24\text{hrs}} = 122.92\text{Btu} / \text{hr} \cdot \text{ft}^2$$

3. Natural convection heat transfer at the outer surfaces of the concrete cask.

Natural convection heat transfer at the outer surfaces of the concrete cask is evaluated by using the heat transfer correlation for vertical and horizontal plates [17, 29]. This method assumes a surface temperature and then estimates Grashof (Gr) or Rayleigh (Ra) numbers to determine whether a heat transfer correlation for a laminar flow model or for a turbulent flow model should be used. Since Grashof or Rayleigh numbers are much higher than the critical values, correlation for the turbulent flow model is used as shown in the following.

Side surface [17]:

$$\begin{aligned} \text{Nu} &= 0.13(\text{Gr} \cdot \text{Pr})^{1/3} \\ h_c &= \text{Nu} \cdot k_f / H_{\text{VCC}} \end{aligned} \quad \text{for } \text{Gr} > 10^9$$

Top surface [29]:

$$\begin{aligned} \text{Nu} &= 0.15\text{Ra}^{1/3} \\ h_c &= \text{Nu} \cdot k_f / L \end{aligned} \quad \text{for } \text{Ra} > 10^7$$

where:

| | |
|-----------|---|
| Gr | Grashof number |
| h_c | Average natural convection heat transfer coefficient |
| H_{vcc} | Height of the vertical concrete cask |
| k_f | Conductivity |
| L | Top surface characteristic length, $L = \text{area} / \text{perimeter}$ |
| Nu | Average Nusselt number |
| Pr | Prandtl number |
| Ra | Rayleigh number |

All material properties required in the above equations are evaluated based on the film temperature, that is, the average value of the surface temperature and the ambient temperature.

4. Radiation heat transfer at the concrete cask outer surfaces.

The radiation heat transfer between the outer surfaces and the ambient is evaluated in the model by calculating an equivalent radiation heat transfer coefficient.

$$h_{rad} = \frac{\sigma(T_1^2 + T_2^2)(T_1 + T_2)}{\frac{1}{\epsilon_1} + \frac{1}{\epsilon_2} + \frac{1}{F_{12}} - 2}$$

where:

| | |
|-----------------------------|--|
| h_{rad} | Equivalent radiation heat transfer coefficient |
| F_{12} | View factor |
| T_1 & T_2 | Surface (T_1) and ambient (T_2) temperatures |
| ϵ_1 & ϵ_2 | Surface (ϵ_1) and ambient ($\epsilon_2=1$) emissivities |
| σ | Stefan-Boltzmann Constant |

At the concrete cask side, an emissivity for a concrete surface of $\epsilon_1 = 0.9$ is used and a calculated view factor (F_{12}) = 0.182 [29] is applied. The view factor is determined by conservatively assuming that the cask is surrounded by eight casks.

At the cask top, an emissivity, ϵ_1 , of 0.8 is conservatively used (emissivity for concrete is 0.9), and a view factor, F_{12} , of 1 is applied.

Accuracy Check of the Numerical Simulation

To ensure the accuracy of the numerical simulation of the air flow in the concrete cask, and to ensure reliable numerical results, the following checks and confirmations are performed.

1. Global convergence of the iteration process for the nonlinear system.

The system controlling air flow through the cask and, therefore, the temperature field is nonlinear and is solved iteratively.

The global iteration process is monitored by checking the variation of parameters with the global iteration—e.g., the maximum air temperature, the mass flow rate, and the net heat carried out of the concrete cask by air convection. All of the results presented are at the converged state.

2. Overall energy balance and mass balance.

This step validates the overall energy balance and mass balance. The mass balance is also shown in Figure 4.4.1.1-5. At the converged state, the mass flow rate at the air inlets matches the mass flow rate at the air outlets, showing that an excellent mass balance has been obtained.

The overall energy balance is checked by computing the total heat input (Q_{in}) and total heat output (Q_{out}). The total heat input includes the total heat from the fuel (Q_{fuel}) and the total absorbed solar energy (Q_{sun}) incident on the concrete cask outer surfaces. The total heat output is the sum of the net heat carried out of the cask by air (Q_{air}) and by convection and radiation heat loss at the concrete cask outer surfaces (Q_{con}).

For the normal storage condition with the PWR design heat load of 23.0 kW:

$$Q_{in} = Q_{fuel} + Q_{sun} = 23.0 \text{ kW} + 9.18 \text{ kW} = 32.18 \text{ kW}$$

$$Q_{out} = Q_{air} + Q_{con} = 20.97 \text{ kW} + 11.72 \text{ kW} = 32.69 \text{ kW}$$

$$Q_{out}/Q_{in} = 1.016$$

For the normal storage condition with the BWR design heat load of 23.0 kW:

$$Q_{in} = Q_{fuel} + Q_{sun} = 23.0 \text{ kW} + 9.52 \text{ kW} = 32.52 \text{ kW}$$

$$Q_{out} = Q_{air} + Q_{con} = 20.70 \text{ kW} + 12.12 \text{ kW} = 32.82 \text{ kW}$$

$$Q_{out}/Q_{in} = 1.009$$

The overall energy balance is demonstrated to be within 2 percent for all design conditions.

3. Finite Element Mesh Adequacy Study.

A sensitivity evaluation is performed to assess the effect of the number of elements used in the Two-dimensional Axisymmetric Air Flow and Concrete Cask Models. The sensitivity evaluation is performed with a reduced element model based on the model for the PWR fuel configuration. The total number of elements in the reduced-element model (13,371 elements) is 21% less than the number of elements used in the axisymmetric air flow and concrete cask model described above. The reduction in the number of elements occurs in the air flow region in the radial direction, which has the largest gradients in velocity and temperature. As shown below, the temperatures calculated by the reduced element model (Case ES1) are essentially the same as the temperatures calculated by the axisymmetric air flow and concrete cask model (Case ES2).

| Case | Number of Elements in Model | Max. Air Temp. in Annular Region (Canister Surface) | Maximum Concrete Temp. | Average Air Temp. at the Outlet | Maximum Canister Shell Temp. |
|---------|-----------------------------|---|------------------------|---------------------------------|------------------------------|
| ES1 | 13,371 | 451 K | 360 K | 335 K | 452 K |
| ES2 | 16,835 | 448 K | 359 K | 339 K | 449 K |
| ES1/ES2 | 0.79 | 1.01 | 1.00 | 0.99 | 1.01 |

A comparison of the two models (Case ES1/ES2) shows that the maximum difference is 1%. Therefore, the number of elements used in the Two-dimensional Axisymmetric Air Flow and Concrete Cask Model (16,835) is adequate.

Supplemental Shielding Fixture Evaluation

The effect of the installation of an optional supplemental shielding fixture, shown in Drawing 790-613, installed in the air inlet is evaluated based on one-half of the air inlets blocked. The analysis results show that the maximum temperature increase is 5°F, which remains well below normal condition allowables. The pipes in the shielding fixture are offset to block (gamma) radiation, but allow air flow.

Figure 4.4.1.1-1 Two-Dimensional Axisymmetric Air Flow and Concrete Cask Model: PWR

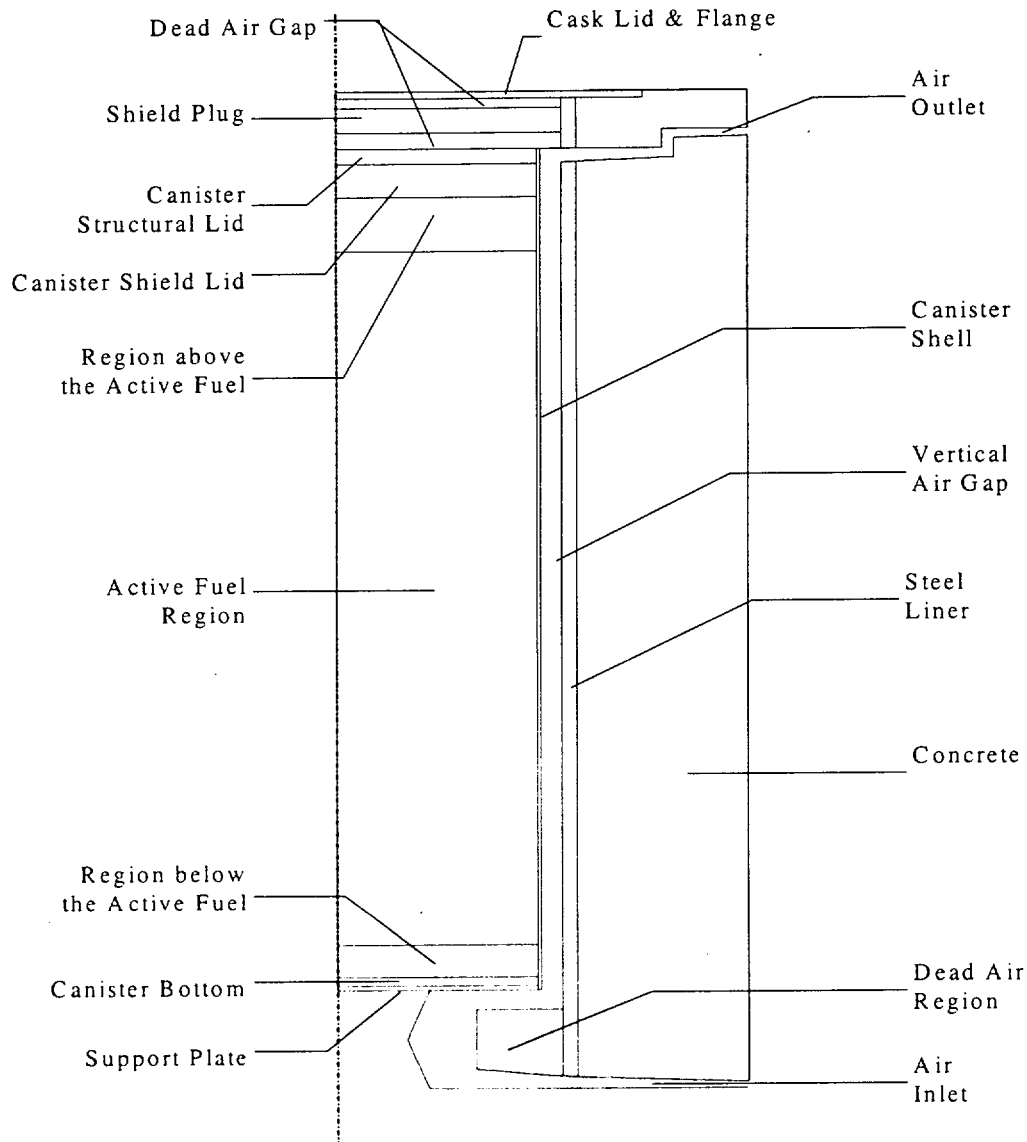


Figure 4.4.1.1-2 Two-Dimensional Axisymmetric Air Flow and Concrete Cask Finite Element Model: PWR

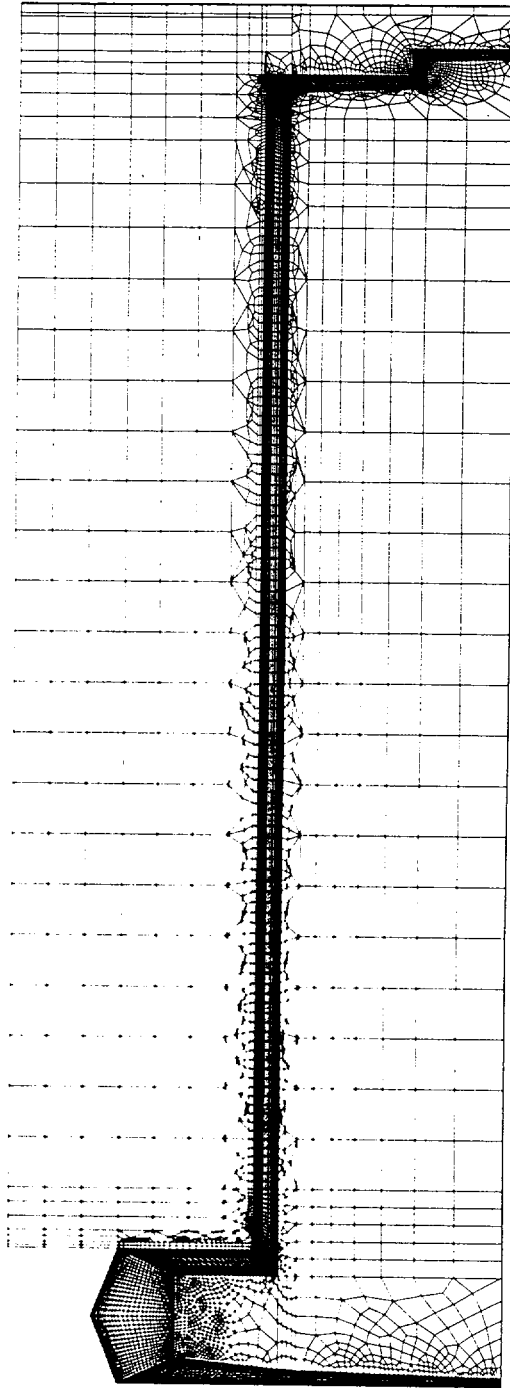


Figure 4.4.1.1-3 Axial Power Distribution for PWR Fuel

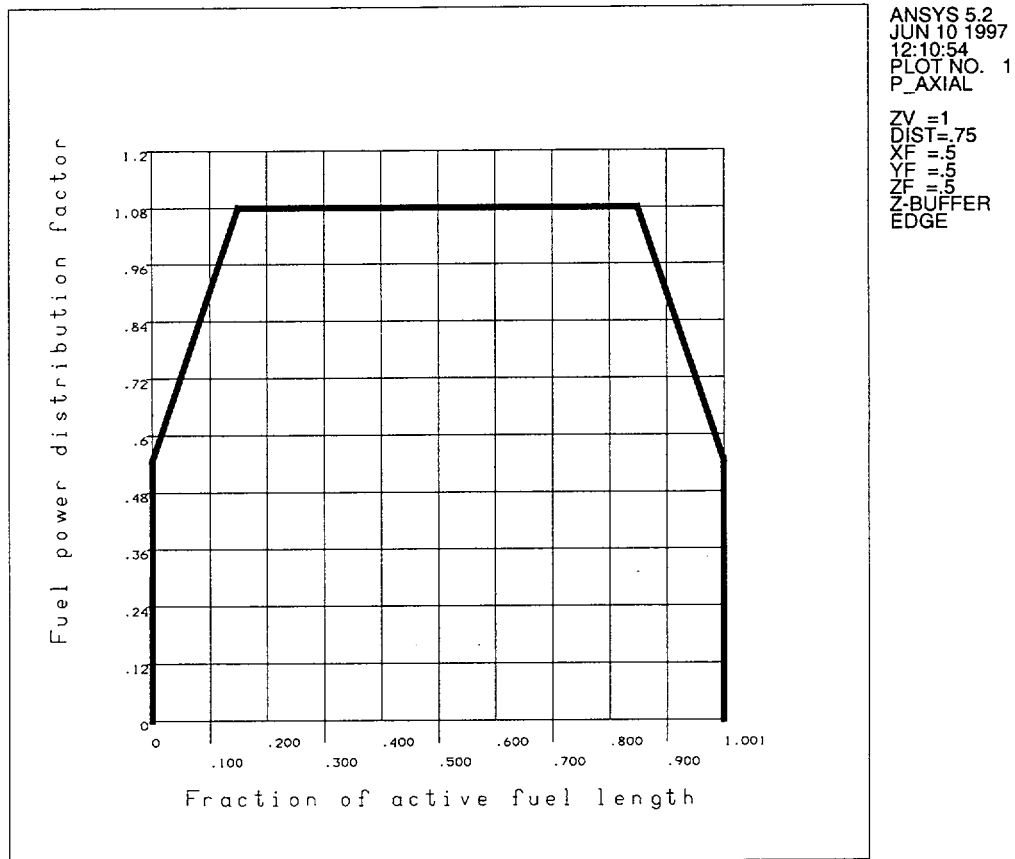
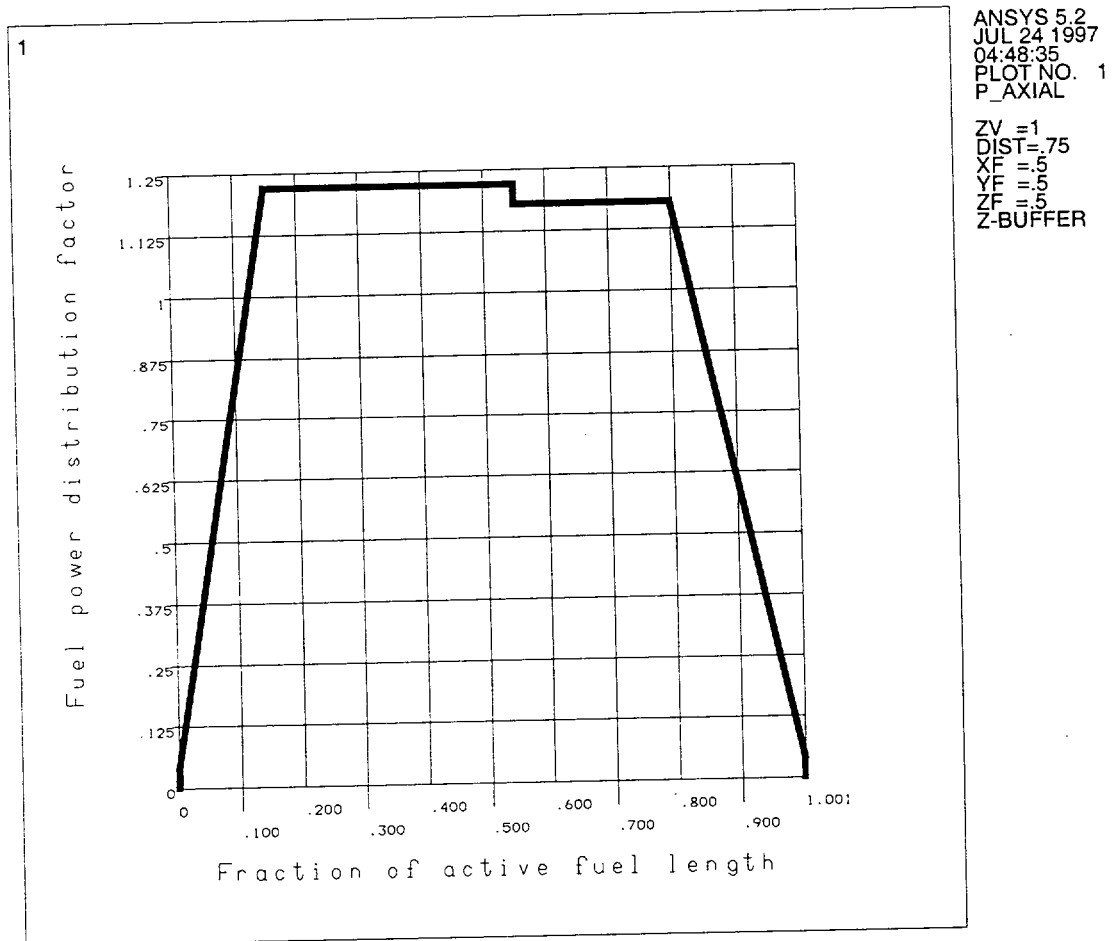


Figure 4.4.1.1-4 Axial Power Distribution for BWR Fuel



4.4.1.2 Three-Dimensional Canister Models

Two three-dimensional canister models are used to evaluate the temperature distribution of the fuel cladding and basket components inside the canister for the PWR and BWR configurations, respectively. The model for PWR fuel is shown in Figures 4.4.1.2-1 and 4.4.1.2-2. The model for BWR fuel is shown in Figures 4.4.1.2-3 and 4.4.1.2-4.

ANSYS SOLID70 three-dimensional conduction elements and LINK31 radiation elements are used to construct the model. The model includes the fuel assemblies, fuel tubes, support disks, heat transfer disks, top and bottom weldments, canister shell, lids, bottom plate and gas inside the canister (helium). Based on symmetry, only half of the canister is modeled. The plane of symmetry is considered to be adiabatic.

The canister outer surface temperatures obtained from the two-dimensional axisymmetric air flow and concrete cask model (Section 4.4.1.1) are applied at the canister surfaces in the model as boundary conditions. In the model, the fuel assemblies are considered to be centered in the fuel tubes. The fuel tubes are centered in the slots of the support disks and heat transfer disks. The basket is centered in the canister. These assumptions are conservative, since any contact between components will provide a more efficient path to reject the heat.

The gaps used in the three-dimensional canister model between the support disks and canister shell, as well as between the heat transfer disk and the canister shell, are shown in the following table.

| | | Nominal Gap At Room Temperature (inch) | Gap Used in the 3-D Thermal Model (inch) | |
|------------|---|--|--|-------------------------|
| | | | At Room Temperature | At Elevated Temperature |
| PWR | Gap between Support Disk and Canister Shell | 0.120 | 0.155 | 0.165 |
| | Gap between Heat Transfer Disk and Canister Shell | 0.245 | 0.280 | 0.195 |
| BWR | Gap between Support Disk and Canister Shell | 0.120 | 0.155 | 0.165 |
| | Gap between Heat Transfer Disk and Canister Shell | 0.280 | 0.315 | 0.232 |

The gaps at room temperature are first used in the model to calculate preliminary temperature distribution and to determine the differential thermal expansion of the disks and canister shell at the elevated temperatures. The gaps at elevated temperature are then established, based on the differential thermal expansions between components, and used in the model for final solution. As shown above, the room temperature gaps used in the thermal model bound the actual nominal gaps at room temperature.

These gap sizes are adjusted in the model to account for differential thermal expansion of the disks and canister shell based on thermal conditions. The gaps used in the model are shown to be larger than the actual gap size based on thermal expansion calculation using the thermal analysis results; therefore, the model is conservative.

A sensitivity study was performed to assess the effect of gap sizes on temperature results, with consideration of fabrication tolerance of the canister and basket. The ANSYS three-dimensional canister model for the PWR fuel is used for the study. The gaps between the disks and canister shell are increased to account for the worst case fabrication tolerance of the canister and basket. The gaps are also adjusted based on the differential thermal expansion of the canister and basket at elevated temperature. Compared to the gaps used in the original three-dimensional thermal model, the gap between the support disk and the canister shell is increased by 27% and the gap between the heat transfer disk and the canister shell is increased by 24%. The results of the sensitivity study indicate that the increase in the maximum fuel cladding and basket temperatures is less than 9°F, which is less than 3% of the temperature difference between the maximum temperature of the fuel cladding/basket and the canister shell. Therefore, the effect of the thermal model gap size on the maximum temperature of the basket and fuel cladding is not significant.

The structural lid and the shield lid are expected to be in full contact due to the weight of the structural lid. The thermal resistance across the contact surface is considered to be negligible and, therefore, no gap is modeled between the lids.

All material properties used in the model, except the effective properties discussed below, are shown in Tables 4.2-1 through 4.2-12.

The fuel assemblies and fuel tubes are modeled as homogenous regions with effective conductivities, determined by the two-dimensional fuel models (Section 4.4.1.5) and the two-dimensional fuel tube models (Section 4.4.1.6), respectively. The effective properties are listed in Tables 4.4.1.2-1 through 4.4.1.2-4. The properties corresponding to the PWR 14 × 14 assemblies are used for the PWR model, since the 14 × 14 assemblies have lower conductivities as compared to other PWR assemblies. For the same reason, the properties corresponding to the BWR 9 × 9 assemblies are used in the BWR model.

In the model, radiation heat transfer is taken into account in the following locations:

1. From the top of the fuel region to the bottom surface of the canister shield lid.
2. From the bottom of the fuel region to the top surface of the canister bottom plate.
3. From the exterior surfaces of the fuel tubes (surface between disks) to the inner surface of the canister shell.
4. From the edge of the PWR support disks to the inner surface of the canister shell.
5. From the edge of heat transfer disks to the inner surface of the canister shell.
6. Between disks in the PWR model in the canister axial direction.

The radiation heat transfer from the BWR support disk is conservatively neglected by using an emissivity value of 0.0001 for the BWR support disk in the model. An emissivity of 0.22 is used for the heat transfer disk, except the water-jet cut surfaces (the circumferential surfaces at the edges of the disks facing the canister shell and the inner surfaces of each slot). The surface condition of the water-jet cut surfaces is similar to that of the sandblasted surface and, therefore, an emissivity of 0.4 is used.

Radiation elements (LINK31) are used to model the radiation effect for the first three locations. Radiation across the gaps (Locations No. 4 through 6) is accounted for by establishing effective conductivities for the gas in the gap, as shown below. The gaps are small compared to the surfaces separated by the gaps.

Radiation heat transfer between two nodes i (hotter node) and j (colder node) is accounted for by the expression:

$$q_r = \sigma \epsilon A F (T_i^4 - T_j^4)$$

where:

- σ = the Stefan-Boltzman constant
- ϵ = effective emissivity between two surfaces
- A = surface area
- F = the gray body shape factor for the surfaces
- T_i = temperature of the i th node
- T_j = temperature of the j th node

The total heat transfer can be expressed as the sum of the radiation and the conduction processes:

$$Q_t = q_r + q_k$$

where q_r is specified above for the radiation heat transfer and q_k , which is the heat transfer by conduction is expressed as:

$$q_k = \frac{KA}{g} (T_i - T_j)$$

where:

- T_i = temperature of the i th node
- T_j = temperature of the j th node
- g = gap distance (between the two surfaces defined by node i and node j)
- K = conductivity of the gas in the gap
- A = area of gap surface

By combining the two expressions (for q_k and q_r) and factoring out the term $A(T_i - T_j)/g$,

$$Q_t = [g\sigma\epsilon F(T_i^2 + T_j^2)(T_i + T_j) + K][A(T_i - T_j)/g]$$

or

$$Q_t = K_{\text{eff}} A (T_i - T_j) / g$$

where:

$$K_{\text{eff}} = g\sigma\epsilon F(T_i^2 + T_j^2)(T_i + T_j) + K$$

The material conductivity used in the analysis for the elements comprising the gap includes the heat transfer by both conduction and radiation.

Effective emissivities (ϵ) are used for all radiation calculations, based on the formula below [17]. The view factor is taken to be unity.

$$\epsilon = 1 / (1/\epsilon_1 + 1/\epsilon_2 - 1) \quad \text{where } \epsilon_1 \text{ \& } \epsilon_2 \text{ are the emissivities of two parallel plates}$$

Radiation between the exterior surfaces of the fuel tubes is conservatively ignored in the model.

Volumetric heat generation (Btu/hr-in³) is applied to the active fuel region based on design heat load, active fuel length of 144 inches and an axial power distribution as shown in Figures 4.4.1.1-3 and 4.4.1.1-4 for PWR and BWR fuel, respectively.

Figure 4.4.1.2-1 Three-Dimensional Canister Model for PWR Fuel

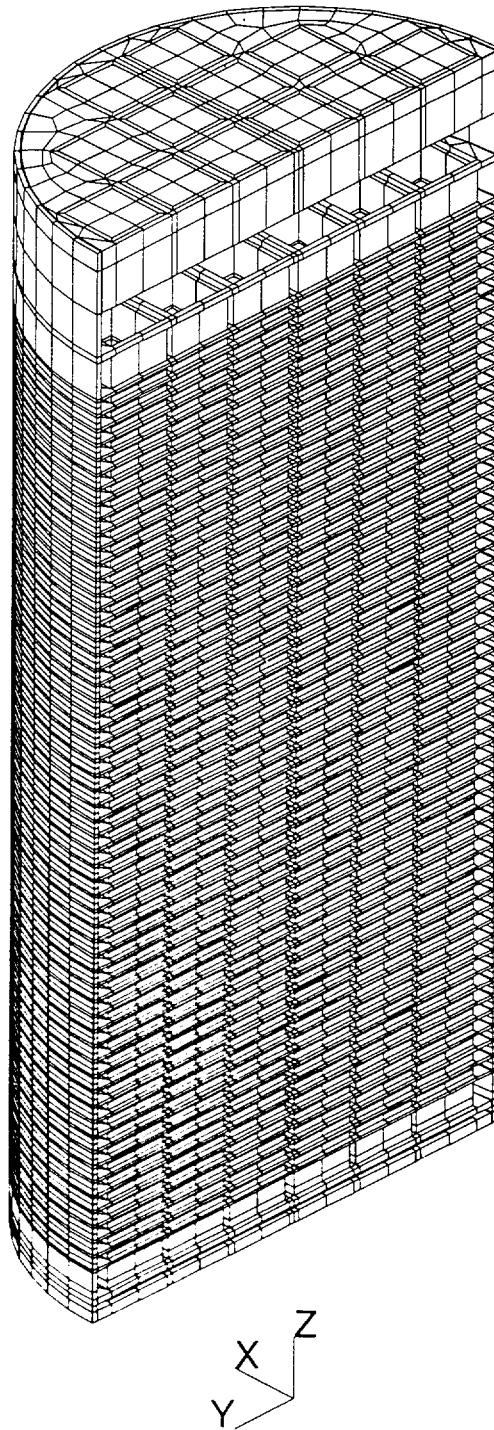


Figure 4.4.1.2-2 Three-Dimensional Canister Model for PWR Fuel – Cross Section

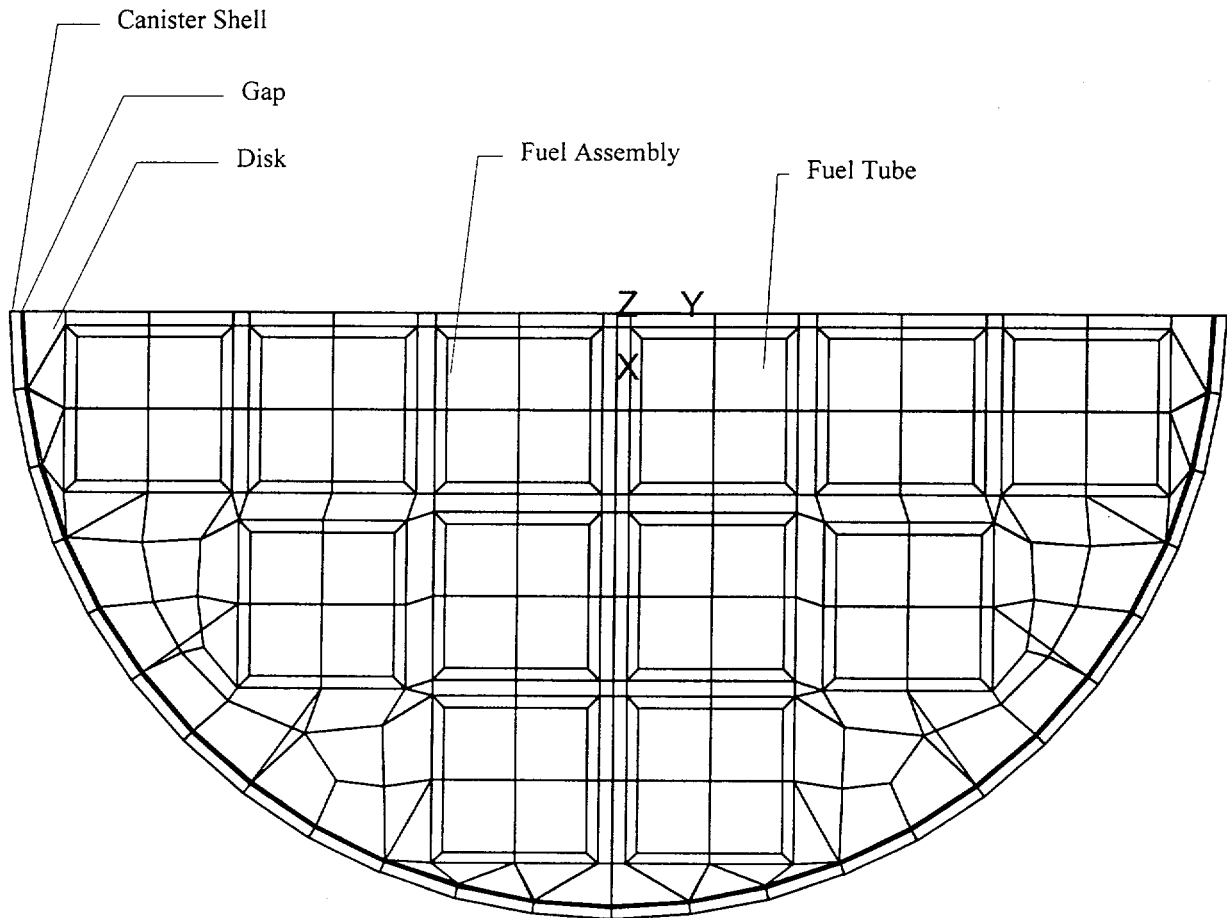


Figure 4.4.1.2-3 Three-Dimensional Canister Model for BWR Fuel

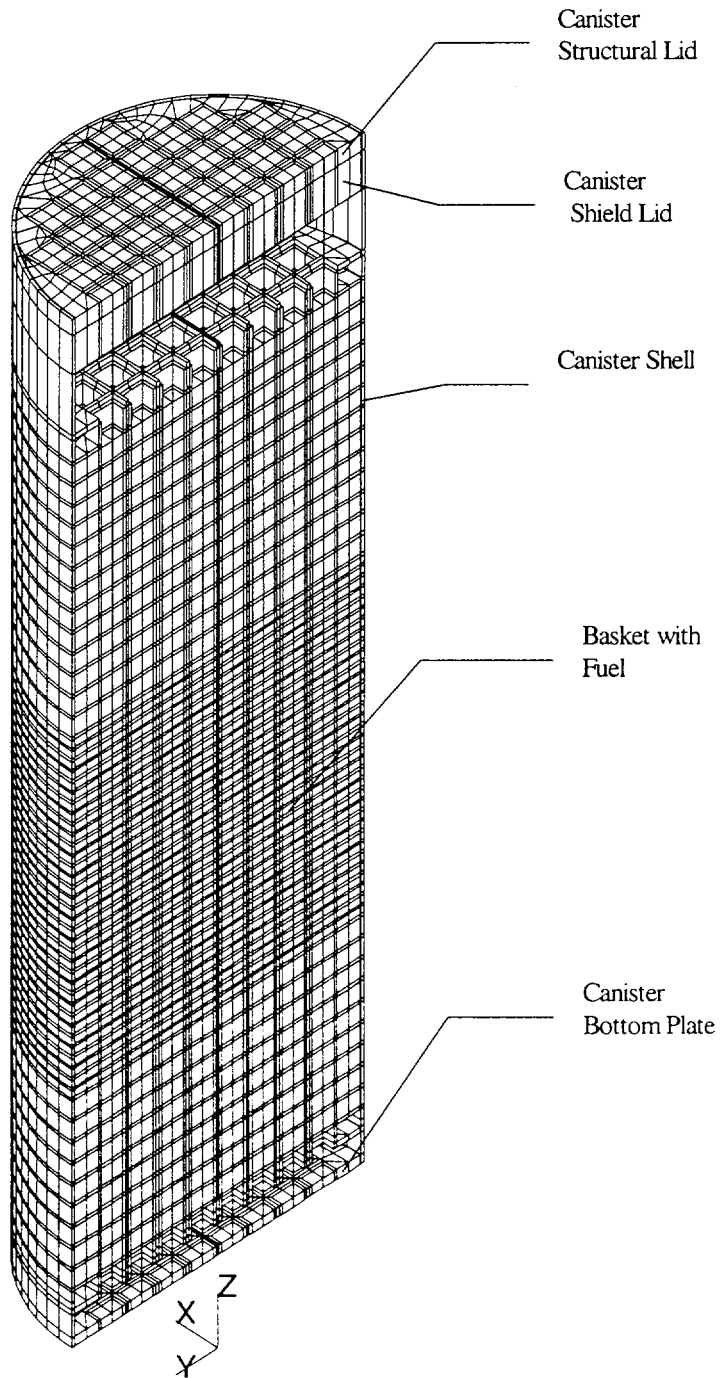


Figure 4.4.1.2-4 Three-Dimensional Canister Model for BWR Fuel – Cross Section

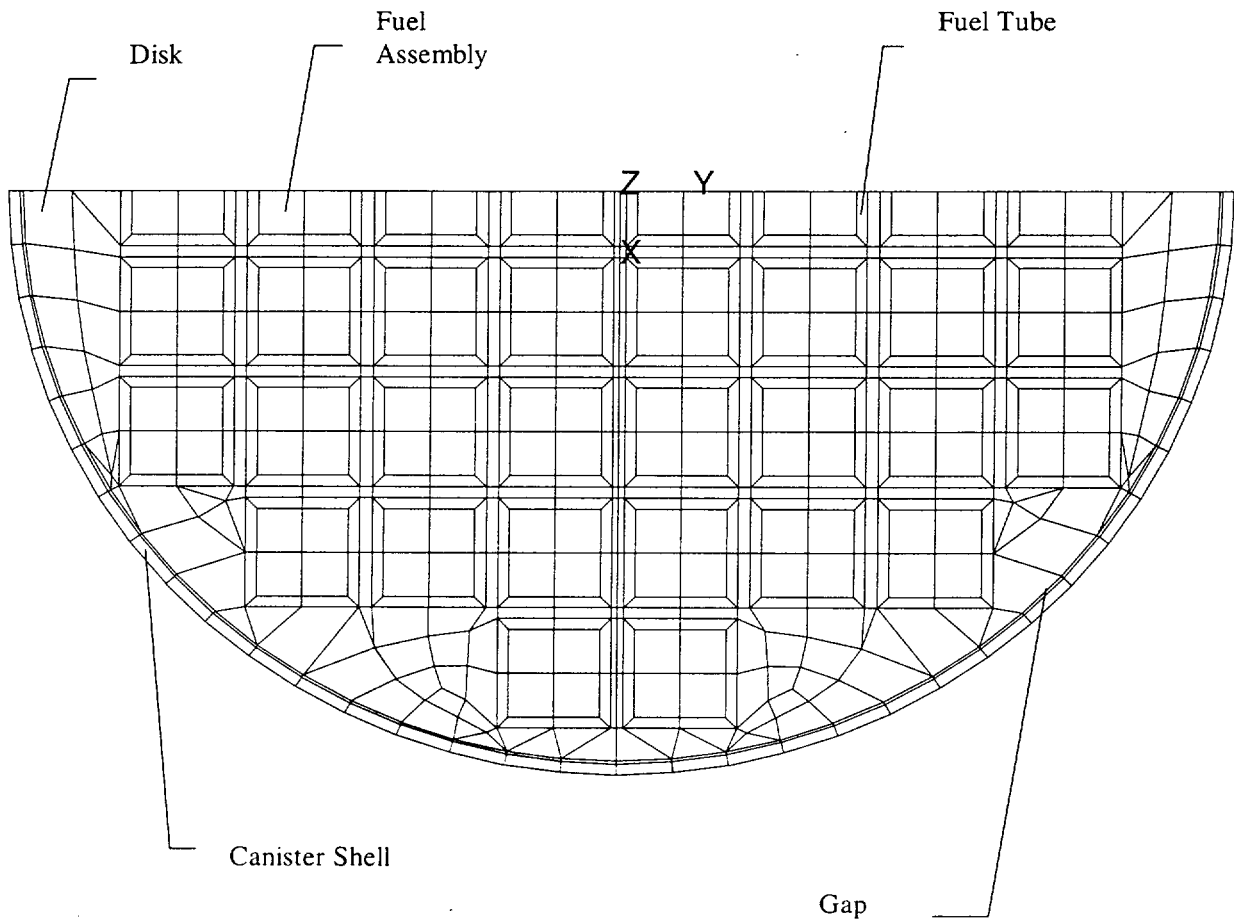


Table 4.4.1.2-1 Effective Thermal Conductivities for PWR Fuel Assemblies

| Conductivity (Btu/hr-in-°F) | Temperature (°F) | | | |
|--------------------------------|------------------|-------|-------|-------|
| | 220 | 414 | 617 | 812 |
| K _{xx} | 0.020 | 0.027 | 0.037 | 0.049 |
| K _{yy} | 0.020 | 0.027 | 0.037 | 0.049 |
| K _{zz} | 0.171 | 0.154 | 0.145 | 0.142 |

Note: x, y and z are in the coordinate system shown in Figure 4.4.1.2-1.

Table 4.4.1.2-2 Effective Thermal Conductivities for BWR Fuel Assemblies

| Conductivity (Btu/hr-in-°F) | Temperature (°F) | | | |
|--------------------------------|------------------|-------|-------|-------|
| | 186 | 389 | 593 | 799 |
| K _{xx} | 0.021 | 0.029 | 0.041 | 0.056 |
| K _{yy} | 0.021 | 0.029 | 0.041 | 0.056 |
| K _{zz} | 0.181 | 0.165 | 0.157 | 0.156 |

Note: x, y and z are in the coordinate system shown in Figure 4.4.1.2-3.

Table 4.4.1.2-3 Effective Thermal Conductivities for PWR Fuel Tubes

| Fuel Assembly Group | Conductivity (Btu/hr-in-°F) | Temperature (°F) | | | |
|---------------------|--------------------------------|------------------|-------|-------|-------|
| | | 206 | 405 | 604 | 803 |
| In SS disk region | | | | | |
| | Kxx | 0.022 | 0.028 | 0.033 | 0.040 |
| | Kyy | 1.54 | 1.57 | 1.59 | 1.61 |
| | Kzz | 1.54 | 1.57 | 1.59 | 1.61 |
| In AL disk region | | | | | |
| | Kxx | 0.022 | 0.027 | 0.032 | 0.038 |
| | Kyy | 1.54 | 1.57 | 1.59 | 1.61 |
| | Kzz | 1.54 | 1.57 | 1.59 | 1.61 |

Note: Kxx is in the direction across the thickness of the fuel tube wall.

Kyy is in the direction parallel to the fuel tube wall.

Kzz is in the canister axial direction.

Table 4.4.1.2-4 Effective Thermal Conductivities for BWR Fuel Tubes

| Tubes with Neutron Absorber | Conductivity | Temperature (°F) | | | |
|---------------------------------------|----------------|------------------|------------|------------|------------|
| | (Btu/hr-in-°F) | 200 | 400 | 600 | 800 |
| In CS disk region | | | | | |
| | Kxx | 0.017 | 0.022 | 0.027 | 0.032 |
| | Kyy | 1.665 | 1.759 | 1.815 | 1.830 |
| | Kzz | 1.665 | 1.759 | 1.815 | 1.830 |
| In AL disk region | | | | | |
| | Kxx | 0.017 | 0.022 | 0.027 | 0.033 |
| | Kyy | 1.665 | 1.759 | 1.815 | 1.830 |
| | Kzz | 1.665 | 1.759 | 1.815 | 1.830 |
| | | | | | |
| Tubes without Neutron Absorber | | 200 | 400 | 600 | 800 |
| In CS disk region | | | | | |
| | Kxx | 0.012 | 0.015 | 0.018 | 0.021 |
| | Kyy | 0.191 | 0.202 | 0.218 | 0.236 |
| | Kzz | 0.191 | 0.202 | 0.218 | 0.236 |
| In AL disk region | | | | | |
| | Kxx | 0.012 | 0.015 | 0.019 | 0.023 |
| | Kyy | 0.191 | 0.202 | 0.218 | 0.236 |
| | Kzz | 0.191 | 0.202 | 0.218 | 0.236 |
| | | | | | |

Note: Kxx is in the direction across the thickness of fuel tube wall.

Kyy is in the direction parallel to fuel tube wall.

Kzz is in the canister axial direction.

4.4.1.3 Three-Dimensional Transfer Cask and Canister Models

The three-dimensional half-symmetry transfer cask model is a representation of the canister and transfer cask assembly. The model is used to perform a transient thermal analysis to determine the maximum water temperature in the canister for the period beginning immediately after removing the transfer cask and canister from the spent fuel pool. The model is also used to calculate the maximum temperature of the fuel cladding, the transfer cask and canister components during the vacuum drying condition and after the canister is back-filled with helium. The transfer cask is evaluated separately for PWR or BWR fuel using two models. For each fuel type, the class of fuel with the shortest associated canister and transfer cask is modeled in order to maximize the contents heat generation rate per unit volume and minimize the heat rejection from the external surfaces. The models for PWR and BWR fuel are shown in Figures 4.4.1.3-1 and 4.4.1.3-2, respectively. ANSYS SOLID70 three-dimensional conduction elements, LINK31 (PWR model) and MATRIX50 (BWR model) radiation elements are used. The model includes the transfer cask and the canister and its internals. The details of the canister and contents are modeled using the same methodology as that presented in Section 4.4.1.2 (Three-Dimensional Canister Models). Effective thermal properties for the fuel regions and the fuel tube regions are established using the fuel models and fuel tube models presented in Sections 4.4.1.5 and 4.4.1.6 respectively. The effective specific heat and density are calculated on the basis of material mass and volume ratio, respectively.

Radiation across the gaps was represented by the LINK31 elements or the MATRIX50 elements, which used the gray body emissivities for stainless and carbon steels. Convection is considered at the top of the canister lid, the exterior surfaces of the transfer cask, as well as at the annulus between the canister and the inner surface of the transfer cask. The combination of radiation and convection at the transfer cask exterior vertical surfaces and canister lid top surface is taken into account in the model using the same method described in Section 4.4.1.2 for the three-dimensional canister models. The bottom of the transfer cask is modeled as being in contact with the concrete floor. Volumetric heat generation (Btu/hr-in^3) is applied to the active fuel region based on a total heat load of 23 kW for both PWR and BWR fuel. The model considers the active fuel length of 144 inches and an axial power distribution, as shown in Figure 4.4.1.1-3 and 4.4.1.1-4 for PWR and BWR fuel, respectively.

An initial temperature of 100°F is considered in the model on the basis of typical maximum average water temperature in the spent fuel pool. Under typical operations, the water inside the

canister is drained within 17 hours and the canister is back-filled with helium immediately after the vacuum drying and transferred to the concrete cask. The transient analysis is performed for 17 hours with the water inside the canister, 32 hours (PWR) and 25 hours (BWR) for the vacuum-dried condition, and 10 hours (PWR) and 16 hours (BWR) for the helium condition, followed by a steady state analysis (in helium condition). The temperature history of the fuel cladding and the basket components, as well as the transfer cask components, is determined and compared with the short-term temperature limits presented in Table 4.1-3.

The evaluation for the 100-ton transfer cask is bounded by the evaluation using the models presented in this section. The overall wall thickness for the 100-ton transfer cask is less than that for the standard transfer cask. The water-neutron shield for the 100-ton transfer cask has better heat transfer capability (conduction and convection) than the NS-4-FR used for the standard transfer cask. The 100-ton transfer cask may be handled in a horizontal orientation. Since there will be contact between basket, canister and transfer cask components when the cask is in the horizontal orientation, a more effective path for heat rejection results. The maximum temperatures for the fuel and basket components are expected to be lower compared with the condition when the transfer cask is in the vertical orientation. The three-dimensional finite element model for the transfer cask and canister for the PWR configuration is modified to simulate the horizontal condition. As shown in Figure 4.4.1.3-3, the contact between components is modeled by nodal couplings at the contact locations (between the transfer cask inner shell and the canister shell, between the canister shell and the disks, and between the disks and the fuel tubes). As a representative case, the transient analysis for the PWR configuration is performed using this model for the thermal evaluation of the system in a horizontal position.

Figure 4.4.1.3-1 Three-Dimensional Standard Transfer Cask and Canister Model - PWR

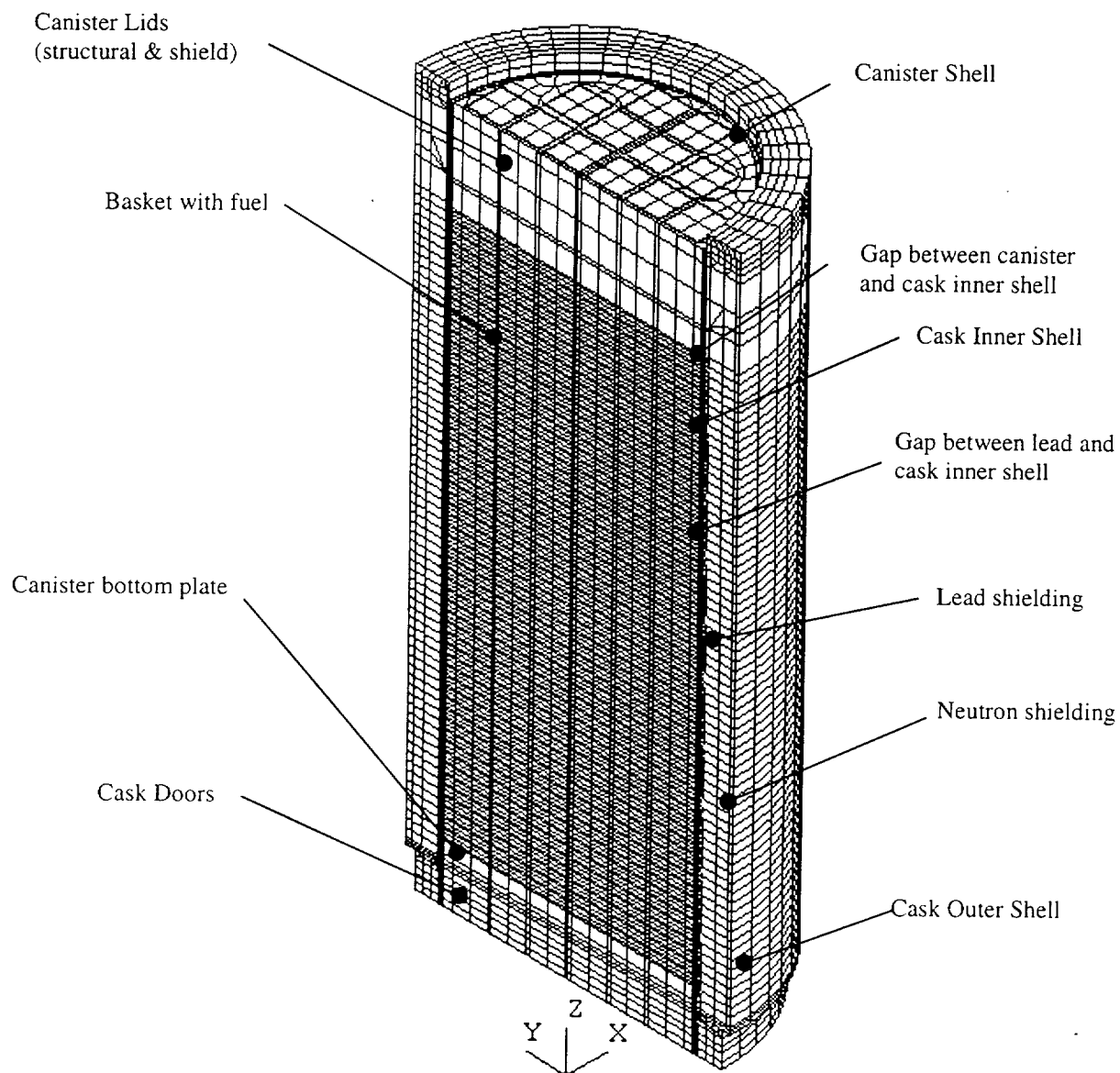
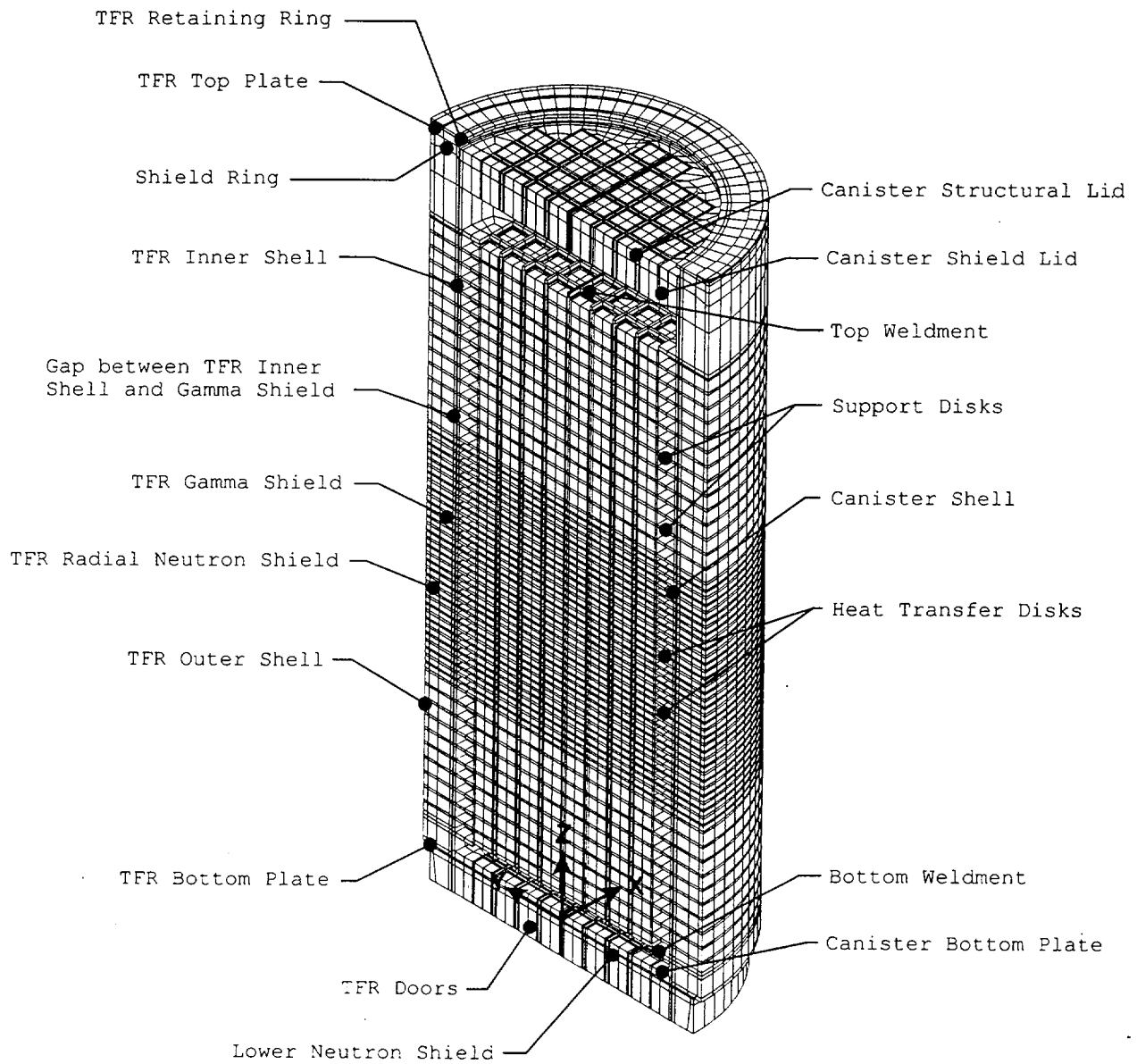
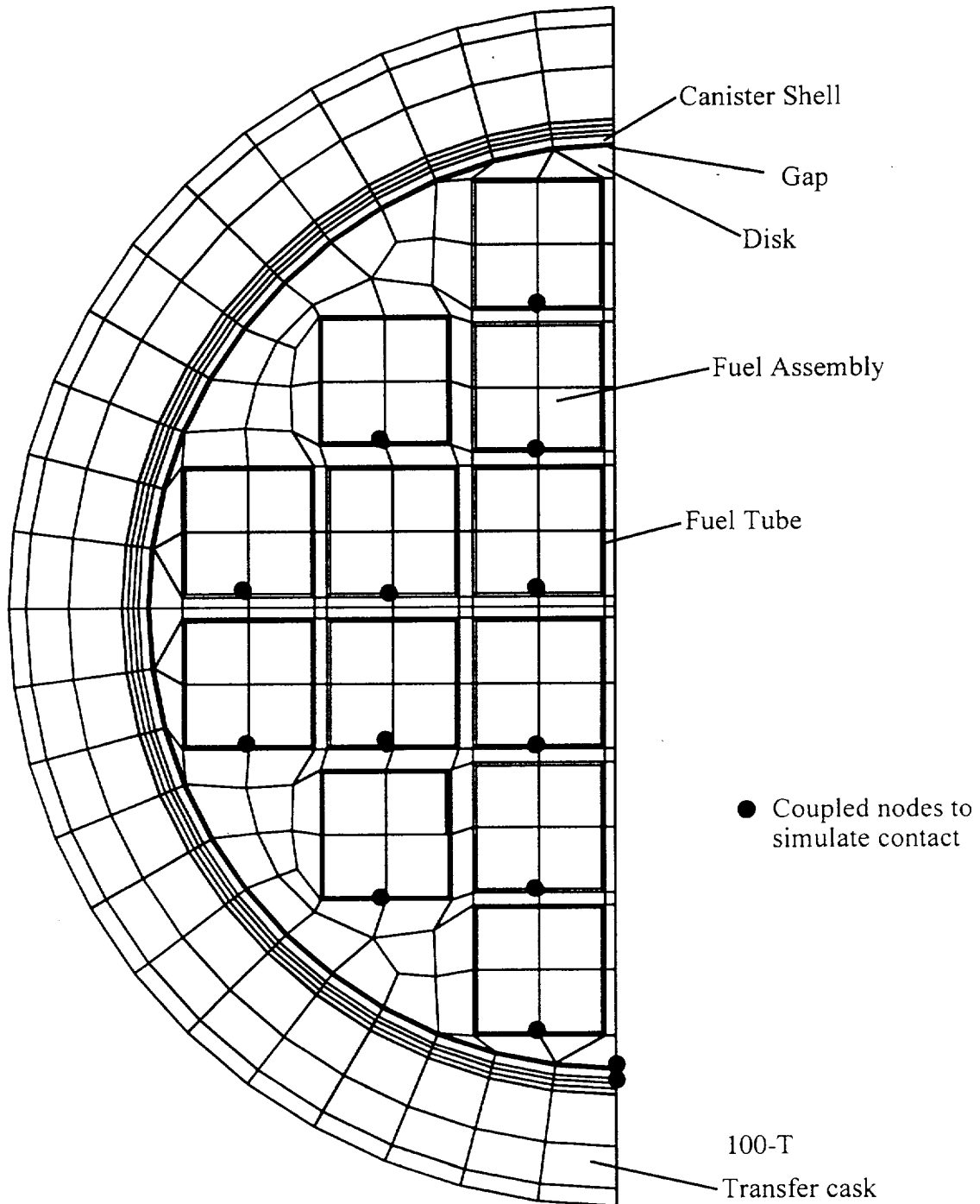


Figure 4.4.1.3-2 Three-Dimensional Standard Transfer Cask and Canister Model - BWR



Canister media and TFR media not shown for clarity.

Figure 4.4.1.3-3 Cross-section of the 100-Ton Transfer Cask and Canister Thermal Model – Cask in Horizontal Position



4.4.1.4 Three-Dimensional Periodic Canister Internal Models

The three-dimensional periodic canister internal model consists of a periodic section of the canister internals. A total of three models are used: one for PWR fuel and two for BWR fuel. For the PWR canister, the model contains one support disk with two heat transfer disks (half thickness) on its top and bottom, the fuel assemblies, the fuel tubes and the media in the canister, as shown in Figure 4.4.1.4-1. The first BWR model, shown in Figure 4.4.1.4-2, represents the central region of the BWR canister, which contains one heat transfer disk with two support disks (half thickness) on its top and bottom, the fuel assemblies, the fuel tubes and the media in the canister. The second BWR model (not shown), for the region without heat transfer disks, contains two support disks (half thickness), the fuel assemblies, the fuel tubes and the media in the canister. The difference between the two BWR models is that the second model does not have the heat transfer disk. The purpose of these models is to determine the effective thermal conductivity of the canister internals in the canister radial direction. The effective conductivities are used in the two-dimensional axisymmetric air flow and concrete cask models. The media in the canister is considered to be helium. The fuel assemblies and fuel tubes in this model are represented by homogeneous regions with effective thermal properties. The effective conductivities for the fuel assemblies and the fuel tubes are determined by the two-dimensional fuel models (Section 4.4.1.5) and the two-dimensional fuel tube models (Section 4.4.1.6) respectively. The properties corresponding to the PWR 14 × 14 assemblies are used for the PWR model, since the 14 × 14 assemblies have the lowest conductivities as compared to other PWR assemblies. For the same reason, the properties corresponding to the BWR 9 × 9 assemblies are used for the BWR models.

The effective thermal conductivity (k_{eff}) of the fuel region in the radial direction is determined by considering the canister internals as a solid cylinder with heat generation. The temperature distribution in the cylinder may be expressed as [17]:

$$T - T_o = \frac{q'''R^2}{4k_{eff}} \left[1 - \left(\frac{r}{R} \right)^2 \right]$$

where:

T_o = the surface temperature of the cylinder

T = temperature at radius "r" of the cylinder

R = the outer radius of the cylinder,

r = radius

$$q''' = \text{the heat generation rate} = \frac{Q}{\pi R^2 H}$$

where: Q = total heat generated in the cylinder

H = length of the cylinder

Considering the temperature at the center of the canister to be T_{\max} , the above equation can be simplified and used to compute the effective thermal conductivity (k_{eff}):

$$k_{\text{eff}} = \frac{Q}{4\pi H(T_{\max} - T_o)} = \frac{Q}{4\pi H\Delta T}$$

where:

Q = total heat generated by the fuel

H = length of the active fuel region

T_o = temperature at outer surface internals (inside surface of the canister)

$$\Delta T = T_{\max} - T_o$$

The value of ΔT is obtained from thermal analysis using the three-dimensional periodic canister internal model with the boundary temperature constrained to be T_o . The effective conductivity (k_{eff}) is then determined by using the above formula. Analysis is repeated by applying different boundary temperatures so that temperature-dependent conductivities can be determined.

Figure 4.4.1.4-1 Three-Dimensional Periodic Canister Internal Model - PWR

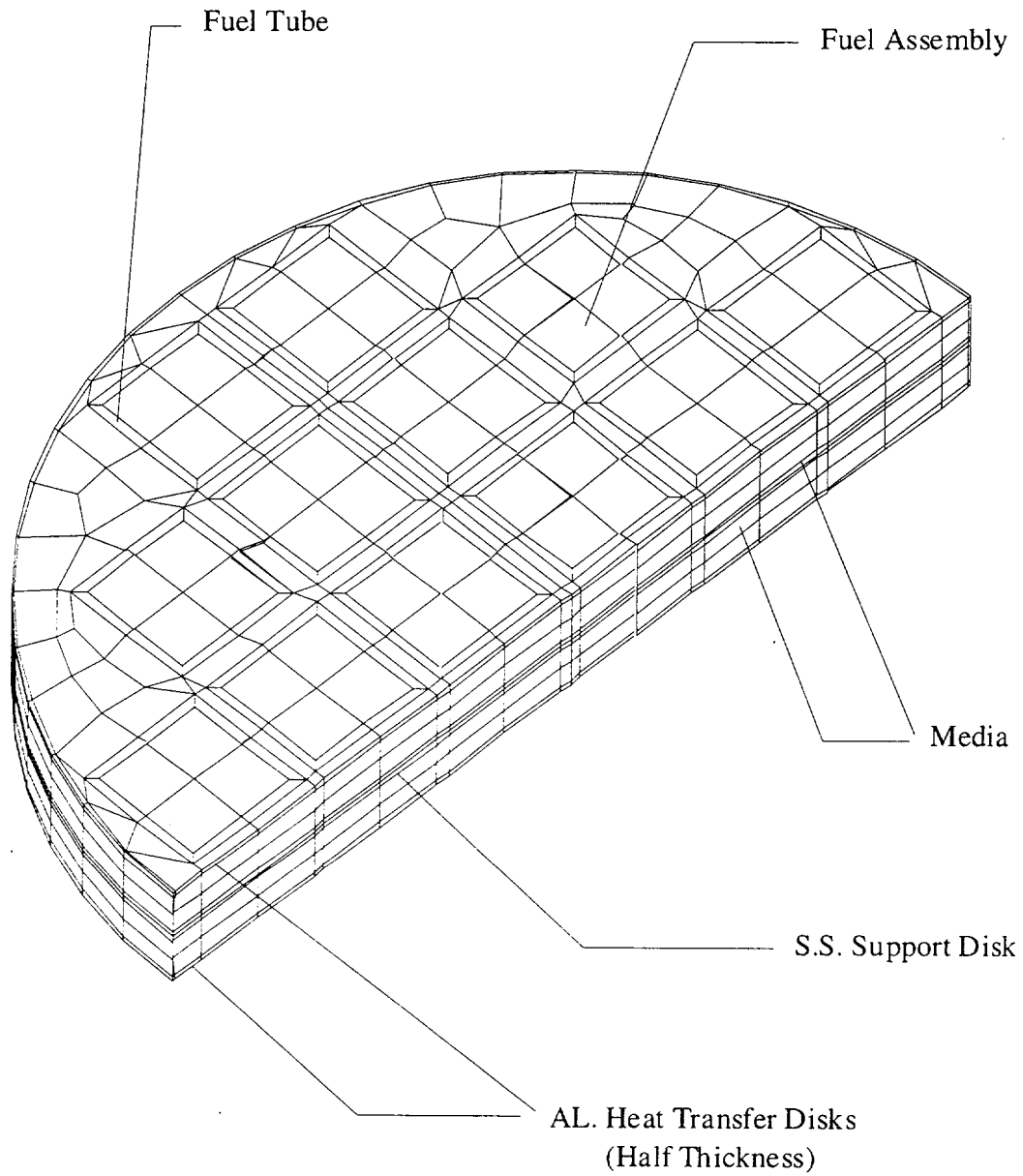
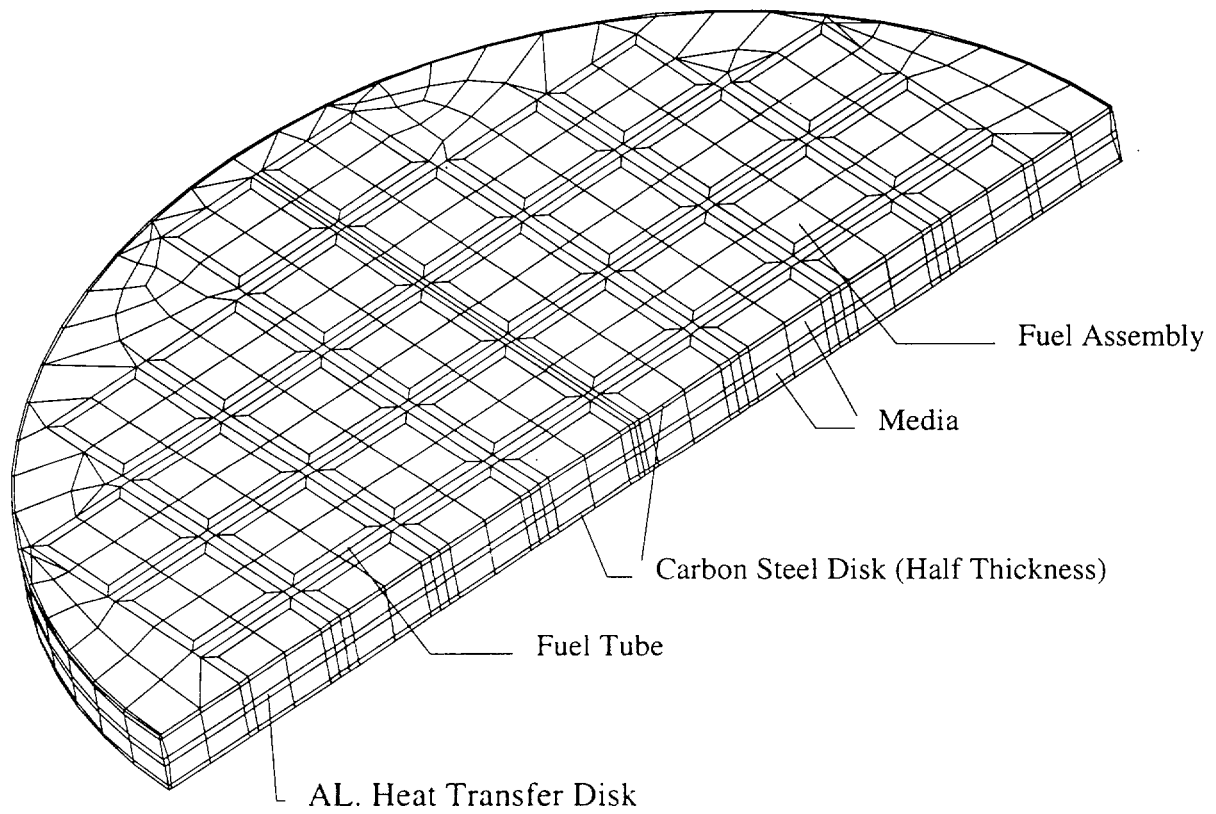


Figure 4.4.1.4-2 Three-Dimensional Periodic Canister Internal Model - BWR



4.4.1.5 Two-Dimensional Fuel Models

The effective conductivity of the fuel is determined by the two-dimensional finite element model of the fuel assembly. The effective conductivity is used in the three-dimensional canister models (Section 4.4.1.2) and the three-dimensional periodic canister internal models (Section 4.4.1.4). A total of seven models are required: four models for the 14×14, 15×15, 16×16 and 17×17 PWR fuels and three models for the 7×7, 8×8 and 9×9 BWR fuels. Because of similarity, only the figure for the PWR 17×17 model is shown in this section (Figure 4.4.1.5-1). All models contain a full cross-section of an assembly to accommodate the radiation elements.

The model includes the fuel pellets, cladding, media between fuel rods, media between the fuel rods and the inner surface of the fuel tube (PWR) or fuel channel (BWR), and helium at the gap between the fuel pellets and cladding. Three types of media are considered: helium, water and a vacuum. Modes of heat transfer modeled include conduction and radiation between individual fuel rods for the steady-state condition. ANSYS PLANE55 conduction elements and MATRIX50 radiation elements are used to model conduction and radiation. Radiation elements are defined between fuel rods and from rods to the wall. Radiation at the gap between the pellets and the cladding is conservatively ignored.

The effective conductivity for the fuel is determined by using an equation defined in a Sandia National Laboratory Report [30]. The equation is used to determine the maximum temperature of a square cross-section of an isotropic homogeneous fuel with a uniform volumetric heat generation. At the boundary of the square cross-section, the temperature is constrained to be uniform. The expression for the temperature at the center of the fuel is given by:

$$T_c = T_e + 0.29468 (Qa^2 / K_{eff})$$

where: T_c = the temperature at the center of the fuel (°F)

T_e = the temperature applied to the exterior of the fuel (°F)

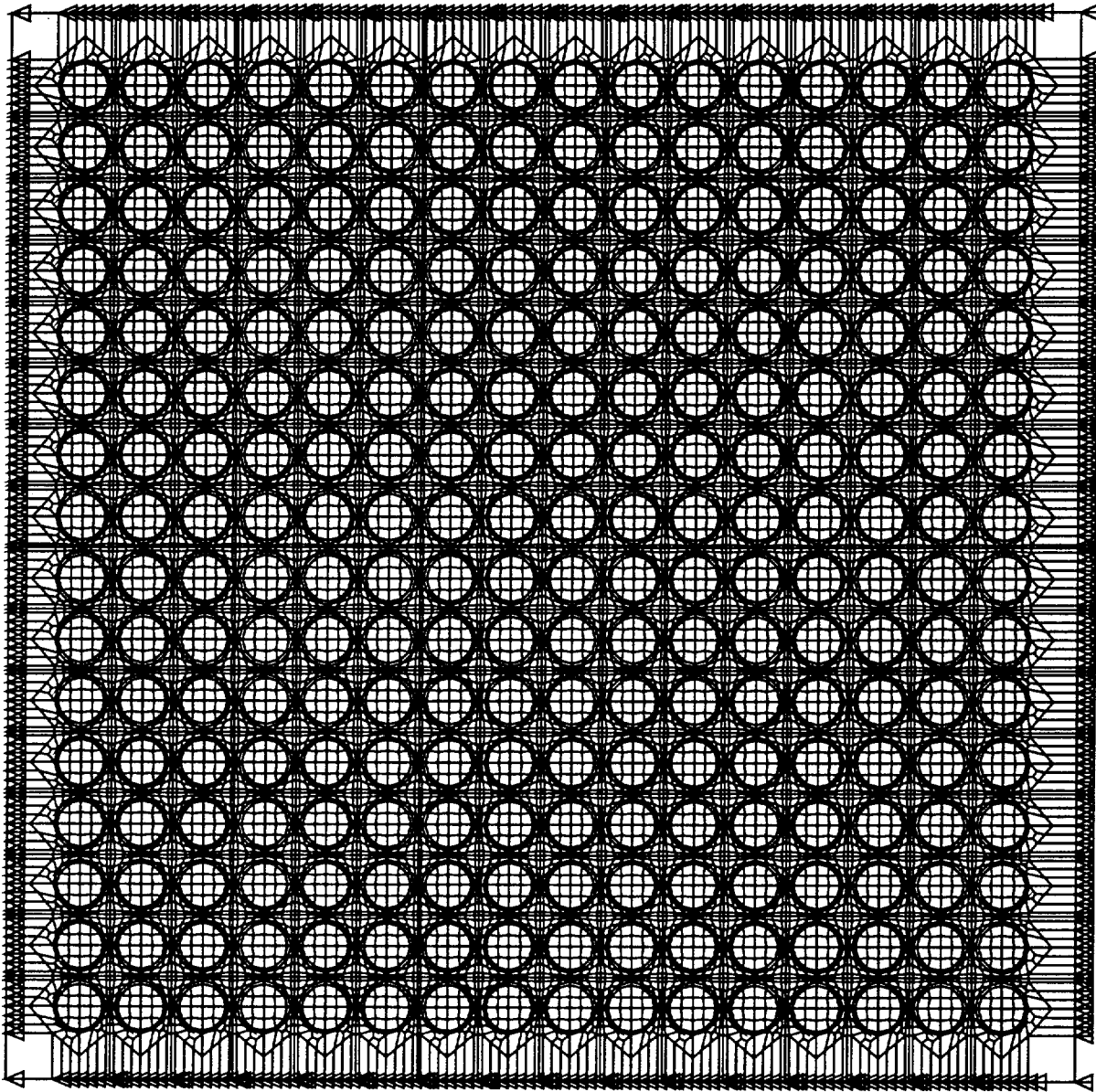
Q = volumetric heat generation rate (Btu/hr-in³)

a = half length of the square cross-section of the fuel (inch)

K_{eff} = effective thermal conductivity for the isotropic homogeneous fuel material (Btu/hr-in-°F)

Volumetric heat generation (Btu/hr-in³) based on the design heat load is applied to the pellets. The effective conductivity is determined based on the heat generated and the temperature difference from the center of the model to the edge of the model. Temperature-dependent effective properties are established by performing multiple analyses using different boundary temperatures. The effective conductivity in the axial direction of the fuel assembly is calculated on the basis of the material area ratio.

Figure 4.4.1.5-1 Two-Dimensional PWR (17x17) Fuel Model



4.4.1.6 Two-Dimensional Fuel Tube Models

The two-dimensional fuel tube model is used to calculate the effective conductivities of the fuel tube wall and BORAL plate. These effective conductivities are used in the three-dimensional canister models (Section 4.4.1.2), the three-dimensional transfer cask and canister models (Section 4.4.1.3) and the three-dimensional periodic canister internal models (Section 4.4.1.4). A total of three models are required: one PWR model and two BWR models (one with the neutron absorber plate, one without the neutron absorber plate), corresponding to the enveloping configurations of the 7×7, 8×8 and 9×9 BWR fuels.

Two forms of the neutron absorber plates are evaluated. The configuration shown in the fuel tube models in Figures 4.4.1.6-1 and 4.4.1.6-2 (for PWR and BWR fuel, respectively) incorporates the BORAL core matrix sandwiched between two layers of aluminum cladding. An alternate design substitutes a single layer of METAMIC for the BORAL. The properties of these materials are presented in Tables 4.2-10 and 4.2-13, respectively. The difference in thermal performance between the two neutron absorber materials is considered to be insignificant, since the primary thermal resistance in the fuel tube design is not the neutron absorber material, but rather the gaps between the fuel tube and the disks.

As shown in Figure 4.4.1.6-1, the PWR model includes the fuel tube, the BORAL plate (including the core matrix sandwiched by aluminum cladding), the stainless steel cladding and the gap between the stainless steel cladding and the support disk or heat transfer disk. Three conditions of media are considered in the gaps: helium, water and a vacuum.

ANSYS PLANE55 conduction elements and LINK31 radiation elements are used to construct the model. The model consists of six layers of conduction elements and two radiation elements (radiation elements are not used for water condition) that are defined at the gaps (two for each gap). The thickness of the model (x-direction) is the distance measured from the outside face of the fuel assembly to the inside face of the slot in the support disk (assuming the fuel tube is centered in the hole in the disk). The tolerance of the neutron absorber plate thickness, 0.003 inch, is used as the gap size between the neutron absorber plate and the stainless steel cladding. The height of the model is defined as equal to the width of the model.

The fuel tubes in the BWR fuel basket differ from those in the PWR fuel basket in that not all sides of the fuel tubes contain neutron absorber. In addition, the BWR fuel assembly is contained in a fuel channel. Therefore, two effective conductivity models are necessary, one fuel tube model with the neutron absorber plate (a total of eight layers of materials) and another fuel tube model with a gap replacing the neutron absorber plate (a total of four layers of materials).

As shown in Figure 4.4.1.6-2, the BWR fuel tube model with neutron absorber includes the fuel channel, the gap between the fuel channel and fuel tube, the fuel tube, the neutron absorber plate (including the core matrix sandwiched by aluminum claddings), and a gap between the stainless steel cladding for the neutron absorber plate and the support disk or heat transfer disk. The effective conductivity of the fuel tube without the neutron absorber plate is determined using the second BWR fuel tube model. As shown in Figure 4.4.1.6-3, this model includes the gap between fuel assembly and the fuel channel, the fuel channel, gap between the fuel channel and stainless steel fuel tube, the fuel tube, and a gap between the fuel tube and the support disk or heat transfer disk. An emissivity value of 0.0001 is conservatively used for the BWR support disk in the model.

Heat flux is applied at the left side of the model (fuel tube for PWR models and fuel channel for BWR models), and the temperature at the right boundary of the model is constrained. The heat flux is determined based on the design heat load. The maximum temperature of the model (at the left boundary) and the temperature difference (ΔT) across the model are calculated by the ANSYS model. The effective conductivity (K_{xx}) is determined using the following formula:

$$q = K_{xx} (A/L) \Delta T$$

or

$$K_{xx} = q L / (A \Delta T)$$

where:

K_{xx} = effective conductivity (Btu/hr-in-^oF) in X direction in Figure 4.4.1.6-1.

q = heat rate (Btu/hr)

A = area (in²)

L = length (thickness) of model (in)

ΔT = temperature difference across the model (^oF)

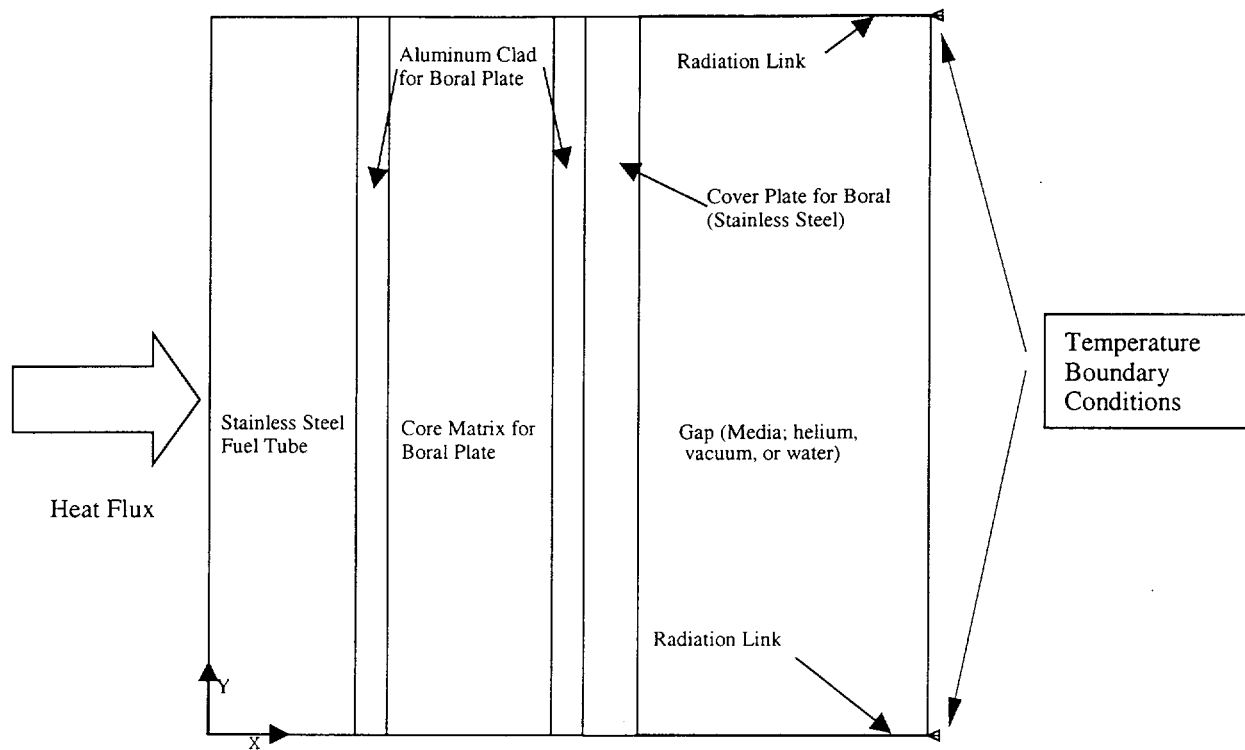
The temperature-dependent conductivity is determined by varying the temperature constraints at one boundary of the model and resolving for the heat rate (q) and temperature difference. The effective conductivity for the parallel path (the Y direction in Figure 4.4.1.6-1) is calculated by:

$$K_{yy} = \frac{\sum K_i t_i}{L}$$

where:

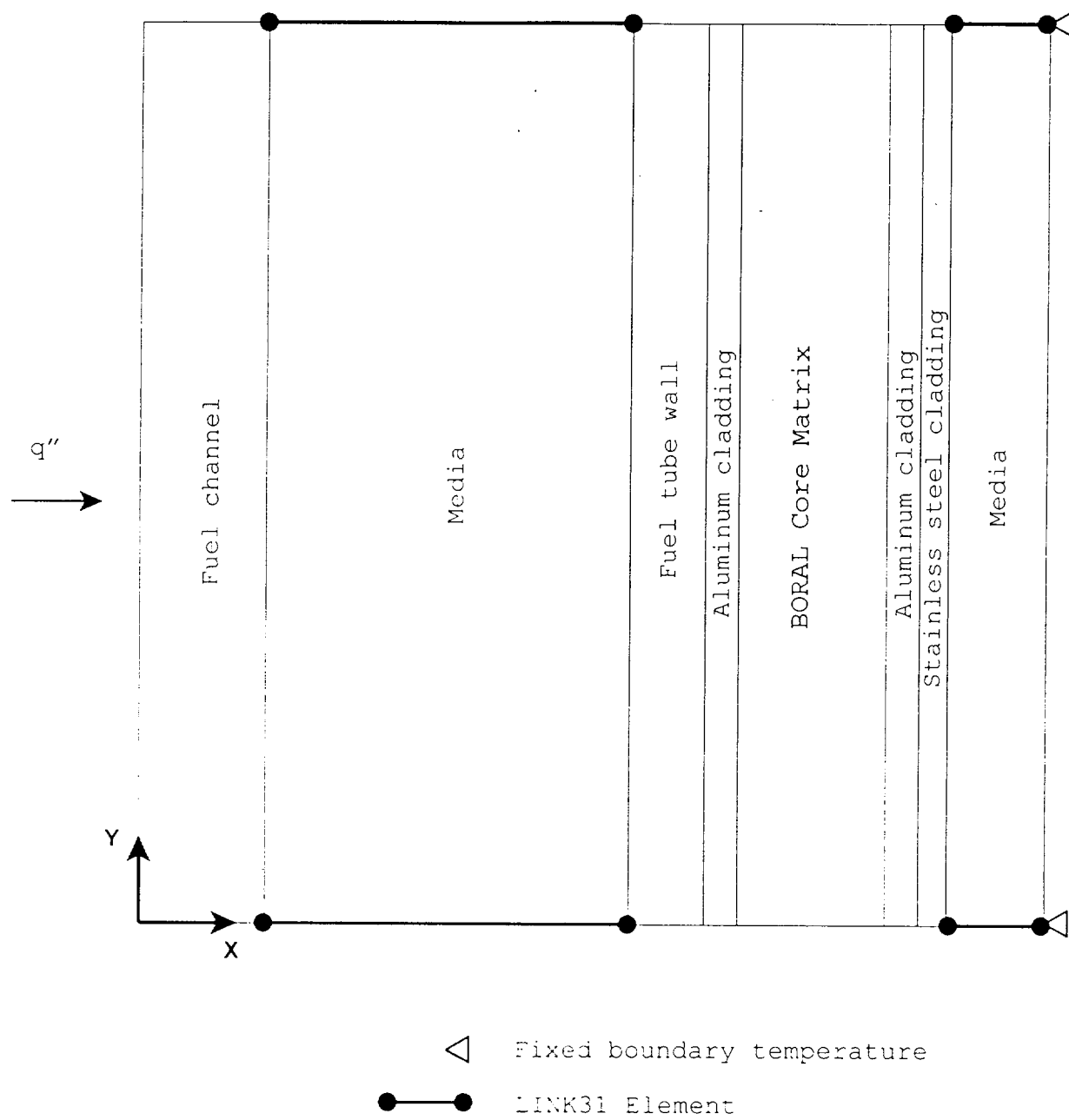
- K_i = thermal conductivity of each layer
- t_i = thickness of each layer
- L = total length (thickness) of the model

Figure 4.4.1.6-1 Two-Dimensional Fuel Tube Model: PWR Fuel



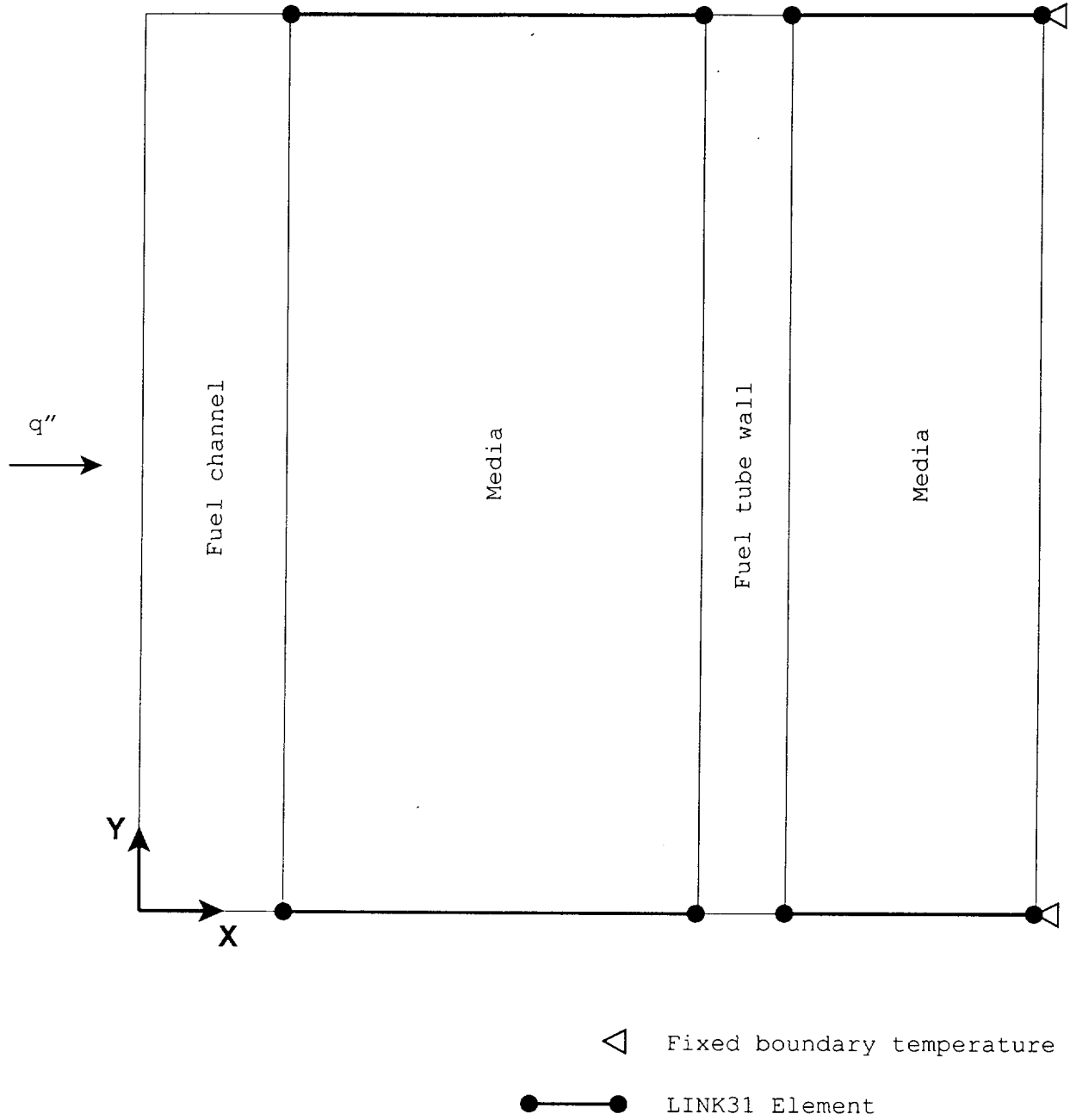
*Media can be water, vacuum, or helium.

Figure 4.4.1.6-2 Two-Dimensional Fuel Tube Model: BWR Fuel Tube with Neutron Absorber



*Media can be water, vacuum, or helium.

Figure 4.4.1.6-3 Two-Dimensional Fuel Tube Model: BWR Fuel Tube without Neutron Absorber



*Media can be water, vacuum, or helium.

4.4.1.7 Two-Dimensional Forced Air Flow Model for Transfer Cask Cooling

A two-dimensional axisymmetric air flow model is used to determine the air flow rate needed to ensure that the maximum temperature of the canister shell and canister components inside the transfer cask do not exceed those presented in Tables 4.4.3-3 and 4.4.3-4 for the helium condition. This air flow model considers a 0.34-inch air annulus between the outer surface of the canister shell and the inner surface of the transfer cask, and has a total length of 191-inches. The fuel canister is cooled by forced convection in the air annulus resulting from air pumped in through fill/drain ports in the body of the transfer cask. The radiation heat transfer between the vertical annulus surfaces (the canister shell outer surface and the transfer cask inner surface) is conservatively neglected. All heat is considered to be removed by the air flow.

ANSYS FLOTTRAN FLUID141 fluid thermal elements are used to construct the two-dimensional axisymmetric air flow finite element model for transfer cask cooling. The model and the boundary conditions applied to the model, are shown in Figures 4.4.1.7-1, 4.4.1.7-2 and 4.4.1.7-3.

As shown in Tables 4.4.3-3 and 4.4.3-4, the temperature margin of the governing component (the heat transfer disk) for the PWR fuel configuration is lower than the margin for the BWR fuel configuration; therefore, the thermal loading for the PWR configuration is used. The non-uniform heat generation applied in the model, shown in Figure 4.4.1.7-4, is based on the axial power distribution shown in Figure 4.4.1.1-3 for PWR fuel.

The inlet air velocity is specified based on the volume flow rate. Room temperature (76°F) is applied to the inlet nodes, while zero air velocity, in both the X and Y directions, is defined as the boundary condition for the vertical solid sides.

Results of the analyses of forced air cooling of the canister inside the transfer cask are shown in Figure 4.4.1.7-5. As shown in the figure, the maximum canister shell temperature is less than 416°F for a forced air flow rate of 275 ft³/minute, or higher, where 416°F is the calculated maximum canister shell temperature for the typical transfer operation for the PWR configuration (Table 4.4.3-3). A forced air volume flow rate of 375 ft³/minute is conservatively specified for cooling the canister in the event that forced air cooling is required. Evaluation of a forced air volume flow rate of 375 ft³/minute, results in a maximum canister shell temperature of 321°F, which is significantly less than the design basis temperature of 416°F.

Figure 4.4.1.7-1 Two-Dimensional Axisymmetric Finite Element Model for Transfer Cask Forced Air Cooling

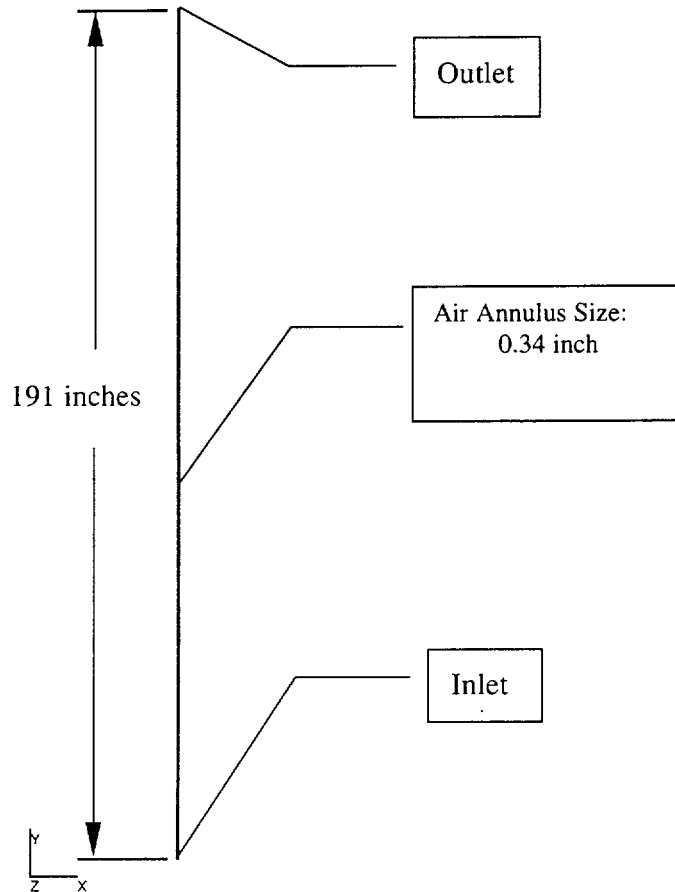


Figure 4.4.1.7-2 Two-Dimensional Axisymmetric Outlet Air Flow Model for Transfer Cask Cooling

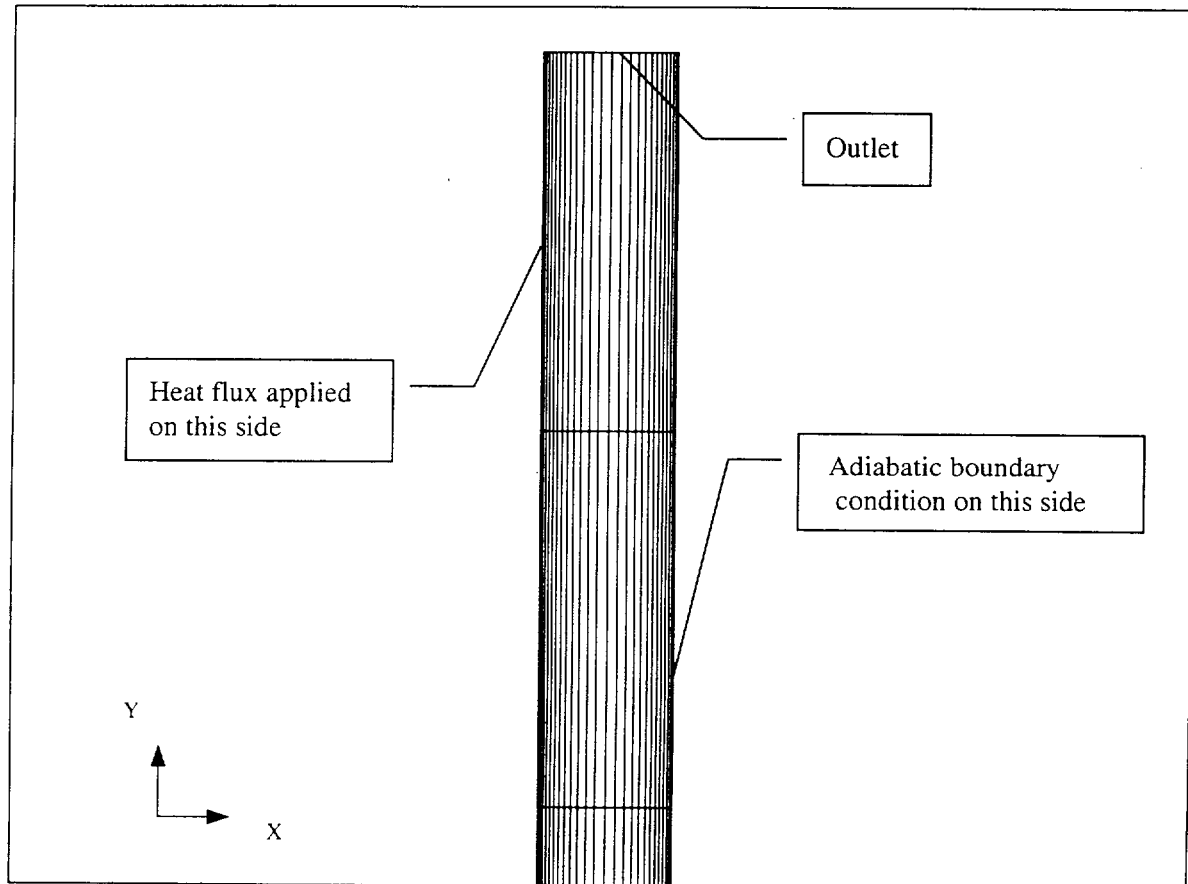


Figure 4.4.1.7-3 Two-Dimensional Axisymmetric Inlet Air Flow Model for Transfer Cask Cooling

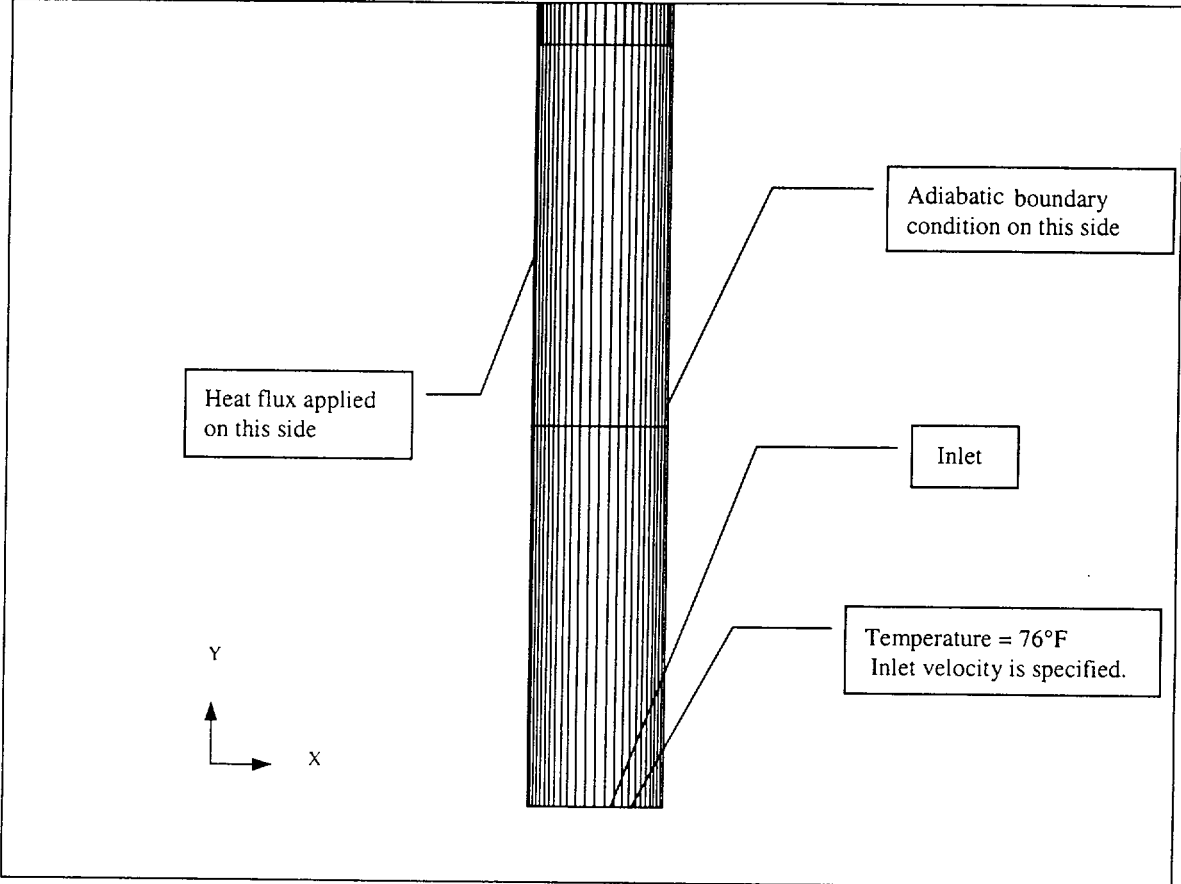


Figure 4.4.1.7-4 Non-Uniform Heat Load from Canister Contents

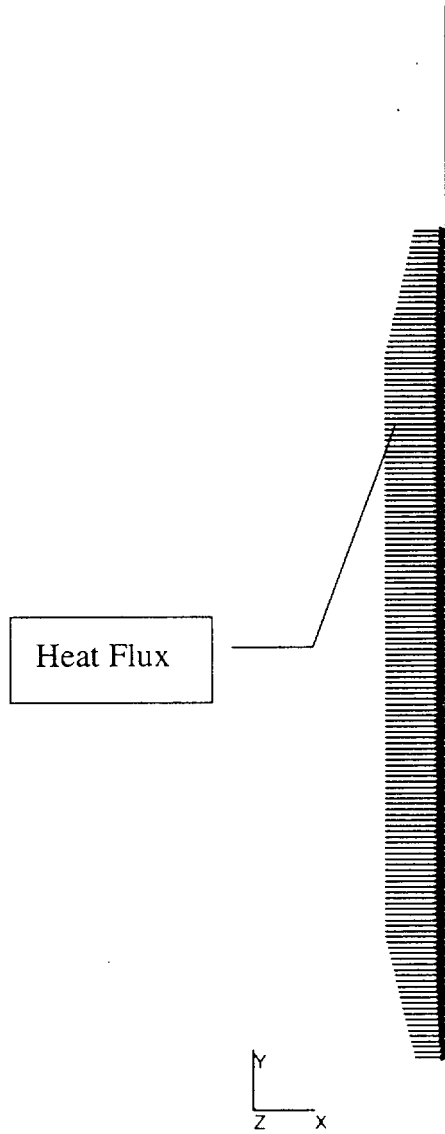
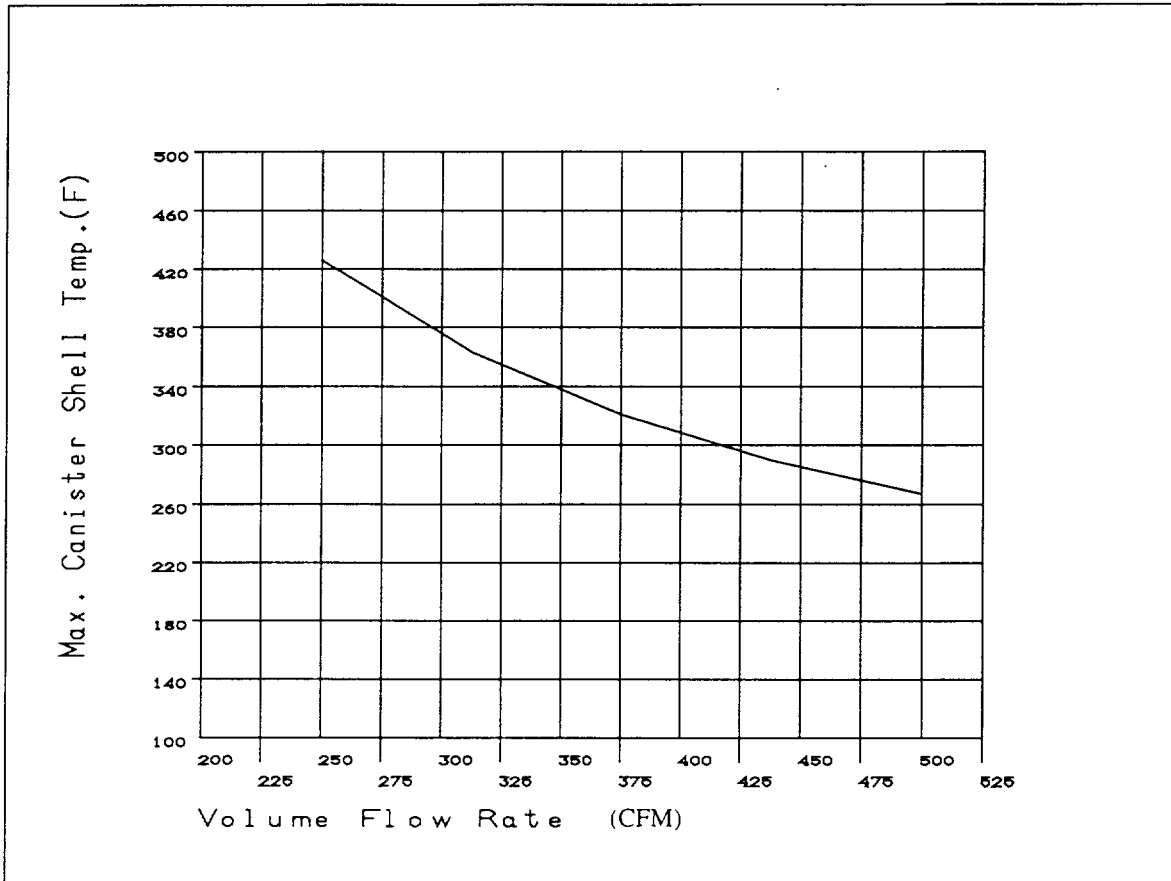


Figure 4.4.1.7-5 Maximum Canister Temperature Versus Air Volume Flow Rate



THIS PAGE INTENTIONALLY LEFT BLANK

4.4.2 Test Model

The Universal Storage System is conservatively designed by analysis. Therefore, no physical model is employed for thermal analysis.

THIS PAGE INTENTIONALLY LEFT BLANK

4.4.3 Maximum Temperatures for PWR and BWR Fuel

Temperature distribution and maximum component temperatures for the Universal Storage System under the normal conditions of storage and transfer, based on the use of the standard transfer cask, are provided in this section. Components of the Universal Storage System containing PWR and BWR fuels are addressed separately. Temperature distributions for the evaluated off-normal and accident conditions are presented in Sections 11.1 and 11.2.

Figure 4.4.3-1 shows the temperature distribution of the Vertical Concrete Cask and the canister containing the PWR design basis fuel for the normal, long-term storage condition. The air flow pattern and air temperatures in the annulus between the PWR canister and the concrete cask liner for the normal condition of storage are shown in Figures 4.4.3-2 and 4.4.3-3, respectively. The temperature distribution in the concrete portion of the concrete cask for the PWR assembly is shown in Figure 4.4.3-4. The temperature distribution for the BWR design basis fuel is similar to that of the PWR fuel and is, therefore, not presented. Table 4.4.3-1 shows the maximum component temperatures for the normal condition of storage for the PWR design basis fuel. The maximum component temperatures for the normal condition of storage for the BWR design basis fuel are shown in Table 4.4.3-2.

As shown in Figure 4.4.3-3, a high-temperature gradient exists near the wall of the canister and the liner of the concrete cask, while the air in the center of the annulus exhibits a much lower temperature gradient, indicating significant boundary layer features of the air flow. The temperatures at the concrete cask steel liner surface are higher than the air temperature, which indicates that salient radiation heat transfer occurs across the annulus. As shown in Figure 4.4.3-4, the local temperature in the concrete, directly affected by the radiation heat transfer across the annulus, can reach 186°F (less than the 200°F allowable temperature). The bulk temperature in the concrete, as determined using volume average of the temperatures in the concrete region, is 135°F, less than the allowable value of 150°F.

Under typical operations, the transient history of maximum component temperatures for the transfer conditions (canister, inside the transfer cask, containing water for 17 hours, vacuum for 32 hours for PWR and 25 hours for BWR and for steady state condition (unlimited time) helium for PWR and 16 hours in helium for BWR) is shown in Figures 4.4.3-5 and 4.4.3-6 for PWR and BWR fuels, respectively. The maximum component temperatures for the transfer conditions (vacuum and helium conditions) are shown in Tables 4.4.3-3 and 4.4.3-4, for PWR and BWR

fuels, respectively. The maximum calculated water temperature is 204°F and 203°F for PWR and BWR fuels, respectively, at the end of 17 hours based on an initial water temperature of 100°F. Using the three-dimensional transfer cask and canister models as described in Section 4.4.1.3, the thermal transient analysis is performed for the 100-ton transfer cask in the horizontal position. The maximum temperatures for the fuel cladding and heat transfer disk are calculated to be 761°F and 701°F, respectively. These temperatures are below the results for the vertical configuration due to contact between components. However, the maximum temperature difference between the center and the edge of the support disk increased from 388°F to 394°F. This temperature remains bounded by the ΔT (425°F) used in Section 3.4.4.1.8.1 for the thermal stress evaluation for the PWR support disk. Based on the results for the PWR configuration, it is expected that the maximum ΔT for the BWR support disk for the 100-ton transfer cask in the horizontal position will remain bounded by the ΔT (400°F) used in Section 3.4.4.1.8.2 for the thermal stress evaluation for the BWR support disk. Note that the maximum ΔT for the BWR support disk for the 100-ton transfer cask in the vertical position is 356°F, which is well below 400°F.

4.4.3.1 Maximum Temperatures at Reduced Total Heat Loads

This section provides the evaluation of component temperatures for fuel heat loads less than the design basis heat load of 23 kW. Transient thermal analyses are performed for PWR fuel heat loads of 20, 17.6, 14, 11 and 8 kW to establish the allowable time limits for the vacuum condition in the canister as described in the Technical Specifications (Chapter 12) for the Limiting Conditions of Operation (LCO), LCOs 3.1.1 and 3.1.4. The time limits ensure that the allowable temperatures of the limiting components – the heat transfer disks and the fuel cladding – are not exceeded. A steady state evaluation is also performed for heat loads of 11 kW and 8 kW in the vacuum condition and all heat load cases in the helium condition. If the steady state temperature calculated is less than the limiting component allowable temperature, then the allowable time duration in the vacuum or helium conditions is not limited.

The three-dimensional transfer cask and canister model for the PWR fuel configuration, described in Section 4.4.1.3, is used for the transient and steady state thermal analysis for the reduced heat load cases. To obtain the bounding temperatures for all possible loading configurations, thermal analyses are performed for a total of fourteen (14) cases as tabulated below. The basket locations are shown in Figure 4.4.3-7. Since the maximum temperature for the limiting components (fuel cladding and heat transfer disk) always occurs at the central region

of the basket, hotter fuels (maximum allowable heat load for 5-year cooled fuel: 0.958 kW = 23 kW/24) are specified at the central basket locations. The bounding cases for each heat load condition are noted with an asterisk (*) in the tabulation which follows. Six cases (cases 3 through 8) are evaluated for the 17.6 kW heat load condition. The first four cases (cases 3 through 6) represent standard UMS system fuel loadings. The remaining two cases (cases 7 and 8) account for the preferential loading configuration for Maine Yankee site specific high burnup fuel (Section 4.5.1.2.2), with case 8 being the bounding case for the Maine Yankee high burnup fuel. Based on the analysis results of the 17.6 kW heat load cases, only two loading cases are required to establish the bounding condition for the 20, 14, 11 and 8 kW heat loads.

| Canister Heat Load (kW) | Heat Load Case | Heat Load (kW) Evaluated in Each Basket Location (See Figure 4.4.3-7) | | | | | |
|-------------------------|----------------|---|-------|-------|-------|-------|-------|
| | | 1 | 2 | 3 | 4 | 5 | 6 |
| 20 | 1 | 0.958 | 0.958 | 0.709 | 0.958 | 0.709 | 0.709 |
| 20* | 2 | 0.958 | 0.958 | 0.958 | 0.958 | 0.958 | 0.210 |
| 17.6 | 3 | 0.958 | 0.958 | 0.509 | 0.958 | 0.509 | 0.509 |
| 17.6* | 4 | 0.958 | 0.958 | 0.568 | 0.958 | 0.958 | 0.000 |
| 17.6 | 5 | 0.958 | 0.958 | 0.958 | 0.958 | 0.568 | 0.000 |
| 17.6 | 6 | 0.958 | 0.958 | 0.284 | 0.958 | 0.958 | 0.284 |
| 17.6 | 7 | 0.958 | 0.146 | 1.050 | 0.146 | 1.050 | 1.050 |
| 17.6 | 8 | 0.958 | 0.958 | 1.050 | 0.384 | 1.050 | 0.000 |
| 14 | 9 | 0.958 | 0.958 | 0.209 | 0.958 | 0.209 | 0.209 |
| 14* | 10 | 0.958 | 0.958 | 0.000 | 0.958 | 0.626 | 0.000 |
| 11 | 11 | 0.958 | 0.896 | 0.000 | 0.896 | 0.000 | 0.000 |
| 11* | 12 | 0.958 | 0.958 | 0.000 | 0.834 | 0.000 | 0.000 |
| 8 | 13 | 0.958 | 0.521 | 0.000 | 0.521 | 0.000 | 0.000 |
| 8* | 14 | 0.958 | 0.958 | 0.000 | 0.084 | 0.000 | 0.000 |

The heat load (23 kW/24 Assemblies = 0.958 kW) at the four (4) central basket locations corresponds to the maximum allowable canister heat load for 5-year cooled fuel (Table 4.4.7-8). The non-uniform heat loads evaluated in this section bound the equivalent uniform heat loads, since they result in higher maximum temperatures of the fuel cladding and heat transfer disk.

Volumetric heat generation (Btu/hr-in³) is applied to the active fuel region in each fuel assembly location of the model using the axial power distribution for PWR fuel (Figure 4.4.1.1-3) in the axial direction.

The thermal analysis results for the closure and transfer of a loaded PWR fuel canister in the transfer cask for the reduced heat load cases are shown in Table 4.4.3-5, with a comparison to the results for the design basis heat load case. The temperatures shown are the maximum

temperatures for the limiting components (fuel cladding and heat transfer disk). The maximum temperatures of the fuel cladding and the heat transfer disk are less than the allowable temperatures (Table 4.1-3) of these components for the short-term conditions of vacuum drying and helium backfill. As shown in Table 4.4.3-5, there is no time limit for movement of the canister out of the transfer cask for all the heat load cases, after the canister is filled with helium. For all heat load cases, the maximum fuel cladding/heat transfer disk temperatures for the steady state condition are below the short-term allowable temperatures of the fuel cladding and the heat transfer disk. Similarly, there is no time limit for the vacuum stage for the heat load cases at or below 11 kW. Note that the maximum water temperature at the end of the "water period" is considered to be the volumetric average temperature of the calculated cladding temperatures in the active fuel region of the hottest fuel assembly. The results indicate that the volumetric average water temperature is below 212°F for all cases evaluated. This is consistent with the thermal model that only considers conduction in the fuel assembly region and between the disks. This approach does not include consideration of convection of the water or the energy absorbed by latent heat of vaporization.

The Technical Specifications specify the remedial actions, either in-pool or forced air cooling, required to ensure that the fuel cladding and basket component temperatures do not exceed their short-term allowable temperatures, if the time limits are not met. LCOs 3.1.1 and 3.1.4 incorporate the operating times for heat loads that are less than the design basis heat loads as evaluated in this section.

Using the same three-dimensional transfer cask/canister models, analysis is performed for the conditions of in-pool cooling and forced air cooling followed by the vacuum drying and helium backfill operation (LCO 3.1.1). The conditions at the end of the vacuum drying as shown in Tables 4.4.3-5 (PWR) and 4.4.3-8 (BWR) are used as the initial conditions of the analyses. The LCO 3.1.1 "Action" analysis results are shown in Tables 4.4.3-6 and 4.4.3-7 for the PWR configuration and Tables 4.4.3-9 and 4.4.3-10 for the BWR configuration. Note that the duration of the second vacuum (after completion of the in-pool or forced air cooling) is limited (calculated based on the heat-up rate of the first vacuum), so the maximum temperatures at the end of the second vacuum cycle will not exceed those at the end of the first vacuum cycle. The maximum temperatures at the end of the first vacuum (Table 4.4.3-5 for PWR and Table 4.4.3-8 for BWR) are conservatively presented as the maximum temperatures for the second vacuum condition. The maximum temperatures for the fuel cladding and the heat transfer disk are below the short-term allowable temperatures.

The in-pool cooling and the forced-air cooling followed by the helium backfill operation in LCO 3.1.4 are also evaluated for the BWR configuration for 23 kW and 20 kW cases. The condition at the end of the helium condition, as shown in Table 4.4.3-8, is used as the initial condition. The results are shown in Tables 4.4.3-11 and 4.4.3-12 for the in-pool cooling and forced-air cooling, respectively. Note that the time limit for the first helium backfill condition is used for second helium backfill condition (after completion of the in-pool or forced air cooling). Based on the heat-up rate of the first helium condition, the maximum component temperatures at the end of the second helium are well below the maximum temperatures at the end of the first helium condition. The maximum temperatures at the end of the first helium (Table 4.4.3-8) are conservatively presented as the maximum temperatures for the second helium backfill condition, as shown in Tables 4.4.3-11 and 4.4.3-12.

Figure 4.4.3-1 Temperature Distribution (°F) for the Normal Storage Condition:
PWR Fuel

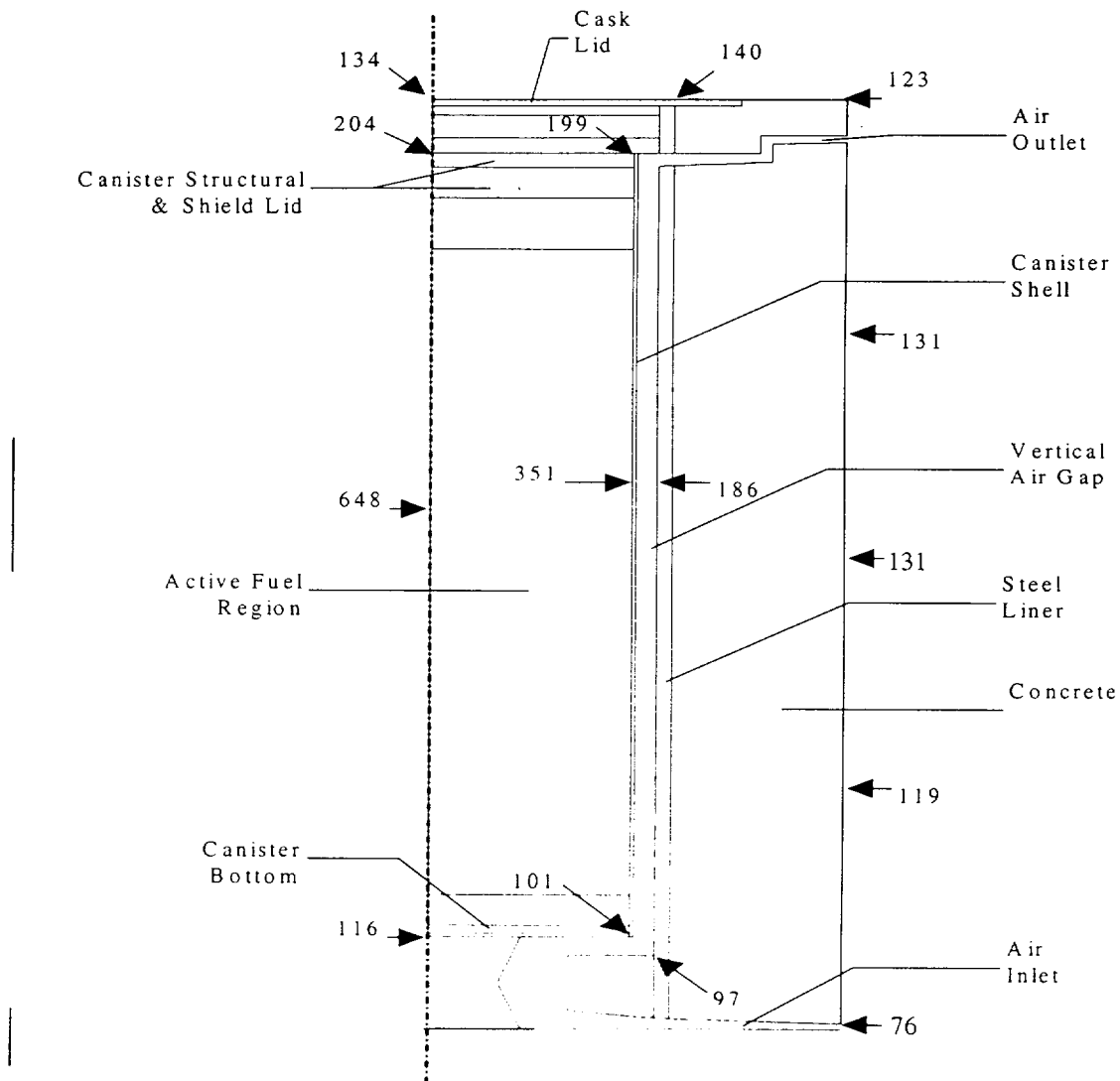


Figure 4.4.3-2 Air Flow Pattern in the Concrete Cask in the Normal Storage Condition:
PWR Fuel

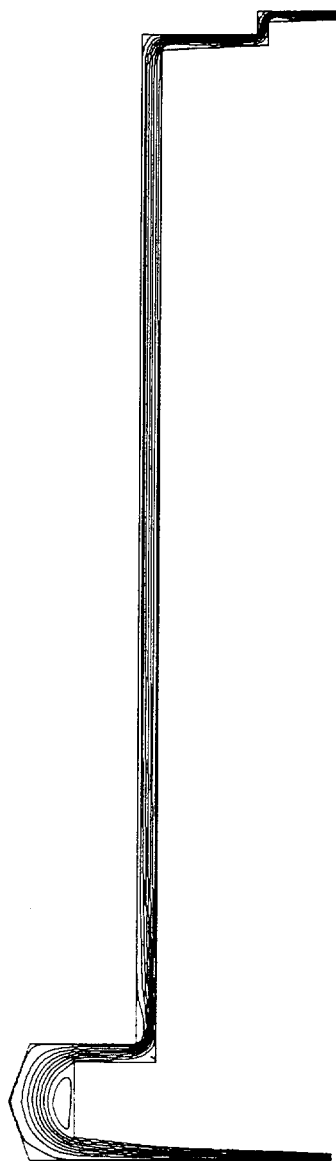


Figure 4.4.3-3 Air Temperature (°F) Distribution in the Concrete Cask During the Normal Storage Condition: PWR Fuel

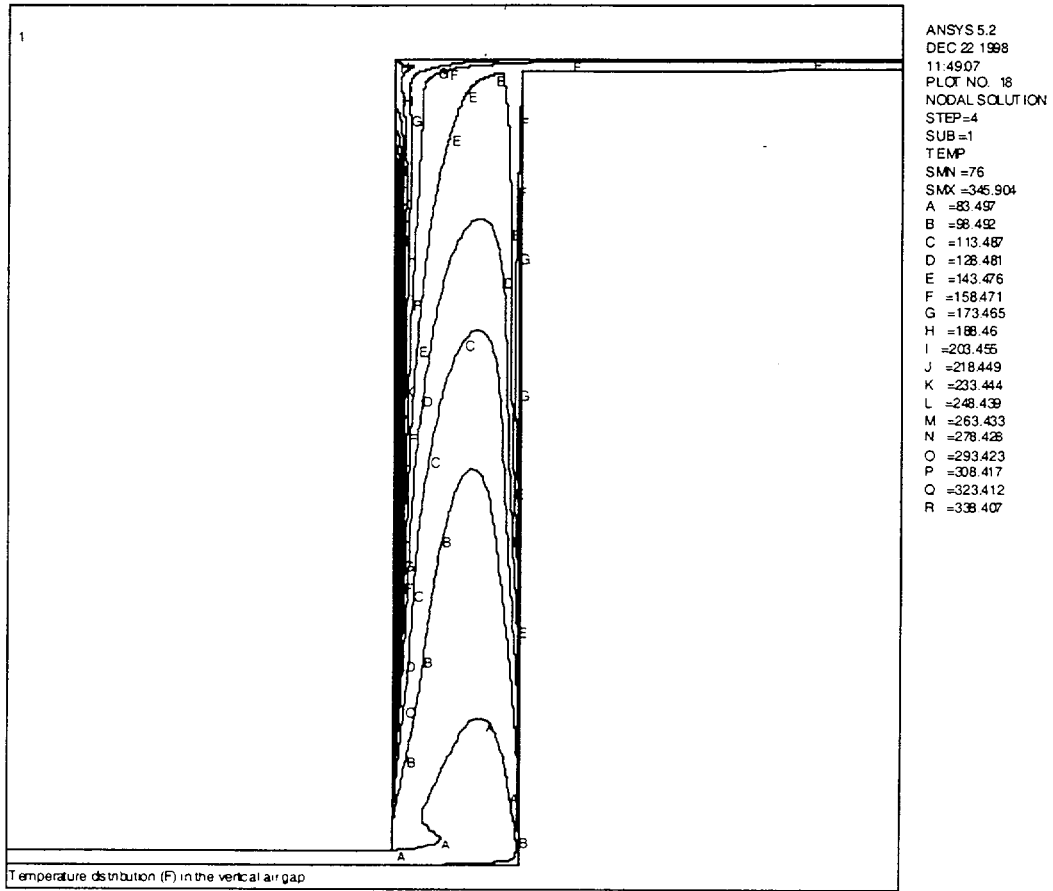


Figure 4.4.3-4 Concrete Temperature (°F) Distribution During the Normal Storage
Condition: PWR Fuel

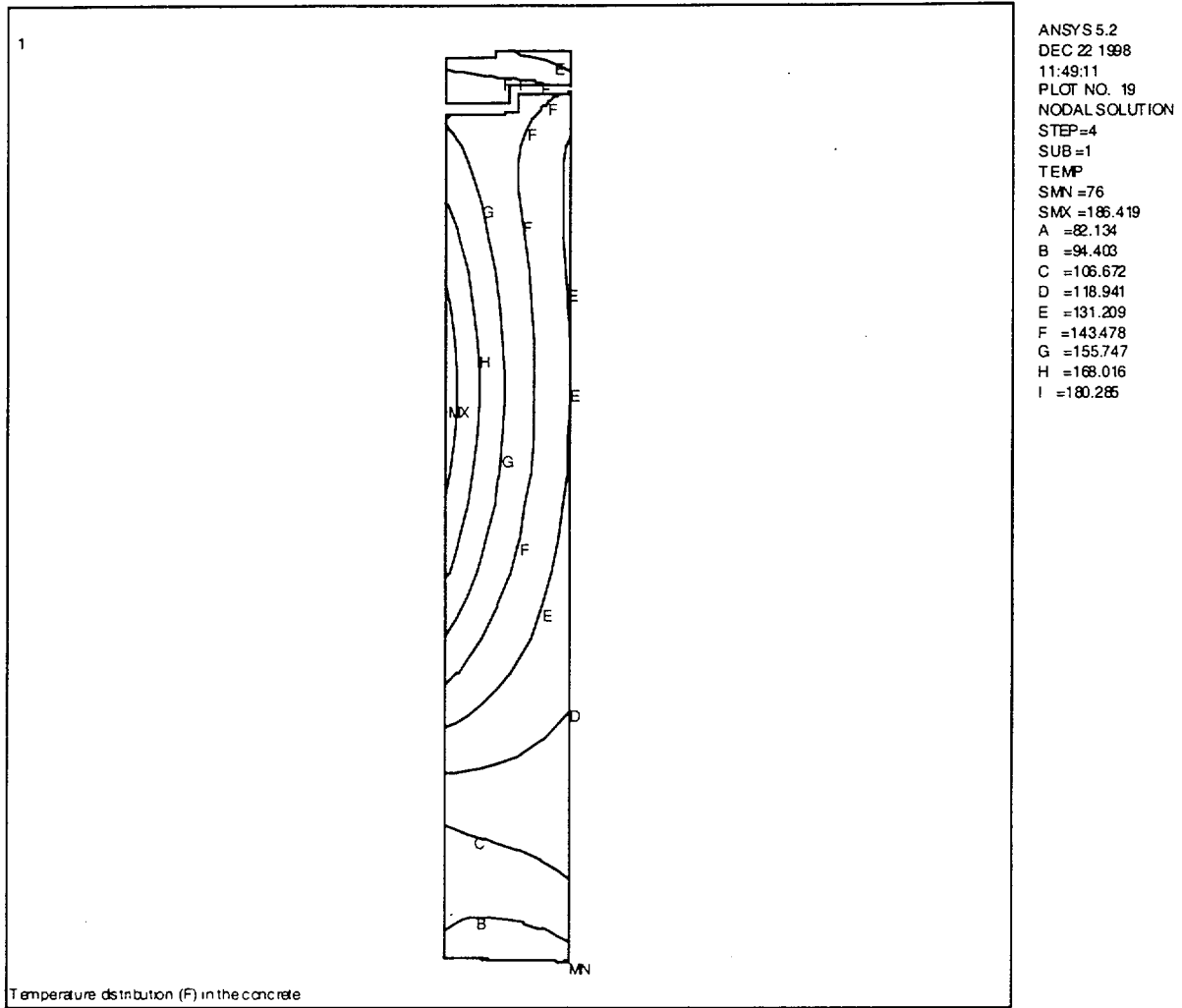
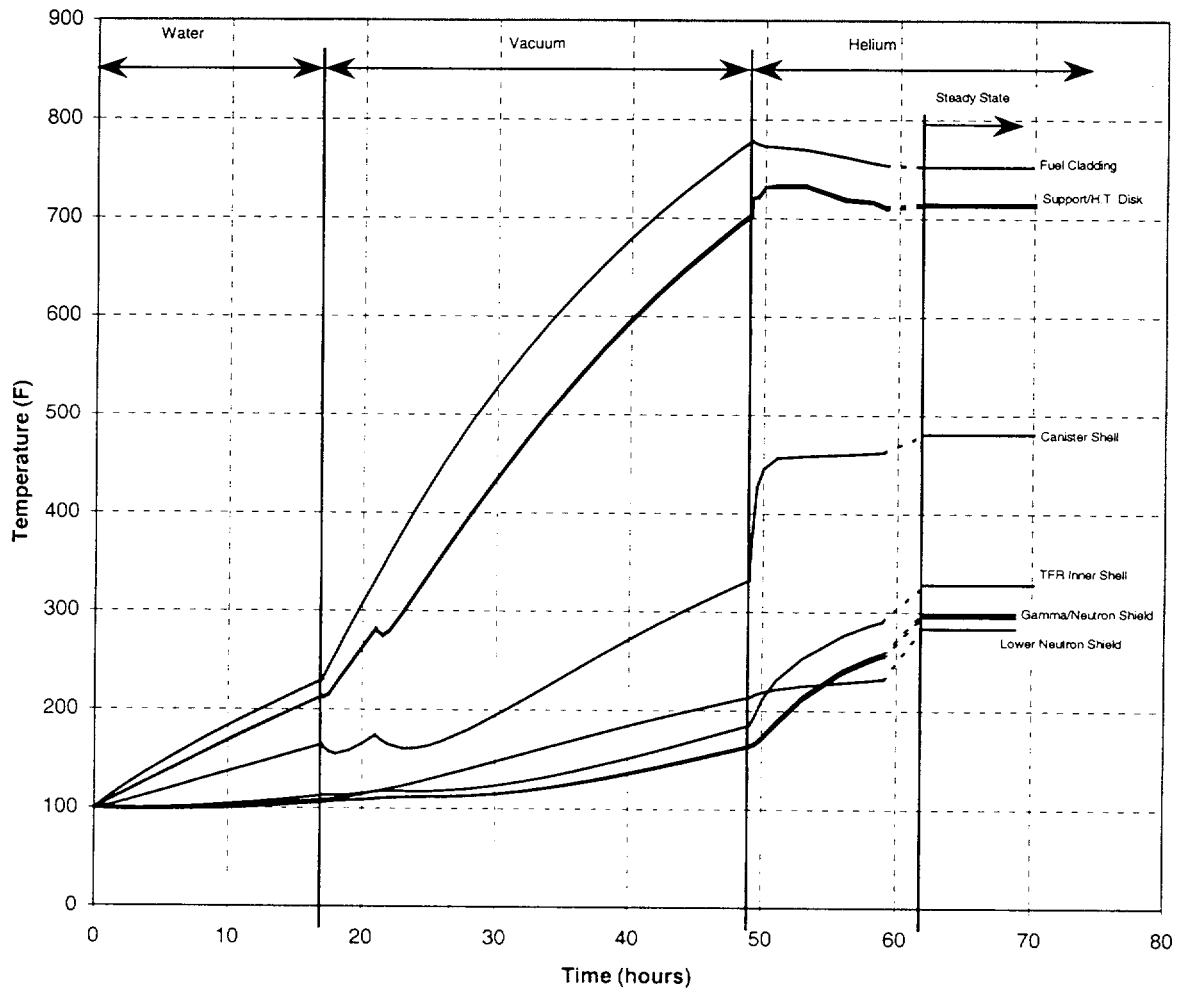


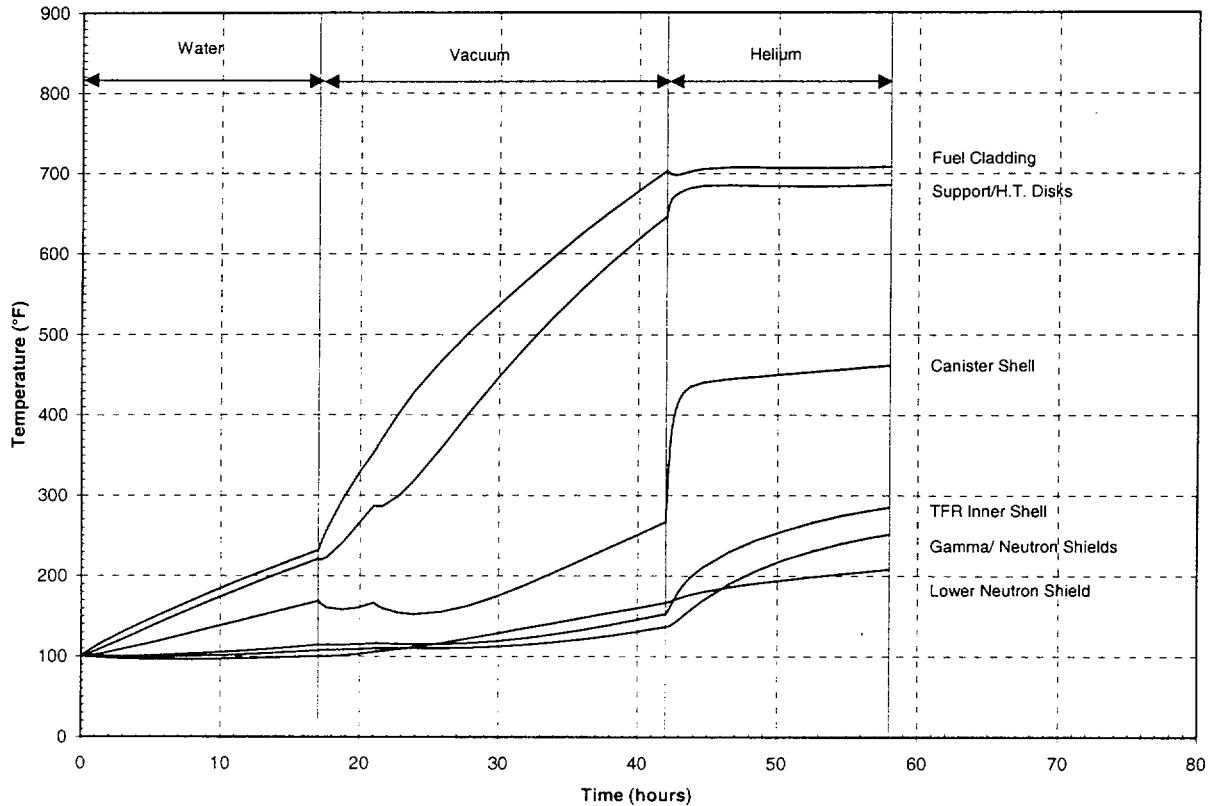
Figure 4.4.3-5 History of Maximum Component Temperature (°F) for Transfer Conditions for PWR Fuel with Design Basis 23 kW Uniformly Distributed Heat Load



Notes:

1. This graph corresponds to a canister containing water for 17 hours, vacuum for 32 hours and with an unlimited time in the helium condition. The results correspond to a uniformly distributed decay heat load of 23 kW.
2. "TFR" refers to the standard transfer cask.

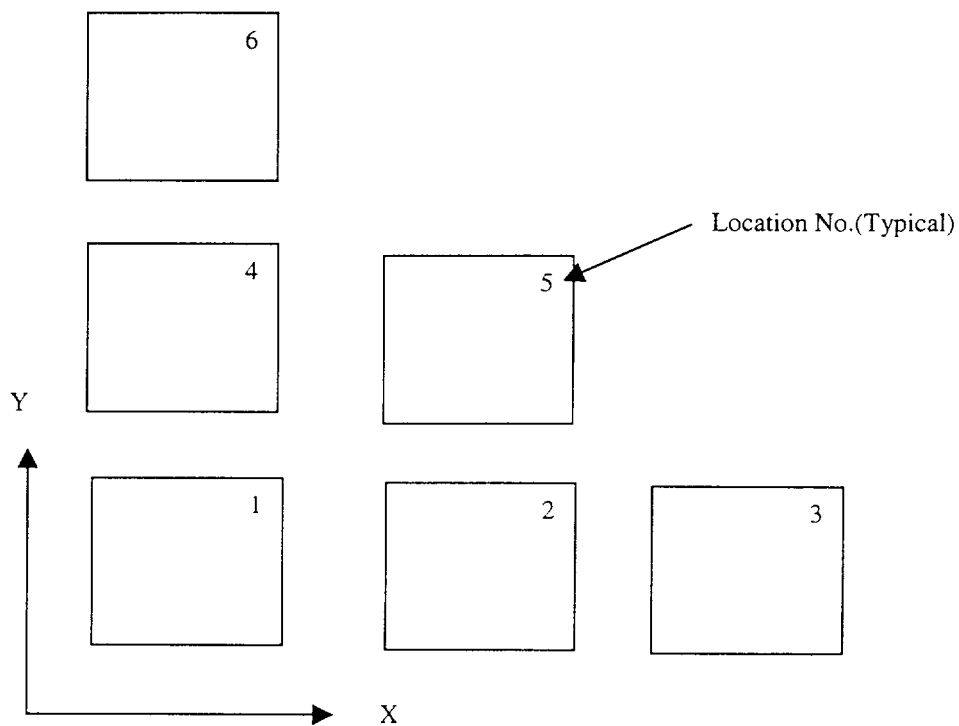
Figure 4.4.3-6 History of Maximum Component Temperature (°F) for Transfer Conditions for BWR Fuel with Design Basis 23 kW Uniformly Distributed Heat Load



Notes:

1. This graph corresponds to a canister containing water for 17 hours, vacuum for 25 hours and 16 hours in the helium condition. The results correspond to a uniformly distributed decay heat load of 23 kW.
2. "TFR" refers to the standard transfer cask.

Figure 4.4.3-7 Basket Location for the Thermal Analysis of PWR Reduced Heat Load Cases



A quarter symmetry configuration is considered. X and Y axes are at the centerlines of the basket.

Figure 4.4.3-8 BWR Fuel Basket Location Numbers

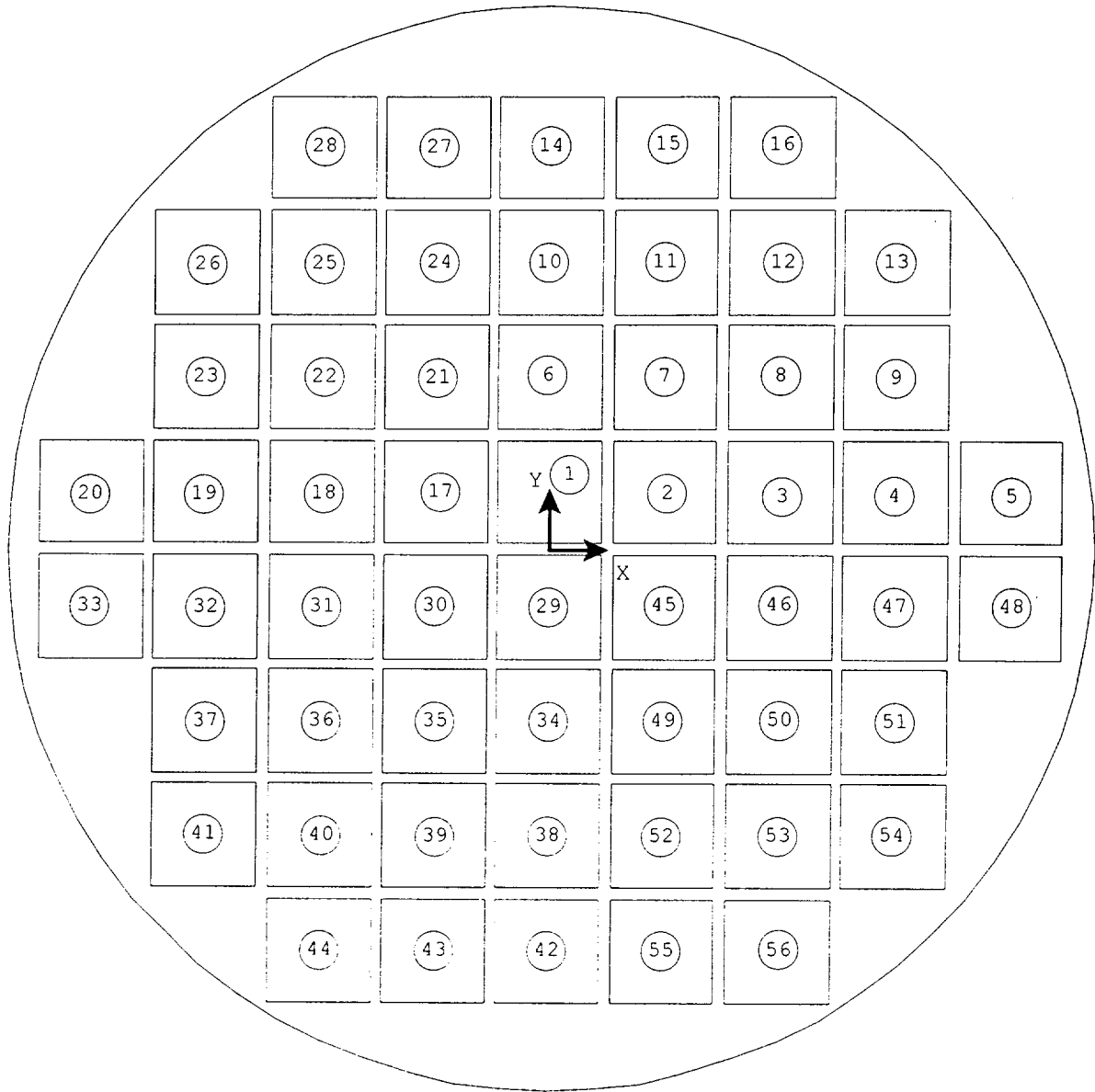


Table 4.4.3-1 Maximum Component Temperatures for the Normal Storage Condition - PWR

| Component | Maximum Temperature (°F) | Allowable Temperatures (°F) |
|-------------------------|-------------------------------------|--|
| Fuel Cladding | 648 | 716 |
| Heat Transfer Disk | 599 | 650 |
| Support Disk | 601 | 650 |
| Top Weldment | 399 | 800 |
| Bottom Weldment | 159 | 800 |
| Canister Shell | 351 | 800 |
| Canister Structural Lid | 204 | 800 |
| Canister Shield Lid | 212 | 800 |
| Concrete | 186 (local) 135 (bulk*) | 300 (local) 150 (bulk) |

* The volume average temperature of the concrete region is used as the bulk concrete temperature.

Table 4.4.3-2 Maximum Component Temperatures for the Normal Storage Condition - BWR

| Component | Maximum Temperature (°F) | Allowable Temperatures (°F) |
|-------------------------|-------------------------------------|--|
| Fuel Cladding | 642 | 716 |
| Heat Transfer Disk | 612 | 650 |
| Support Disk | 614 | 700 |
| Top Weldment | 361 | 800 |
| Bottom Weldment | 276 | 800 |
| Canister Shell | 376 | 800 |
| Canister Structural Lid | 180 | 800 |
| Canister Shield Lid | 185 | 800 |
| Concrete | 192 (local) 136 (bulk*) | 300 (local) 150 (bulk) |

*The volume average temperature of the concrete region is used as the bulk concrete temperature.

Table 4.4.3-3 Maximum Component Temperatures for the Transfer Condition – PWR Fuel with Design Basis 23 kW Uniformly Distributed Heat Load

| Component | Maximum Temperature (°F) | | Allowable Temperature (°F) |
|----------------------|--------------------------|---------------------|----------------------------|
| | Vacuum ¹ | Helium ¹ | |
| Fuel | 779 | 779 | 1058 |
| Lead | 165 | 299 | 600 |
| Neutron Shield | 213 | 295 | 300 |
| Heat Transfer Disk | 702 | 732 | 750 |
| Support Disk | 705 | 734 | 800 |
| Canister | 332 | 481 | 800 |
| Transfer Cask Shells | 185 | 328 | 700 |

1. See Figure 4.4.3-5 for history of maximum component temperatures.

Table 4.4.3-4 Maximum Component Temperatures for the Transfer Condition – BWR Fuel with Design Basis 23 kW Uniformly Distributed Heat Load

| Component | Maximum Temperature (°F) | | Allowable Temperature (°F) |
|----------------------|--------------------------|---------------------|----------------------------|
| | Vacuum ¹ | Helium ¹ | |
| Fuel | 703 | 708 | 1058 |
| Lead | 137 | 252 | 600 |
| Neutron Shield | 135 | 249 | 300 |
| Heat Transfer Disk | 645 | 683 | 750 |
| Support Disk | 646 | 686 | 700 |
| Canister | 267 | 462 | 800 |
| Transfer Cask Shells | 153 | 286 | 700 |

1. See Figure 4.4.3-6 for history of maximum component temperatures.

Table 4.4.3-5 Maximum Limiting Component Temperatures in Transient Operations for the Reduced Heat Load Cases for PWR Fuel

| Heat Load (kW) | Water | | | Vacuum | | | Helium | | |
|-------------------|------------------|--------------------------|--------------------|------------------|--------------------------|--------------------|------------------|---|--------------------|
| | Duration (hours) | Maximum Temperature (°F) | | Duration (hours) | Maximum Temperature (°F) | | Duration (hours) | Max. Temp. / Temp. at Steady-state (°F) | |
| | | Fuel | Heat Transfer Disk | | Fuel | Heat Transfer Disk | | Fuel | Heat Transfer Disk |
| 23.0 | 17 | 230 | 213 | 32 | 779 | 702 | No Limit | 779/752 | 732/713 |
| 20.0 | 18 | 232 | 214 | 37 | 785 | 695 | No Limit | 785/707 | 723/664 |
| 17.6 | 20 | 239 | 219 | 44 | 797 | 697 | No Limit | 797/672 | 725/625 |
| 17.6 ¹ | 20 | 232 | 214 | 44 | 783 | 684 | No Limit | 783/658 | 703/611 |
| 14.0 | 22 | 240 | 219 | 68 | 811 | 700 | No Limit | 811/613 | 724/560 |
| 11.0 | 24 | 237 | 215 | No Limit | 822 | 702 | No Limit | 822/555 | 727/496 |
| 8.0 | 26 | 224 | 199 | No Limit | 751 | 588 | No Limit | 751/484 | 622/413 |

1. Preferential loading configuration 2, site specific case for Maine Yankee.

Table 4.4.3-6 Maximum Limiting Component Temperatures in Transient Operations for PWR Fuel after In-Pool Cooling

| Heat Load (kW) | In-Pool (helium) | | | Vacuum | | | Helium | | |
|----------------|------------------|----------------------|--------------------|-------------------------------|---------------------------------------|--------------------|------------------|---|--------------------|
| | Duration (hours) | End Temperature (°F) | | Duration ¹ (hours) | Maximum Temperature (°F) ² | | Duration (hours) | Max. Temp. / Temp. at Steady-state (°F) | |
| | | Fuel | Heat Transfer Disk | | Fuel | Heat Transfer Disk | | Fuel | Heat Transfer Disk |
| 23.0 | 24 | 507 | 434 | 19 | 779 | 702 | No Limit | 779/752 | 732/713 |
| 20.0 | 24 | 489 | 407 | 26 | 785 | 695 | No Limit | 785/707 | 723/664 |
| 17.6 | 24 | 481 | 400 | 33 | 797 | 697 | No Limit | 797/672 | 725/625 |
| 14.0 | 24 | 468 | 385 | 61 | 811 | 700 | No Limit | 811/613 | 724/560 |

1. The maximum allowable time in the Technical Specification for this condition is equal to 2 hours less than the maximum allowable time shown in this table. This 2-hour reduction allows the handling time required to enter the next stage.
2. The maximum temperatures at the end of the first vacuum (Table 4.4.3-5) are conservatively presented.

Table 4.4.3-7 Maximum Limiting Component Temperatures in Transient Operations for PWR Fuel after Forced-Air Cooling

| Heat Load (kW) | Forced-Air (helium) | | | Vacuum | | | Helium | | |
|----------------|---------------------|----------------------|--------------------|-------------------------------|--------------------------|--------------------|------------------|---|--------------------|
| | Duration (hours) | End Temperature (°F) | | Duration ¹ (hours) | Maximum Temperature (°F) | | Duration (hours) | Max. Temp. / Temp. at Steady-state (°F) | |
| | | Fuel | Heat Transfer Disk | | Fuel | Heat Transfer Disk | | Fuel | Heat Transfer Disk |
| 23.0 | 24 | 648 | 594 | 9 | 779 | 702 | No Limit | 779/752 | 732/713 |
| 20.0 | 24 | 619 | 558 | 14 | 785 | 695 | No Limit | 785/707 | 723/664 |
| 17.6 | 24 | 600 | 544 | 21 | 797 | 697 | No Limit | 797/672 | 725/625 |
| 14.0 | 24 | 572 | 506 | 45 | 811 | 700 | No Limit | 811/613 | 724/560 |

1. The maximum allowable time in the Technical Specification for this condition is equal to 2 hours less than the maximum allowable time shown in this table. This 2-hour reduction allows the handling time required to enter the next stage.
2. The maximum temperatures at the end of the first vacuum (Table 4.4.3-5) are conservatively presented.

Table 4.4.3-8 Maximum Limiting Component Temperatures in Transient Operations for BWR Fuel

| Heat Load (kW) | Water | | | Vacuum | | | Helium | | |
|----------------|------------------|--------------------------|--------------------|------------------|--------------------------|--------------------|------------------|---|--------------------|
| | Duration (hours) | Maximum Temperature (°F) | | Duration (hours) | Maximum Temperature (°F) | | Duration (hours) | Max. Temp. / Temp. at Steady-state (°F) | |
| | | Fuel | Heat Transfer Disk | | Fuel | Heat Transfer Disk | | Fuel | Heat Transfer Disk |
| 23 | 17 | 232 | 221 | 25 | 703 | 645 | 16 | 708 | 683 |
| 20 | 18 | 234 | 222 | 27 | 694 | 627 | 30 | 694 | 661 |
| 17 | 19 | 234 | 221 | 33 | 701 | 629 | No Limit | 701/660 | 659/631 |
| 14 | 20 | 232 | 219 | 45 | 719 | 643 | No Limit | 719/606 | 671/574 |
| 11 | 23 | 234 | 220 | 72 | 733 | 653 | No Limit | 733/543 | 679/508 |
| 8 | 31 | 236 | 220 | No Limit | 724 | 639 | No Limit | 724/467 | 639/427 |

Table 4.4.3-9 Maximum Limiting Component Temperatures in Transient Operations after Vacuum for BWR Fuel after In-Pool Cooling

| Heat Load (kW) | In-Pool (helium) | | | Vacuum | | | Helium | | |
|----------------|------------------|----------------------|--------------------|-------------------------------|--------------------------|--------------------|------------------|---|--------------------|
| | Duration (hours) | End Temperature (°F) | | Duration ¹ (hours) | Maximum Temperature (°F) | | Duration (hours) | Max. Temp. / Temp. at Steady-state (°F) | |
| | | Fuel | Heat Transfer Disk | | Fuel | Heat Transfer Disk | | Fuel | Heat Transfer Disk |
| 23 | 24 | 488 | 444 | 12 | 703 | 645 | 16 | 708 | 683 |
| 20 | 24 | 476 | 431 | 13 | 694 | 627 | 30 | 694 | 661 |
| 17 | 24 | 467 | 419 | 19 | 701 | 629 | No Limit | 701/660 | 659/631 |
| 14 | 24 | 455 | 404 | 28 | 719 | 643 | No Limit | 719/606 | 671/574 |
| 11 | 24 | 439 | 383 | 54 | 733 | 653 | No Limit | 733/543 | 679/508 |

1. The maximum allowable time in the Technical Specification for this condition is equal to 2 hours less than the maximum allowable time shown in this table. This 2-hour reduction allows the handling time required to enter the next stage.
2. The maximum temperatures at the end of the first vacuum (Table 4.4.3-8) are conservatively presented.

Table 4.4.3-10 Maximum Limiting Component Temperatures in Transient Operations after Vacuum for BWR Fuel after Forced-Air Cooling

| Heat Load (kW) | Forced-Air (helium) | | | Vacuum | | | Helium | | |
|----------------|---------------------|----------------------|--------------------|-------------------------------|--------------------------|--------------------|------------------|---|--------------------|
| | Duration (hours) | End Temperature (°F) | | Duration ¹ (hours) | Maximum Temperature (°F) | | Duration (hours) | Max. Temp. / Temp. at Steady-state (°F) | |
| | | Fuel | Heat Transfer Disk | | Fuel | Heat Transfer Disk | | Fuel | Heat Transfer Disk |
| 23 | 24 | 623 | 591 | 4 | 703 | 645 | 16 | 708 | 683 |
| 20 | 24 | 592 | 558 | 5 | 694 | 627 | 30 | 694 | 661 |
| 17 | 24 | 565 | 528 | 10 | 701 | 629 | No Limit | 701/660 | 659/631 |
| 14 | 24 | 541 | 503 | 20 | 719 | 643 | No Limit | 719/606 | 671/574 |
| 11 | 24 | 519 | 477 | 43 | 733 | 653 | No Limit | 733/543 | 679/508 |

1. The maximum allowable time in the Technical Specification for this condition is equal to 2 hours less than the maximum allowable time shown in this table. This 2-hour reduction allows the handling time required to enter the next stage.
2. The maximum temperatures at the end of the first vacuum (Table 4.4.3-8) are conservatively presented.

Table 4.4.3-11 Maximum Limiting Component Temperatures in Transient Operations after Helium for BWR Fuel after In-Pool Cooling

| Heat Load (kW) | In-Pool (helium) | | | Helium | | |
|----------------|------------------|----------------------|--------------------|------------------|------------------------------|--------------------|
| | Duration (hours) | End Temperature (°F) | | Duration (hours) | Max. Temp. (°F) ¹ | |
| | | Fuel | Heat Transfer Disk | | Fuel | Heat Transfer Disk |
| 23 | 24 | 489 | 444 | 16 | 708 | 683 |
| 20 | 24 | 477 | 431 | 30 | 694 | 661 |

1. The maximum temperatures at the end of helium in Table 4.4.3-8 are conservatively used.

Table 4.4.3-12 Maximum Limiting Component Temperatures in Transient Operations after Helium for BWR Fuel after Forced-Air Cooling

| Heat Load (kW) | Forced-Air (helium) | | | Helium | | |
|----------------|---------------------|----------------------|--------------------|------------------|------------------------------|--------------------|
| | Duration (hours) | End Temperature (°F) | | Duration (hours) | Max. Temp. (°F) ¹ | |
| | | Fuel | Heat Transfer Disk | | Fuel | Heat Transfer Disk |
| 23 | 24 | 630 | 598 | 16 | 708 | 683 |
| 20 | 24 | 601 | 566 | 30 | 694 | 661 |

1. The maximum temperatures at the end of helium in Table 4.4.3-8 are conservatively used.

THIS PAGE INTENTIONALLY LEFT BLANK

4.4.4 Minimum Temperatures

The minimum temperatures of the Vertical Concrete Cask and components occur at -40°F with no heat load. The temperature distribution for this off-normal environmental condition is provided in Section 11.1. At this extreme condition, the component temperatures are above their minimum material limits.

THIS PAGE INTENTIONALLY LEFT BLANK

4.4.5 Maximum Internal Pressures

The maximum internal operating pressures for normal conditions of storage are calculated in the following sections for the PWR and BWR Transportable Storage Canisters.

4.4.5.1 Maximum Internal Pressure for PWR Fuel Canister

The internal pressures within the PWR fuel canister are a function of fuel type, fuel condition (failure fraction), burnup, UMS[®] canister type, and the backfill gases in the canister cavity. Gases included in the canister pressure evaluation include rod-fill, rod fission and rod backfill gases, canister backfill gases and burnable poison generated gases. Each of the fuel types expected to be loaded into the UMS[®] canister system is separately evaluated to arrive at a bounding canister pressure.

Fission gases include all fuel material generated gases including long-term actinide decay generated helium. Based on detailed SAS2H calculations of the maximum fissile material mass assemblies in each canister class, the quantity of gas generated by the fuel rods rises as burnup and cool time is increased and enrichment is decreased. To assure the maximum gas is available for release, the PWR inventories are extracted from 60,000 MWD/MTU burnup cases at an enrichment of 1.9 wt. % ²³⁵U and a cool time of 40 years. Gas inventories at 60,000 MWD/MTU bound those calculated at 45,000 MWD/MTU, the maximum allowable burnup. Gases included are all krypton, iodine, and xenon isotopes in addition to helium and tritium (³H). Molar quantities for each of the maximum fissile mass assemblies are summarized in Table 4.4.5-1. Fuel generated gases are scaled by fissile mass to arrive at molar contents of other UMS[®] fuel types.

Fuel rod backfill pressure varies significantly between the PWR fuel types. The maximum reported backfill pressure is listed for the Westinghouse 17×17 fuel assembly at 500 psig. With the exception of the B&W fuel assemblies, which are limited to 435 psig, all fuel assemblies evaluated are set to the maximum 500 psig backfill reported for the Westinghouse assembly. Backfill quantities are based on the free volume between the pellet and the clad and the plenum volume. The fuel rod backfill gas temperature is conservatively assumed to have an initial temperature of 68°F.

Burnable poison rod assemblies (BPRAs) placed within the UMS[®] storage canister may contribute additional molar gas quantities due to (n,α) reactions of fission generated neutrons with ¹⁰B during in-core operation. ¹⁰B forms the basis of a portion of the neutron poison population. Other neutron poisons, such as gadolinium and erbium, do not produce a significant amount of helium nuclides (alpha particles) as part of their activation chain. Primary BPRAs in existence include Westinghouse Pyrex (borosilicate glass) and WABA (wet annular burnable absorber) configurations, as well as B&W BPRAs and shim rods employed in CE cores. The CE shim rods replace standard fuel rods to form a complete assembly array. The quantity of helium available for release from the BPRAs is directly related to the initial boron content of the rods and the release fraction of gas from the matrix material in question. Release from either of the low temperature, solid matrix materials is likely to be limited, but no release fractions were available in open literature. As such, a 100% release fraction is assumed based on a boron content of 0.0063 g/cm ¹⁰B per rod, with the maximum number of rods per assembly. The maximum number of rods is 16 for Westinghouse core 14×14 assemblies, 20 rods for Westinghouse and B&W 15×15 assemblies, and 24 rods for Westinghouse and B&W 17×17 assemblies. The length of the absorber is conservatively taken as the active fuel length. CE core shim rods are modeled at 0.0126 g/cm ¹⁰B for 16, 12, and 12 rods applied to CE manufactured 14×14, 15×15 and 16×16 cores, respectively.

The canister backfill gases are conservatively assumed to be at 250°F, which is significantly below the canister shell maximum initial temperature of 285°F at 9 hours of vacuum drying. The initial pressure of the canister backfill gas is 1 atm (0.0 psig). Free volume inside each PWR canister class is listed in Table 4.4.5-2. The listed free volumes do not include fuel assembly components since these components vary for each assembly type and fuel insert. Subtracting out the rod and guide tube volumes and all hardware components arrives at free volume of the canisters including fuel assemblies and a load of 24 BPRAs. For the Westinghouse BPRAs, the Pyrex volume is employed since it displaces more volume than the WABA rods.

The total pressure for each of the UMS[®] payloads is found by calculating the releasable molar quantity of each gas (30% of the fission gas and 100% of the rod backfill adjusted for the 1% fuel failure fraction), and summing the quantities directly. The quantity of gas is then employed in the ideal gas equation in conjunction with the average gas temperature at normal operating conditions to arrive at system pressures. The normal condition average temperature of the gas within the PWR canister is conservatively considered to be 420°F. This temperature bounds the calculated gas temperature (418°F) for normal conditions of storage using the three-dimensional

canister models. Each of the UMS[®] PWR fuel types is individually evaluated for normal condition pressure, and sets the maximum normal condition pressure at 4.21 psig. A summary of the maximum pressure in each PWR canister class is shown in Table 4.4.5-3. The table also includes the fuel type producing the listed maximum pressures.

4.4.5.2 Maximum Internal Pressure for BWR Fuel Canister

BWR canister maximum pressures are determined in the same manner as those documented for the PWR canister cases. Primary differences between PWR and BWR analysis include a maximum normal condition average gas temperature of 410°F, rod backfill gas pressures of 132 psig, and limits pressurizing gases to fission gases (including helium actinide decay gas), rod backfill gases, and canister backfill gas. The 132 psig employed in this analysis is significantly higher than the 6 atmosphere maximum pressure reported in open literature. BWR assemblies do not contain an equivalent to the PWR BPRAs and, therefore, do not require ¹⁰B helium generated gases to be added. Fissile gas inventories for the maximum fissile material assemblies in each of the three BWR lattices configurations (7×7, 8×8, and 9×9) are shown in Table 4.4.5-4. Free volumes, without fuel components, in UMS[®] canister classes 4 and 5 are shown in Table 4.4.5-5. Maximum pressures for each canister class are listed in Table 4.4.5-6. The maximum normal condition pressure of 3.97 psig is based on a GE 7×7 assembly, designed for a BWR/2-3 reactor, with gas inventories conservatively taken from a 60,000 MWD/MTU source term. The normal condition pressure for a UMS[®] storage canister containing the GE 9×9 fuel assembly with 79 fuel rods is 3.96 psig. Similar fuel masses and displaced volume account for similar canister pressures.

Table 4.4.5-1 PWR Per Assembly Fuel Generated Gas Inventory

| Array | Assy Type | MTU | Moles |
|-------|----------------|--------|-------|
| 14×14 | WE Standard | 0.4144 | 35.52 |
| 15×15 | B&W | 0.4807 | 41.32 |
| 16×16 | CE (System 80) | 0.4417 | 38.10 |
| 17×17 | WE Standard | 0.4671 | 40.18 |

Table 4.4.5-2 PWR Canister Free Volume (No Fuel or Inserts)

| Canister Class | 1 | 2 | 3 |
|---------------------------------------|--------|--------|--------|
| Basket Volume (in ³) | 69800 | 74490 | 77460 |
| Canister Height (inch) | 175.05 | 184.15 | 191.75 |
| Canister Free Volume w/o Fuel (liter) | 7970 | 8400 | 8770 |

Table 4.4.5-3 PWR Maximum Normal Condition Pressure Summary

| Canister Class | Fuel Type | Pressure (psig) |
|----------------|--------------------|-----------------|
| Class 1 | WE 17×17 Standard | 4.20 |
| Class 2 | B&W 17×17 Mark C | 4.21 |
| Class 3 | CE 16×16 System 80 | 4.11 |

Table 4.4.5-4 BWR Per Assembly Fuel Generated Gas Inventory

| Array | Assy Type | MTU | Moles |
|-------|------------------|--------|-------|
| 7×7 | GE 7×7 (49 Rods) | 0.1985 | 16.78 |
| 8×8 | GE 8×8 (63 Rods) | 0.1880 | 16.07 |
| 9×9 | GE 9×9 (79 Rods) | 0.1979 | 16.86 |

Table 4.4.5-5 BWR Canister Free Volume (No Fuel or Inserts)

| Canister Class | 4 | 5 |
|---------------------------------------|--------|--------|
| Basket Volume (in ³) | 73110 | 74680 |
| Canister Height (inch) | 185.55 | 190.35 |
| Canister Free Volume w/o Fuel (liter) | 8500 | 8740 |

Table 4.4.5-6 BWR Maximum Normal Condition Pressure Summary

| Canister Class | Fuel Type | Pressure (psig) |
|----------------|-----------|-----------------|
| Class 4 | GE 7×7 | 3.97 |
| Class 5 | GE 9×9 | 3.96 |

THIS PAGE INTENTIONALLY LEFT BLANK

4.4.6 Maximum Thermal Stresses

The results of thermal stress calculations for normal conditions of storage are reported in Section 3.4.4.

THIS PAGE INTENTIONALLY LEFT BLANK

4.4.7 Maximum Allowable Cladding Temperature and Canister Heat Load

The maximum allowable cladding temperatures are calculated for PWR and BWR systems based on fuel assembly type, maximum burnup, and minimum initial cool time. Allowable heat loads are determined by relating cladding temperature to canister heat load.

Cladding stresses are calculated for a set of representative PWR and BWR assemblies at 40,000 MWD/MTU and 380°C. The limiting, highest stress assemblies, the Westinghouse 14×14 and GE 9×9 (150-inch fuel region), are then evaluated at various burnups to determine the maximum allowable fuel cladding temperature based on PNL-6364 criteria [33]. Maximum allowable cladding temperatures are calculated for burnups ranging from 35,000 MWD/MTU to 45,000 MWD/MTU. After applying a bias to the maximum allowable cladding temperatures, the maximum allowable heat load is calculated as a function of burnup and minimum initial cool time.

4.4.7.1 Maximum Allowable Cladding Temperature

Based on PNL-6364, the cladding temperature limit is expressed as a function of initial dry storage temperature, initial cladding stress at the dry storage temperature, and initial storage time.

The initial cladding stress is a function of the rod internal pressure, temperature, diameter of the fuel rod, and fuel cladding thickness. The initial cladding stress (σ_{mhoop}) for a particular assembly is calculated as [33]:

$$\sigma_{\text{mhoop}} = \frac{(P)(D_{\text{mid}})}{2t} \times \alpha \times \frac{T_2}{T_1} \times \frac{69.684}{10,000}$$

where:

- σ_{mhoop} = dry storage cladding hoop stress, MPa
- P = internal gas pressure of the rod, psi
- T_1 = temperature at which P was determined, °K
- t = cladding wall thickness, in.
- D_{mid} = cladding midwall diameter, in.
- α = a factor, 0.95 for PWR rods or 0.90 for BWR rods
- T_2 = allowable storage temperature for σ_{mhoop} , °K

To account for cladding oxidation during in-core fuel assembly operation and storage of the fuel in the spent fuel pool, the nominal cladding thickness is reduced by 0.06 mm and 0.125 mm for PWR and BWR fuel rods respectively [34].

The pressure in the fuel assembly rods is produced by the combination of fill gas and fission gas.

For a given fuel assembly design, the fill gas quantity is fixed and does not vary with discharge burnup. Based on the initial pressure and temperature of the fill gas, the number of moles of gas are calculated using the ideal gas law:

$$PV = NRT$$

where:

- P = Pressure
- V = Volume (free volume inside fuel rod)
- N = Number of moles of gas
- R = Universal gas constant
- T = Temperature of the gas

The number of moles of fill gas are added to the fission gas quantity and converted to a cladding internal pressure at storage conditions.

The fission gas quantity pressurizing the fuel cladding is calculated on the basis of the burnup and a fission gas release fraction. While the amount of fission gas produced is a predictable quantity (directly correlated to the number of fissions required to produce the desired burnup), the release fraction of the gas from the pellet into the pellet-cladding void depends on fill gas pressure and reactor operating conditions.

The number of fissions (Z) is related to the burnup by:

$$Z = X \text{ Burnup} \frac{\text{MWD}}{\text{MTU}} \times 1.0 \times 10^6 \frac{\text{W}}{\text{MW}} \times 86,400 \frac{\text{sec}}{\text{d}} \times \frac{1 \text{ MeV}}{1.602 \times 10^{-13} \text{ J}} \times \frac{1 \text{ Fission}}{200 \text{ MeV}}$$

$$\times \frac{1 \text{ Mole}}{6.02 \times 10^{23} \text{ Atoms}} \times \text{Mass} \frac{\text{MTU}}{\text{Assembly}} \times \frac{\text{Assembly}}{\# \text{ Rods}}$$

Multiplying the number of fissions by 0.3125 (0.25 × 1.25) atoms/fission then derives the quantity of fission gas produced. Olander's "Fundamental Aspects of Nuclear Reactor Fuel Elements" [31] lists the number of gas atoms from a single fission as 0.25. Based on a detailed SAS2H isotope generated fission gas inventory, this fraction is increased by 25% to account for decay chains not included in Olander (particularly those leading to ¹³⁶Xe). By employing a conservative fission gas fraction rather than the SAS2H output itself, the allowable cladding temperature calculation is decoupled from source term calculations.

Based on Sandia report 90-2406, "A Method for Determining the Spent-Fuel Contribution to Transport Cask Containment Requirements" [30], gas release fractions from the fuel pellets are assumed to be 12% for PWR fuel rods and 25% for BWR fuel rods. Relying on a gas diffusion

model (as applied to pre-pressurized light water reactor fuel rods), the Sandia report indicates a release fraction of approximately 1% for PWR rods and approximately 2% for BWR rods [Page I-62 of Ref. 30]. Experimental release fractions reach as high as 16% for PWR rods and 25% for BWR rods [Page I-64 and I-65 of Ref. 30]. The higher release fractions are associated with unpressurized fuel rods or those rods run at uncharacteristically high temperatures and linear heat generation rates. While these rods show higher release rates, they are not expected to produce higher "burned fuel" pressures, since the partial pressure of the fill gas is not present, thereby allowing a larger number of fission gas molecules to accumulate before reaching limiting cladding pressure. The 12% PWR fission gas release fraction excludes the unpressurized Maine Yankee rod data while including the Calvert Cliff data through a burnup of approximately 56,000 MWD/MTU burnup. An additional analysis is performed comparing the 12% PWR and 25% BWR release fractions to the element specific release fractions in Reg. Guide 1.25 [Ref. 35]. The 12% PWR release fraction results in gas releases similar to those indicated by the Regulatory Guide, while the BWR 25% release fraction is twice the Regulatory Guide indicated gas release. Note that both the Sandia report and the Regulatory Guide release fractions are for punctured fuel rods where the release of the pressurizing gas allows additional gaseous isotopes to migrate from the fuel matrix. Using the 12% PWR and 25% BWR fuel rod release fractions, therefore, results in a conservative cladding pressurization assumption for the intact rod analysis.

Fuel rod free volume is calculated based on the fuel characteristics documented in Table 4.4.7-1 and Table 4.4.7-2 for PWR and BWR fuel assemblies, respectively. Not all assemblies requested for loading are included in the tables, since assemblies with significantly higher free volume or lower fuel mass are bound by the cladding stress evaluations presented. Section 4.4.5 contains a sample free volume calculation of a fuel rod. While the maximum canister pressure calculation conservatively neglected the plenum spring volume, the spring volume is subtracted out of the plenum volume in the cladding maximum stress calculation to increase internal rod pressure.

Substituting the internal gas pressure resulting from the releasable gas inventories produced by 40,000 MWD/MTU burned fuel into Equation 1 at a temperature of 380°C results in the assembly-specific maximum cladding stresses shown in Table 4.4.7-1 and Table 4.4.7-2. The Westinghouse 14×14 and GE 9×9 (150-inch fuel region) are the limiting PWR and BWR assembly types at 113.9 and 70.5 MPa stress levels, respectively.

The stress levels in the limiting assemblies are then evaluated at burnups ranging from 35,000 MWD/MTU to 45,000 MWD/MTU and temperatures of 300°C and 400°C for PWR fuels and 300°C and 450°C for BWR fuel. The evaluation results are presented in Table 4.4.7-3. This data is overlaid on generic stress versus limiting temperature curves to arrive at cool time and burnup-specific maximum cladding allowable temperatures. The data, shown in Table 4.4.7-4, from which the generic curves are constructed, is taken from Table 3.1 of PNL-6189 [5].

The cladding temperature limit curves for the limiting PWR and BWR fuel assemblies are provided in Figure 4.4.7-1 and Figure 4.4.7-2. The intercept of each of the curves represents the maximum allowable cladding temperature at a given cool time and maximum assembly burnup. Fuel rod peak cladding stress level and the allowable cladding temperature are calculated using the assembly average burnup, even though some rods experience a higher burnup than the average. The average burnup is used since the quantity of fission gas formation and the fuel rod gas temperature are conservatively determined. As shown in Table 4.4.7-5, allowable cladding temperature varies only slightly over a wide range of burnup for a given required cooling time. Consequently, the variation in cladding stress with burnup is also small.

4.4.7.2 Maximum Allowable Canister Heat Load

Thermal analysis was performed at three heat loads to determine the corresponding maximum fuel cladding temperature for both PWR and BWR fuel. The thermal models and methods, described in Section 4.4.1, used to determine the temperature of fuel cladding and system components for the design basis heat load are applied to determine the cladding temperature at reduced heat loads. The cladding temperatures versus heat load in Table 4.4.7-6 and Table 4.4.7-7 are the results of rounding the ANSYS calculated temperatures up to provide a conservative, bounding input for correlating allowable cladding temperature to allowable heat load. The temperatures versus heat load curves are plotted in Figure 4.4.7-3. To provide adequate design margin, the maximum allowable cladding temperatures are reduced by a temperature bias, shown in Table 4.4.7-9, prior to their use in the calculation of maximum allowable canister heat load. Maximum allowable canister heat loads are calculated for initial cool times ranging from 5 to 15 years and burnups ranging from 35,000 MWD/MTU to 45,000 MWD/MTU. The results of the PWR and BWR analysis are presented in Table 4.4.7-8. Since these temperatures are based on the PWR and BWR assemblies having the highest cladding stress levels, the maximum heat loads can be applied to all UMS design basis contents.

Figure 4.4-7-1 PWR Fuel Dry Storage Temperature versus Cladding Stress

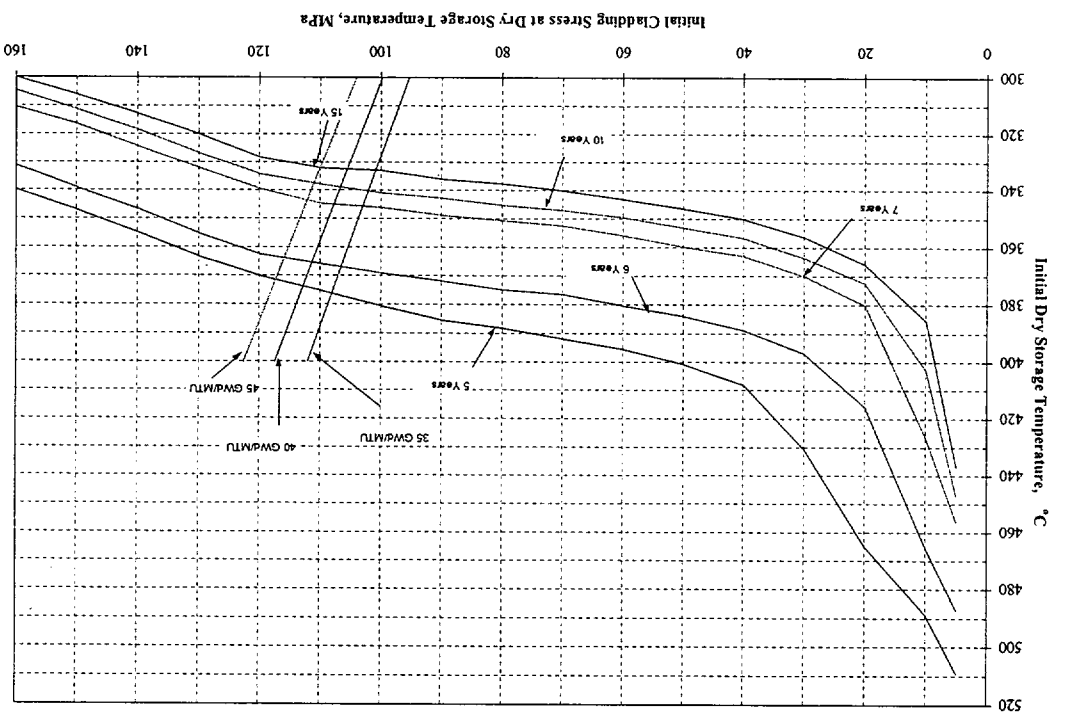


Figure 4.4-7-2 BWR Fuel Dry Storage Temperature versus Cladding Stress

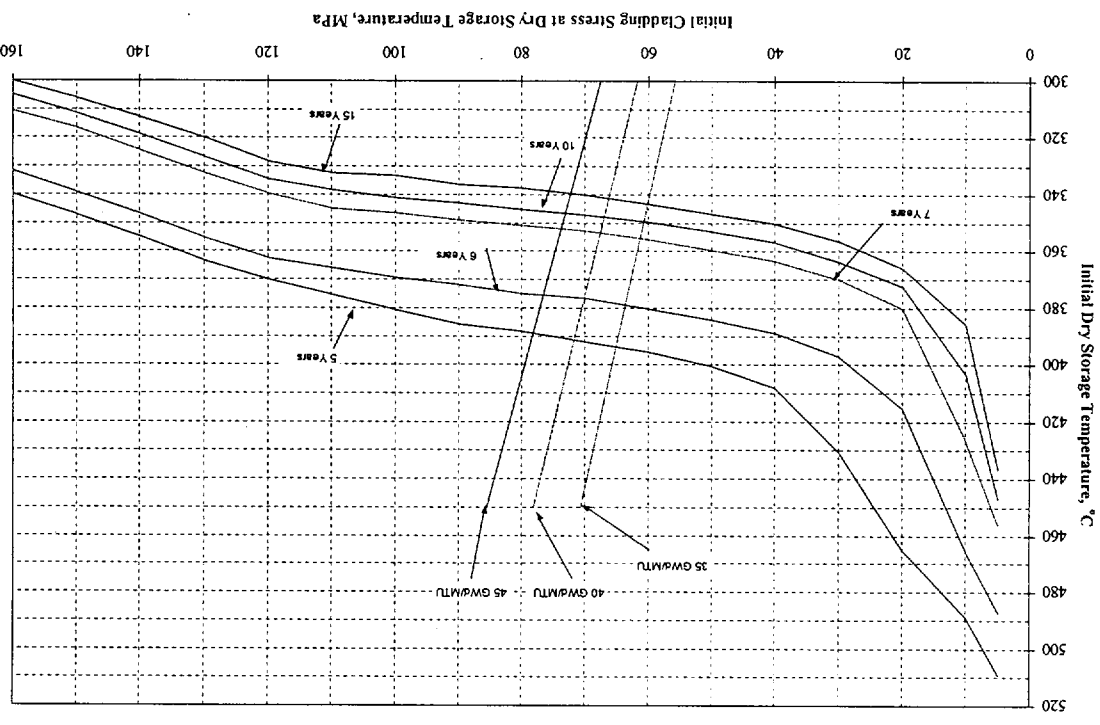


Figure 4.4.7-3 PWR and BWR Fuel Cladding Dry Storage Temperature versus Basket Heat Load

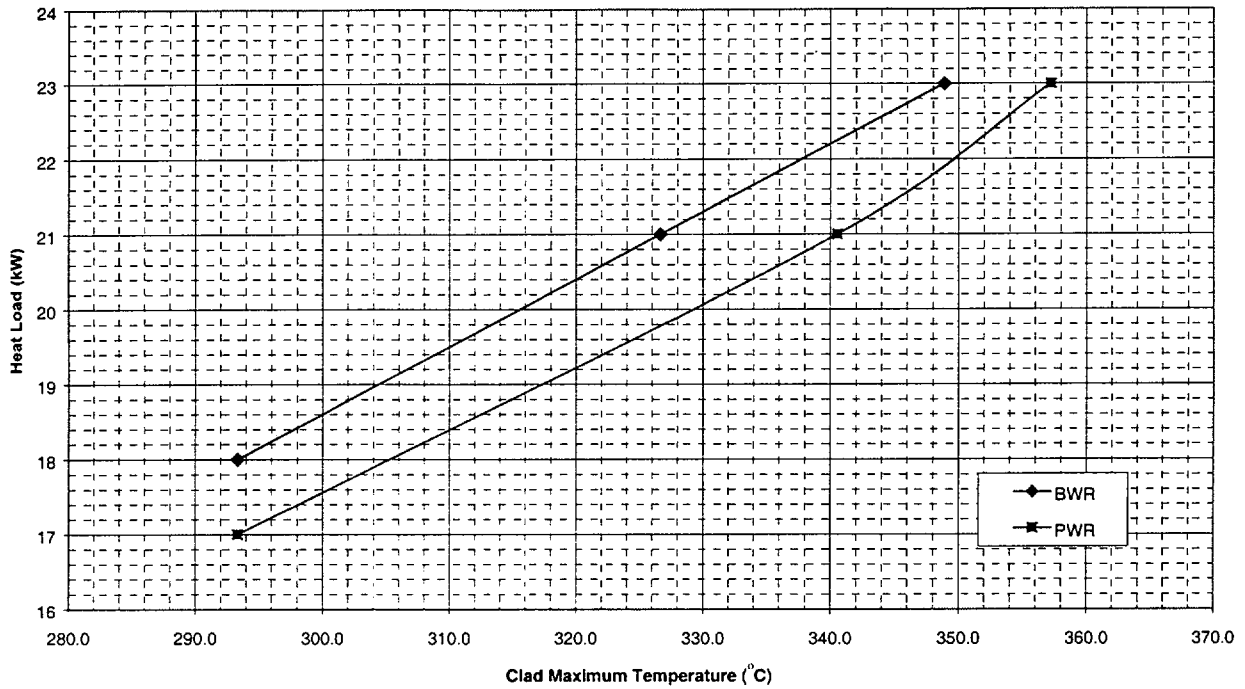


Table 4.4.7-1 PWR Cladding Stress Level Comparison Chart

| Fuel Type | Units | B&W 15×15 | B&W 17×17 | CE 14×14 | CE 16×16 | WE 14×14 | WE 15×15 | WE 17×17 |
|--------------------|-------------------|--------------|--------------|-------------|-------------|-------------|-------------|-------------|
| Rod OD | inch | 0.43 | 0.379 | 0.44 | 0.382 | 0.422 | 0.422 | 0.374 |
| Cladding Thickness | inch | 0.0265 | 0.024 | 0.028 | 0.025 | 0.0225 | 0.0242 | 0.0225 |
| Pellet OD | inch | 0.3686 | 0.3232 | 0.3765 | 0.325 | 0.3674 | 0.3659 | 0.3225 |
| Active Fuel Length | inch | 144 | 143 | 137 | 150 | 145.2 | 144 | 144 |
| Plenum Length | inch | 7.755 | 8.318 | 8.528 | 9.927 | 5.790 | 7.386 | 6.260 |
| Spring Weight | lb | 0.042 | 0.026 | 0.1 | 0.1 | 0.07 | 0.044 | 0.037 |
| Backfill Pressure | psig | 435 | 435 | 500 | 500 | 500 | 500 | 500 |
| Fuel Mass | MTU | 0.4807 | 0.4658 | 0.4037 | 0.4417 | 0.4144 | 0.4646 | 0.4671 |
| # of Fuel Rods | | 208 | 264 | 176 | 236 | 179 | 204 | 264 |
| Free Volume | inch ³ | 1.427 | 1.198 | 1.252 | 1.052 | 1.217 | 1.300 | 0.882 |
| Pressure (380°C) | psia | 1525 | 1478 | 1739 | 1722 | 1762 | 1713 | 1795 |
| Stress Level | MPa | 83.1 | 78.9 | 91.2 | 88.5 | 113.9 | 101.7 | 102.1 |

Table 4.4.7-2 BWR Cladding Stress Level Comparison Chart

| Fuel Type | Units | EX 7×7 | EX 8×8 | EX 9×9 | GE 7×7 | GE 8×8a | GE 8×8b | GE 9×9 |
|--------------------|-------------------|--------|--------|--------|--------|---------|---------|--------|
| Rod OD | inch | 0.57 | 0.484 | 0.424 | 0.563 | 0.493 | 0.483 | 0.441 |
| Cladding Thickness | inch | 0.036 | 0.036 | 0.03 | 0.032 | 0.034 | 0.032 | 0.028 |
| Pellet OD | inch | 0.49 | 0.4045 | 0.3565 | 0.487 | 0.416 | 0.41 | 0.376 |
| Active Fuel Length | inch | 144 | 150 | 150 | 144 | 144 | 150 | 150 |
| Plenum Length | inch | 10.200 | 10.024 | 9.578 | 11.190 | 10.960 | 9.580 | 9.580 |
| Spring Weight | lb | 0.13 | 0.1 | 0.047 | 0.083 | 0.066 | 0.066 | 0.047 |
| Backfill Pressure | psig | 44.1 | 132.0 | 132.0 | 44.1 | 132.0 | 132.0 | 132.0 |
| Fuel Mass | MTU | 0.196 | 0.1793 | 0.1666 | 0.1977 | 0.1855 | 0.1847 | 0.1979 |
| # of Fuel Rods | | 48 | 62 | 74 | 49 | 63 | 62 | 79 |
| Free Volume | inch ³ | 2.426 | 1.708 | 1.469 | 3.236 | 2.181 | 1.970 | 1.758 |
| Pressure (380°C) | psia | 1264 | 1469 | 1359 | 971 | 1236 | 1345 | 1286 |
| Stress Level | MPa | 66.7 | 65.1 | 65.4 | 58.2 | 59.8 | 68.7 | 70.5 |

Table 4.4.7-3 Cladding Stress as a Function of Fuel Assembly Average Burnup and Temperature

| Burnup | PWR | | BWR | |
|----------------|-----------|-----------|----------|----------|
| | 300°C | 400°C | 300°C | 450°C |
| 35,000 MWD/MTU | 95.4 Mpa | 112.3 Mpa | 55.9 Mpa | 70.8 Mpa |
| 40,000 MWD/MTU | 99.9 Mpa | 117.4 Mpa | 61.8 Mpa | 78.2 Mpa |
| 45,000 MWD/MTU | 104.2 Mpa | 122.6 Mpa | 67.6 Mpa | 85.5 Mpa |
| 50,000 MWD/MTU | 122.3 Mpa | 143.9 Mpa | -- | -- |

Table 4.4.7-4 Maximum Allowable Initial Storage Temperature (°C) As a Function of Initial Cladding Stress and Initial Cool Time

| MPa | 5 years | 6 years | 7 years | 10 years | 15 years |
|-----|---------|---------|---------|----------|----------|
| 5 | 509.2 | 487.3 | 455.9 | 447 | 436.5 |
| 10 | 488.8 | 465.5 | 426.4 | 403 | 385.6 |
| 20 | 465.2 | 415.5 | 380.1 | 372.4 | 366 |
| 30 | 430.4 | 397 | 370.1 | 363.8 | 356.5 |
| 40 | 408.1 | 389 | 363.2 | 356.6 | 350 |
| 50 | 400.6 | 384 | 359.7 | 353.1 | 346.5 |
| 60 | 395.6 | 380.4 | 355.9 | 349.6 | 343.1 |
| 70 | 391.9 | 376.5 | 352.5 | 347 | 340 |
| 80 | 388.2 | 375 | 350.8 | 345.2 | 337.6 |
| 90 | 385.7 | 372 | 348.8 | 342.8 | 336.1 |
| 100 | 380.7 | 369.3 | 346.2 | 341 | 333.2 |
| 110 | 375.2 | 365.9 | 344.6 | 338 | 332.1 |
| 120 | 370 | 362.4 | 339.5 | 334.3 | 328.2 |
| 130 | 363.5 | 355.2 | 332.2 | 326.6 | 320 |
| 140 | 355 | 346.6 | 324.2 | 318.6 | 312.6 |
| 150 | 346.9 | 339.1 | 316.5 | 311.2 | 306 |
| 160 | 339.6 | 331.4 | 310.3 | 304.7 | 299.9 |

Table 4.4.7-5 Maximum Allowable Cladding Temperature for PWR and BWR Fuel Assemblies

| Cool Time [years] | PWR Clad Temperature Limit [°C] | | | BWR Clad Temperature Limit [°C] | | |
|----------------------|---------------------------------|--------|--------|---------------------------------|--------|--------|
| | Burnup (MWD/MTU) | | | Burnup (MWD/MTU) | | |
| | 35,000 | 40,000 | 45,000 | 35,000 | 40,000 | 45,000 |
| 5 | 376 | 374 | 371 | 394 | 391 | 389 |
| 6 | 367 | 365 | 364 | 379 | 376 | 376 |
| 7 | 346 | 345 | 343 | 355 | 353 | 352 |
| 10 | 340 | 339 | 338 | 349 | 348 | 346 |
| 15 | 333 | 333 | 332 | 343 | 341 | 339 |

Table 4.4.7-6 Cladding Maximum Temperature as a Function of Basket Heat Load (PWR)

| Fuel Clad | | Heat Load |
|-----------|-----------|-----------|
| Temp (°F) | Temp (°C) | kW |
| 560 | 293.3 | 17 |
| 645 | 340.6 | 21 |
| 675 | 357.2 | 23 |

Table 4.4.7-7 Cladding Maximum Temperature as a Function of Basket Heat Load (BWR)

| Fuel Clad | | Heat Load |
|-----------|-----------|-----------|
| Temp (°F) | Temp (°C) | kW |
| 560 | 293.3 | 18 |
| 620 | 326.7 | 21 |
| 660 | 348.9 | 23 |

Table 4.4.7-8 Maximum Allowable Decay Heat for UMS[®] PWR and BWR Systems

| Cool Time ¹ | PWR Burnup (MWD/MTU) | | | BWR Burnup (MWD/MTU) | | |
|------------------------|-------------------------|---------|---------|-------------------------|---------|---------|
| | 35,000 | 40,000 | 45,000 | 35,000 | 40,000 | 45,000 |
| 5 | 23 kW | 23 kW | 23 kW | 23 kW | 23 kW | 23 kW |
| 6 | 22.4 kW | 22.1 kW | 21.9 kW | 23 kW | 23 kW | 23 kW |
| 7 | 20.2 kW | 20.1 kW | 20 kW | 22.1 kW | 21.9 kW | 21.8 kW |
| 10 | 19.7 kW | 19.6 kW | 19.5 kW | 21.6 kW | 21.5 kW | 21.4 kW |
| 15 | 19.1 kW | 19 kW | 18.9 kW | 21.1 kW | 20.9 kW | 20.7 kW |

1. Based on temperature bias shown in Table 4.4.7-9.

Table 4.4.7-9 Temperature Bias Applied to Maximum Allowable Decay Heats

| Cool Time [years] | PWR Clad Temperature Bias [°C] | | | BWR Clad Temperature Bias [°C] | | |
|----------------------|--------------------------------|--------|--------|--------------------------------|--------|--------|
| | Burnup (MWD/MTU) | | | Burnup (MWD/MTU) | | |
| | 35,000 | 40,000 | 45,000 | 35,000 | 40,000 | 45,000 |
| 5 | -15 | -15 | -14 | -18 | -17 | -18 |
| 6 | -15 | -15 | -16 | -18 | -17 | -19 |
| 7 | -15 | -15 | -14 | -16 | -16 | -17 |
| 10 | -15 | -15 | -15 | -16 | -16 | -15 |
| 15 | -15 | -16 | -16 | -15 | -16 | -16 |

THIS PAGE INTENTIONALLY LEFT BLANK

4.4.8 Evaluation of System Performance for Normal Conditions of Storage

Results of thermal analysis of the Universal Storage System containing PWR or BWR fuel under normal conditions of storage are summarized in Tables 4.4.3-1 through 4.4.3-4. The maximum PWR and BWR fuel rod cladding temperatures are below the allowable temperatures; temperatures of safety-related components during storage and transfer operations under normal conditions are maintained within their safe operating ranges; and thermally induced stresses in combination with pressure and mechanical load stresses are shown in the structural analysis of Chapter 3.0 to be less than the allowable stresses. Therefore, the Universal Storage System performance meets the requirements for the safe storage of design basis fuel under the normal operating conditions specified in 10 CFR 72.

THIS PAGE INTENTIONALLY LEFT BLANK

4.5 Thermal Evaluation for Site Specific Spent Fuel

This section presents the thermal evaluation of fuel assemblies or configurations, which are unique to specific reactor sites or which differ from the UMS[®] Storage System design basis fuel. These site specific configurations result from conditions that occurred during reactor operations, participation in research and development programs, and from testing programs intended to improve reactor operations. Site specific fuel includes fuel assemblies that are uniquely designed to accommodate reactor physics, such as axial fuel blanket and variable enrichment assemblies, and fuel that is classified as damaged. Damaged fuel includes fuel rods with cladding that exhibit defects greater than pinhole leaks or hairline cracks.

Site specific fuel assembly configurations are either shown to be bounded by the analysis of the standard design basis fuel assembly configuration of the same type (PWR or BWR), or are shown to be acceptable contents by specific evaluation.

4.5.1 Maine Yankee Site Specific Spent Fuel

The standard spent fuel assembly for the Maine Yankee site is the Combustion Engineering (CE) 14×14 fuel assembly. Fuel of the same design has also been supplied by Westinghouse and by Exxon. The standard 14×14 fuel assembly is included in the population of the design basis PWR fuel assemblies for the UMS[®] Storage System (See Table 2.1.1-1). The maximum decay heat for the standard Maine Yankee fuel is the design basis heat load for the PWR fuels (23 kW total, or 0.958 kW per assembly). This heat load is bounded by the thermal evaluations in Section 4.4 for the normal conditions of storage, Section 4.4.3.1 for less than design basis heat loads and Chapter 11 for off-normal and accident conditions.

Some Maine Yankee site specific fuel has a burnup greater than 45,000 MWD/MTU, but less than 50,000 MWD/MTU. This fuel is evaluated in Section 4.5.1.2. As shown in that section, loading of fuel assemblies in this burnup range is subject to preferential loading in designated basket positions in the Transportable Storage Canister and certain fuel assemblies in this burnup range must be loaded in a Maine Yankee fuel can.

The site specific fuels included in this evaluation are:

1. Consolidated fuel rod lattices consisting of a 17 × 17 lattice fabricated with 17 × 17 grids, 4 stainless steel support rods and stainless steel end fittings. One of these

- lattices contains 283 fuel rods and 2 rod position vacancies. The other contains 172 fuel rods, with the remaining rod position locations either empty or containing stainless steel dummy rods.
2. Standard fuel assemblies with a Control Element Assembly (CEA) inserted in each one.
 3. Standard fuel assemblies that have been modified by removing damaged fuel rods and replacing them with stainless steel dummy rods, solid zirconium rods, or 1.95 wt % enriched fuel rods.
 4. Standard fuel assemblies that have had the burnable poison rods removed and replaced with hollow Zircaloy tubes.
 5. Standard fuel assemblies with in-core instrument thimbles stored in the center guide tube.
 6. Standard fuel assemblies that are designed with variable enrichment (radial) and axial blankets.
 7. Standard fuel assemblies that have some fuel rods removed.
 8. Standard fuel assemblies that have damaged fuel rods.
 9. Standard fuel assemblies that have some type of damage or physical alteration to the cage (fuel rods are not damaged).
 10. Two (2) rod holders, designated CF1 and CA3. CF1 is a lattice having approximately the same dimensions as a standard fuel assembly. It is a 9×9 array of tubes, some of which contain damaged fuel rods. CA3 is a previously used fuel assembly lattice that has had all of the rods removed, and in which damaged fuel rods have been inserted.
 11. Standard fuel assemblies that have damaged fuel rods stored in their guide tubes.
 12. Standard fuel assemblies with inserted startup sources and other non-fuel items.

The Maine Yankee site specific fuels are also described in Section 1.3.2.1.

The thermal evaluations of these site specific fuels are provided in Section 4.5.1.1. Section 4.5.1.2 presents the evaluation of Maine Yankee fuel inventory that is not bounded by the evaluation performed in Section 4.4.7. This fuel may have higher burnup than the design basis fuel, have a higher decay heat on a per assembly basis, have a burnup/cool time condition that is outside of the cladding temperature evaluation presented in Section 4.4.7, or be subject to all of these differences.

4.5.1.1 Thermal Evaluation for Maine Yankee Site Specific Spent Fuel

The maximum heat load per assembly for site specific fuel considered in this section is limited to the design basis heat load (0.958 kW). The evaluation of fuel configurations having a greater heat load is presented in Section 4.5.1.2.

4.5.1.1.1 Consolidated Fuel

There are two (2) consolidated fuel lattices. One lattice contains 283 fuel rods and the other contains 172 fuel rods. Conservatively, only one consolidated fuel lattice is loaded in any Transportable Storage Canister.

The maximum decay heat of the consolidated fuel lattice having 283 fuel rods is 0.279 kW. This heat load is bounded by the design basis PWR fuel assembly, since it is less than one-third of the design basis heat load.

The second consolidated fuel lattice has 172 fuel rods with 76 stainless steel dummy rods at the outer periphery of the lattice. Due to the existence of the stainless steel rods, the effective thermal conductivities of this assembly may be slightly lower than those of the standard CE 14×14 fuel assembly. While the stainless steel rods provide better conductance in the axial direction, the radiation heat transfer is less effective at the surface of stainless steel rods, as compared to the standard fuel rods. The radiation is a function of surface emissivity and the emissivity for stainless steel (0.36) is less than one-half of that for Zircaloy (0.75). A parametric study is performed to demonstrate that the thermal performance of the UMS PWR basket loading configuration consisting of 23 standard CE 14×14 fuel assemblies and the consolidated fuel lattice with stainless rods is bounded by that of the configuration consisting of 24 standard CE 14×14 fuel assemblies. Two finite element models are used in the study: a two-dimensional fuel assembly model and a three-dimensional periodic canister internal model.

The two-dimensional model is used to determine the effective thermal conductivities of the consolidated fuel lattice with stainless steel rods. Considering the symmetry of the consolidated fuel, the finite element model represents a one-quarter section as shown in Figure 4.5.1.1-1. The methodology used in Section 4.4.1.5 for the two-dimensional fuel model for PWR fuel is employed in this model. The model includes the fuel pellets, cladding, helium between the fuel rods, and helium occupying the gap between the fuel pellets and cladding. In addition, the

rods at the two outer layers are modeled as solid stainless steel rods to represent the configuration of this consolidated fuel lattice. Modes of heat transfer modeled include conduction and radiation between individual rods for steady-state condition. ANSYS PLANE55 conduction elements and LINK31 radiation elements are used in the model. Radiation elements are defined between rods and from rods to the boundary of the model. The effective conductivity for the fuel is determined using the procedure described in Section 4.4.1.5.

The three-dimensional periodic canister internal model consists of a periodic section of the canister internals. The model contains one support disk with two heat transfer disks (half thickness) on its top and bottom, the fuel assemblies, the fuel tubes and the helium in the canister, as shown in Figure 4.5.1.1-2. The purpose of this model is to compare the maximum fuel cladding temperatures of the following cases:

- 1) Base Case: All 24 positions loaded with standard CE 14×14 fuel assemblies.
- 2) Case 2: 23 positions with standard fuel, with one consolidated fuel lattice in position 2.
- 3) Case 3: 23 positions with standard fuel, with one consolidated fuel lattice in position 3.
- 4) Case 4: 23 positions with standard fuel, with one consolidated fuel lattice in position 4.
- 5) Case 5: 23 positions with standard fuel, with one consolidated fuel lattice in position 5.

Positions 2, 3, 4, and 5 are shown in Figure 4.5.1.1-3. Based on symmetry, these locations represent all of the possible locations for consolidated fuel in the basket.

The fuel assemblies and fuel tubes are represented by homogeneous regions with effective thermal conductivities. The effective conductivities for the consolidated fuel are determined by the two-dimensional fuel assembly model discussed above. The effective conductivities for the CE 14×14 fuel assemblies are established based on the model described in Section 4.4.1.5. Effective properties for the fuel tubes are determined by the two-dimensional fuel tube model in Section 4.4.1.6. Volumetric heat generation corresponding to the design basis heat load of 0.958 kW per assembly is applied to the CE 14×14 fuel regions in the model. Similarly, a heat generation rate corresponding to 0.279 kW is applied to the consolidated fuel assembly region. The heat conduction in the axial direction is conservatively ignored by assuming that the top and

bottom surfaces of the model are adiabatic. A constant temperature of 400°F is applied to the outer surface of the model as boundary conditions. Note that the maximum canister temperature is 351°F for PWR configurations for the normal condition of storage (Table 4.1-4). Steady state thermal analysis is performed for all five cases and the calculated maximum fuel cladding temperatures in the model are:

| | Base Case | Case 2 | Case 3 | Case 4 | Case 5 |
|--|-----------|--------|--------|--------|--------|
| Maximum Fuel Cladding Temperature (°F) | 755 | 733 | 738 | 740 | 740 |

As shown, the maximum temperatures for Cases 2 through 5 are less than those of the Base Case. It is concluded that the thermal performance of the configuration consisting of 23 standard CE 14×14 fuel assemblies and one consolidated fuel lattice is bounded by that of the configuration consisting of 24 standard CE 14×14 fuel assemblies. This study shows that a consolidated fuel lattice can be located in any basket position. However, as shown in Table 12B2-6 in Chapter 12, the consolidated fuel assembly must be loaded in a corner position of the fuel basket (e.g., Position 5 shown in Figure 4.5.1.1-3).

4.5.1.1.2 Standard CE 14 × 14 Fuel Assemblies with Control Element Assemblies

A Control Element Assembly (CEA) consists of five solid B₄C rods encapsulated in stainless steel tubes. The B₄C material has a conductivity of 1.375 BTU/hr-in-°F. With the CEA inserted into the guide tubes of the CE 14×14 fuel assembly, the effective conductivity in the axial direction of the fuel assembly is increased because solid material replaces helium in the guide tubes. The change in the effective conductivity in the transverse direction of the fuel assembly is negligible since the CEA is inside of the guide tubes. Note that the total heat load, including the small amount of extra heat generated by the CEA, remains below the design basis heat load. Therefore, the thermal performance of the fuel assemblies with CEAs inserted is bounded by that of the standard fuel assemblies.

4.5.1.1.3 Modified Standard Fuel Assemblies

These assemblies include those standard fuel assemblies that have been modified by removing damaged fuel rods and replacing them with stainless steel dummy rods, solid zirconium rods or 1.95 wt % enriched fuel rods.

The maximum number of fuel rods replaced by stainless steel rods is six (6) per assembly, which is about 3% of the total number of fuel rods in each assembly (176). The conductivity of the stainless steel is similar to that of Zircaloy and better than that of the UO₂. The resultant increase in effective conductivity of the modified fuel assembly in the axial direction offsets the decrease in the effective conductivity in the transverse direction (due to slight reduction of radiation heat transfer at the surface of the stainless steel rods). The maximum number of fuel rods replaced by solid Zirconium rods is five (5) per assembly. Since the solid Zirconium rod has a higher conductivity than the fuel rod (UO₂ with Zircaloy clad), the effective conductivity of the repaired fuel assembly is increased. The thermal properties for the enriched fuel rod remain the same as for standard fuel rods, so there is no change in effective conductivity of the fuel assembly results from the use of fuel rods enriched to 1.95 wt % ²³⁵U. These rods replace other fuel rods in the assembly after the first or second burnup cycles were completed. Therefore, these replacement fuel rods have been burned a minimum of one cycle less than the remainder of the assembly, producing a proportionally lower per rod heat load. The heat load (on a per rod basis) of the fuel rods in a standard assembly, bounds the heat load of the 1.95 wt % ²³⁵U enriched fuel rods. Consequently, the loading of modified fuel assemblies is bounded by the thermal evaluation of the standard fuel assembly.

4.5.1.1.4 Use of Hollow Zircaloy Tubes

Certain standard fuel assemblies have had the burnable poison rods removed. These rods were replaced with hollow Zircaloy tubes.

There are 16 locations where burnable poison rods were removed and hollow Zircaloy tubes were installed in their place. Since the maximum heat load for these assemblies is 0.552 kW per assembly (less than two-thirds of the design basis heat load) and the number of hollow Zircaloy rods is only about one-tenth (16/176) of the total number of the fuel rods, the thermal performance of these fuel assemblies is bounded by that of the standard fuel assemblies.

4.5.1.1.5 Standard Fuel with In-core Instrument Thimbles

Certain fuel assemblies have in-core instrument thimbles stored within the center guide tube of each fuel assembly. Storing an in-core instrument thimble assembly in the center guide tube of a fuel assembly will slightly increase the axial conductance of the fuel assembly (helium replaced by solid material). Therefore, there is no negative impact on the thermal performance of the fuel

assembly with this configuration. The thermal performance of these fuel assemblies is bounded by that of the standard fuel assemblies.

4.5.1.1.6 Standard Fuel Assemblies with Variable Enrichment and Axial Blankets

The Maine Yankee variably enriched fuel assemblies are limited to two batches of fuel, which have a maximum burnup less than 30,000 MWD/MTU. The variably enriched rods in the fuel assemblies have enrichments greater than 3.4 wt % ²³⁵U, except that the axial blankets on one batch are enriched to 2.6 wt % ²³⁵U. As shown in Table 12B2-8, fuel at burnups less than or equal to 30,000 MWD/MTU with any enrichment greater than, or equal to, 1.9 wt % ²³⁵U may be loaded with 5 years cool time.

The thermal conductivities of the fuel assemblies with variable enrichment (radial) and axial blankets are considered to be essentially the same as those of the standard fuel assemblies. Since the heat load per assembly is limited to the design basis heat load, there is no effect on the thermal performance of the system due to this loading configuration.

4.5.1.1.7 Standard Fuel Assemblies with Removed Fuel Rods

Except for assembly number EF0046, the maximum number of missing fuel rods from a standard fuel assembly is 14, or 8% (14/176) of the total number of rods in one fuel assembly. The maximum heat load for any one of these fuel assemblies is conservatively determined to be 0.63 kW. This heat load is 34% less than the design basis heat load of 0.958 kW. Fuel assembly EF0046 was used in the consolidated fuel demonstration program and has only 69 rods remaining in its lattice. This fuel assembly has a heat load of 70 watts, or 7% of the design basis heat load of 0.958 kW. Therefore, the thermal performance of fuel assemblies with removed fuel rods is bounded by that of the standard fuel assemblies.

4.5.1.1.8 Fuel Assemblies with Damaged Fuel Rods

Damaged fuel assemblies are standard fuel assemblies with fuel rods with known or suspected cladding defects greater than hairline cracks or pinhole leaks. Fuel, classified as damaged, will be placed in a Maine Yankee fuel can. The primary function of the fuel can is to confine fuel material within the can and to facilitate handling and retrievability. The Maine Yankee fuel can is shown in Drawings 412-501 and 412-502. The placement of the loaded fuel cans is restricted

by the operating procedures and/or Technical Specifications to loading into the four fuel tube positions at the periphery of the fuel basket as shown in Figure 12B2-1. The heat load for each damaged fuel assembly is limited to the design basis heat load 0.958 kW (23 kW/24).

A steady-state thermal analysis is performed using the three-dimensional canister model described in Section 4.4.1.2 simulating 100% failure of the fuel rods, fuel cladding, and guide tubes of the damaged fuel held in the Maine Yankee fuel can. The canister is assumed to contain twenty (20) design basis PWR fuel assemblies and damaged fuel assemblies in fuel cans in each of the four corner positions.

Two debris compaction levels are considered for the 100% failure condition: (Case 1) 100% compaction of the fuel rod, fuel cladding, and guide tube debris resulting in a 52-inch debris level in the bottom of each fuel can, and (Case 2) 50% compaction of the fuel rod, fuel cladding, and guide tube debris resulting in a 104-inch debris level in the bottom of each fuel can. The entire heat generation rate for a single fuel assembly (i.e., 0.958 kW) is concentrated in the debris region with the remainder of the active fuel region having no heat generation rate applied. To ensure the analysis is bounding, the debris region is located at the lower part of the active fuel region in lieu of the bottom of the fuel can. This location is closer to the center of the basket where the maximum fuel cladding temperature occurs. The effective thermal conductivities for the design basis PWR fuel assembly (Section 4.4.1.5) are used for the debris region. This is conservative since the debris (100% failed rods) is expected to have higher density (better conduction) and more surface area (better radiation) than an intact fuel assembly. In addition, the thermal conductivity of helium is used for the remainder of the active fuel length. Boundary conditions corresponding to the normal condition of storage are used at the outer surface of the canister model (see Section 4.4.1.2). A steady-state thermal analysis is performed. The results of the thermal analyses performed for 100% fuel rod, fuel cladding, and guide tube failure are:

| Description | Maximum Temperature (°F) | | | |
|--------------------------|--------------------------|--------------|--------------|--------------------|
| | Fuel Cladding | Damaged Fuel | Support Disk | Heat Transfer Disk |
| Case 1 (100% Compaction) | 654 | 672 | 598 | 594 |
| Case 2 (50% Compaction) | 674 | 594 | 620 | 616 |
| Design Basis PWR Fuel | 670 | N/A | 615 | 612 |
| Allowable | 716 | N/A | 650 | 650 |

As demonstrated, the extreme case of 100% fuel rod, fuel cladding, and guide tube failure with 50% compaction of the debris results in temperatures that are less than 1% higher than those calculated for the design basis PWR fuel. The maximum temperatures for the fuel cladding, damaged fuel assembly, support disks, and heat transfer disks remain within the allowable temperature range for both 100% failure cases. Additionally, the temperatures used in the structural analyses of the fuel basket envelop those calculated for both 100% failure cases.

Additionally, the above analysis has been repeated to consider a maximum heat load of 1.05 kW/assembly (maximum heat load for the 50,000 MWD/MTU fuel, see Section 4.5.1.2.1) in the Maine Yankee fuel cans. To maintain the 23 kW total heat load per canister, the model considers a heat load of 1.05 kW/assembly in the four (4) Maine Yankee fuel cans and 0.94 kW/assembly in the rest of the twenty (20) basket locations. The analysis results indicate that the maximum temperatures for the fuel cladding and basket components are slightly lower than those for the case with a heat load of 0.958 kW in the damaged fuel can, as presented above. The maximum fuel cladding temperature is 650°F (< 654°F) and 672°F (< 674°F) for 100% and 50% compaction ratio cases, respectively. Therefore, the case with 1.05 kW/assembly in the Maine Yankee fuel can is bounded by the case with 0.958 kW/assembly in the fuel cans.

4.5.1.1.9 Standard Fuel Assemblies with Damaged Lattice

Certain standard fuel assemblies may have damage or physical alteration to the lattice or cage that holds the fuel rods, but not exhibit damage to the fuel rods. Fuel assemblies with lattice damage are evaluated in Section 11.2.16. The structural analysis demonstrates that these assemblies retain their configuration in the design basis accident events and loading conditions.

The effective thermal conductivity for the fuel assembly used in the thermal analyses in Section 4.4 is determined by the two-dimensional fuel model (Section 4.4.1.5). The model conservatively ignores the conductance of the steel cage of the fuel assembly. Therefore, damage or physical alteration to the cage has no effect on the thermal conductivity of the fuel assembly used in the thermal models. The thermal performance of these fuel assemblies is bounded by that of the standard fuel assemblies.

4.5.1.1.10 Damaged Fuel Rod Holders

The Maine Yankee site specific fuel inventory includes two (2) damaged fuel rod holders designated CF1 and CA3. CF1 is a 9×9 array of tubes having roughly the same dimensions as a fuel assembly. Some of the tubes hold damaged fuel rods. CA3 is a previously used fuel assembly cage (i.e., a fuel assembly with all of the fuel rods removed), into which damaged fuel rods have been inserted.

Similar to the fuel assemblies that have damaged fuel rods, the damaged fuel rod holders will be placed in Maine Yankee fuel cans and their location in the basket is restricted to one of the four corner fuel tube positions of the basket. The decay heat generated by the fuel in each of these rod holders is less than one-fourth of the design basis heat load of 0.958 kW. Therefore, the thermal performance of the damaged fuel rod holders is bounded by that of the standard fuel assemblies.

4.5.1.1.11 Assemblies with Damaged Fuel Rods Inserted in Guide Tubes

Similar to fuel assemblies that have damaged fuel rods, fuel assemblies that have up to two damaged fuel rods or poison rods stored in each guide tube are placed in Maine Yankee fuel cans and their loading positions are restricted to the four corner fuel tubes in the basket. The rods inserted in the guide tubes can not be from a different fuel assembly (i.e., any rod in a guide tube originally occupied a rod position in the same fuel assembly). Storing fuel rods in the guide tubes of a fuel assembly slightly increases the axial conductance of the fuel assembly (helium replaced by solid material). The design basis heat load bounds the heat load for these assemblies. Therefore, the thermal performance of fuel assemblies with rods inserted in the guide tubes is bounded by that of the standard fuel assemblies.

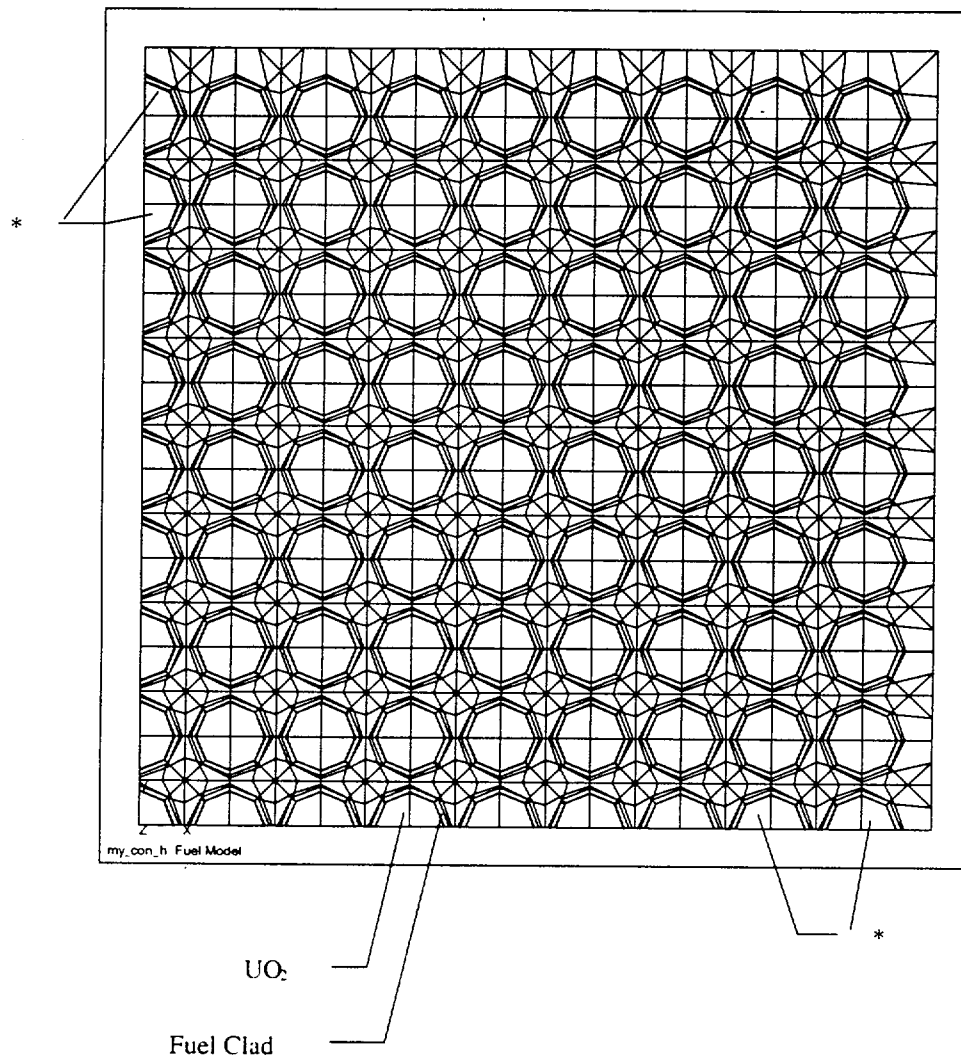
4.5.1.1.12 Standard Fuel Assemblies with Inserted Start-up Sources and Other Non-Fuel Items

Five Control Element Assembly (CEA) fingertips and a 24-inch ICI segment may be placed into the guide tubes of a fuel assembly. In addition, four irradiated start-up neutron sources and one unirradiated source, having a combined total heat load of 15.4 watts, will be loaded into separate fuel assemblies. With the CEA fingertips and the neutron sources inserted into the guide tubes of the fuel assemblies, the effective conductivity in the axial direction of the fuel assembly is increased because solid material replaces helium in the guide tubes. The change in the effective

conductivity in the transverse direction of the fuel assembly is negligible, since the non-fuel items are inside of the guide tubes. In addition, the fuel assemblies that hold these non-fuel items are restricted to basket corner loading locations, which have an insignificant effect on the maximum fuel cladding and basket component temperatures at the center of the basket.

Note that the total heat load of the fuel assembly, including the small amount of extra heat generated by the CEA fingertips, ICI 24-inch segment, and the neutron sources, remains below the design basis heat load. Therefore, the thermal performance of the fuel assemblies with these non-fuel items inserted is bounded by that of the standard fuel assemblies.

Figure 4.5.1.1-1 Quarter Symmetry Model for Maine Yankee Consolidated Fuel



* Two outer layers (rows) of rods are modeled as stainless steel

Figure 4.5.1.1-2 Maine Yankee Three-Dimensional Periodic Canister Internal Model

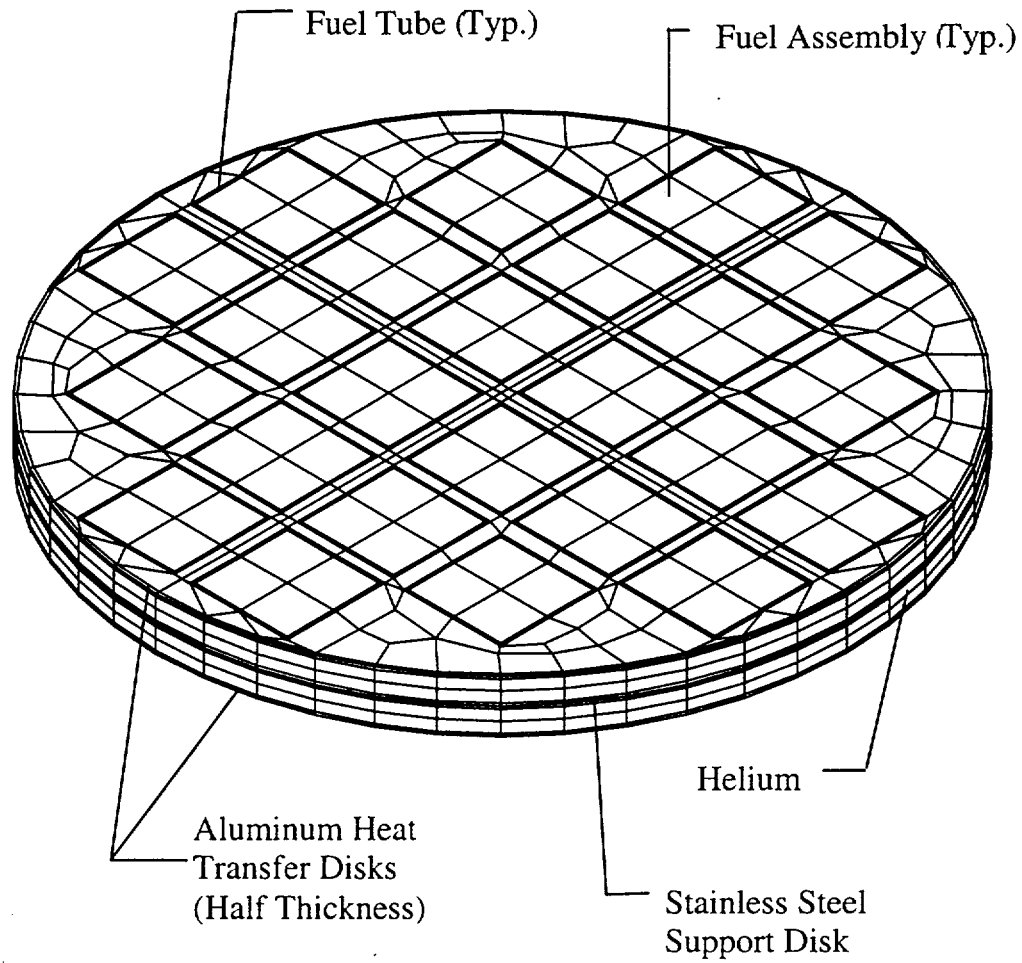


Figure 4.5.1.1-3 Evaluated Locations for the Maine Yankee Consolidated Fuel Lattice in the PWR Fuel Basket

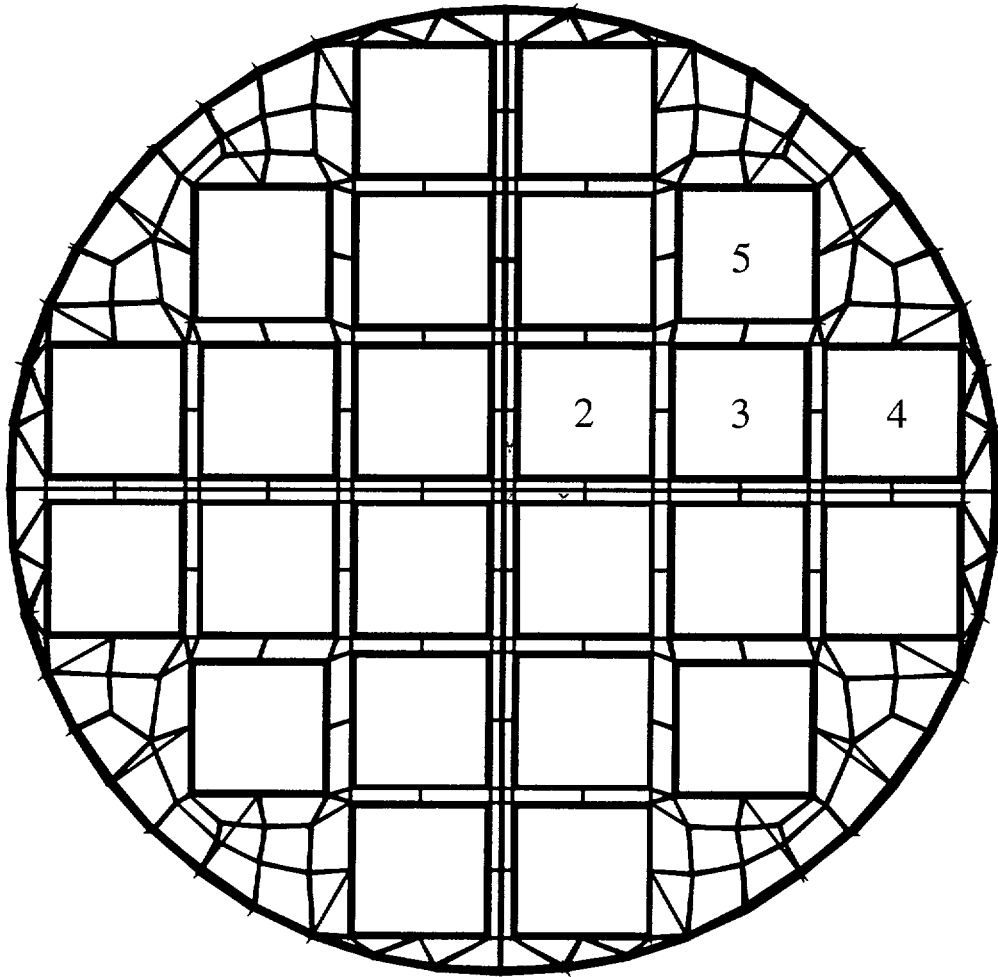
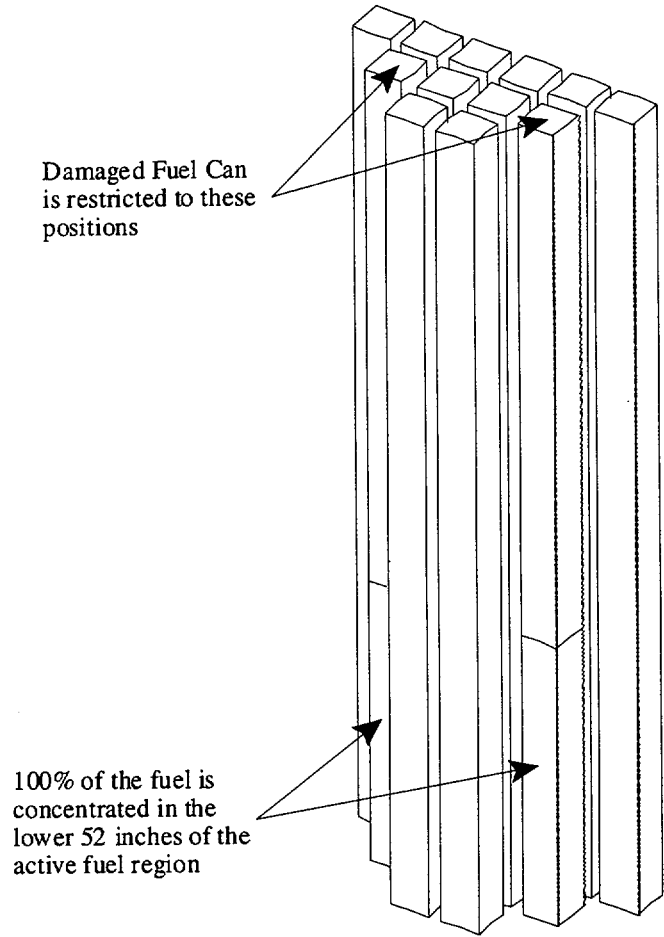
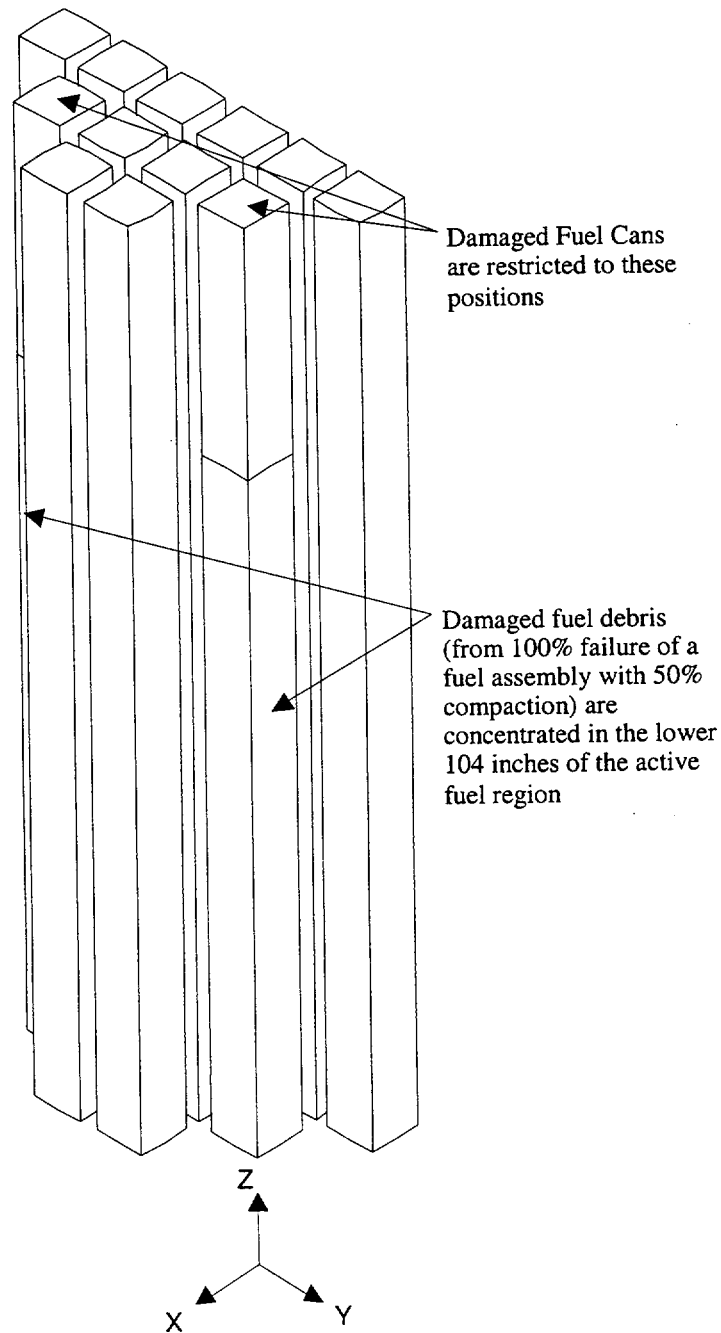


Figure 4.5.1.1-4 Active Fuel Region in the Three-Dimensional Canister Model



Note: Finite element mesh not shown for clarity.

Figure 4.5.1.1-5 Fuel Debris and Damaged Fuel Regions in the Three-Dimensional Canister Model



4.5.1.2 Maximum Allowable Heat Loads for Maine Yankee Site Specific Spent Fuel

This section includes evaluations for the Maine Yankee fuel inventory that is not bounded by the evaluation performed in Section 4.4.7. This fuel may have higher burnup than the design basis fuel, have a higher decay heat on a per assembly basis, have a burnup/cool time condition that is outside of the cladding temperature evaluation presented in Section 4.4.7, or be subject to all of these differences.

Maximum allowable clad temperatures and decay heats are evaluated for:

1. Fuel with burnup in excess of 45,000 MWD/MTU (maximum 50,000 MWD/MTU),
2. Preferential loading patterns with hotter fuel on the periphery of the basket, and
3. Preferential loading with fuel exceeding design basis heat load (0.958 kW) per assembly on the basket periphery.

As shown in Section 4.4.7, the standard CE 14×14 fuel assembly has a significantly lower cladding stress level than the equivalent burnup Westinghouse 14×14 assembly. It is, therefore, conservative to apply the characteristics of the design basis assembly to the CE 14×14 Maine Yankee fuel assemblies (Note that the Westinghouse 14×14 assembly evaluated in Section 4.4.7 is the fuel assembly used in Westinghouse reactors, but it is not the Westinghouse 14×14 assembly built for use in the CE reactors, such as the Maine Yankee reactor).

The maximum allowable decay heat, listed either on a per canister or per assembly basis, is combined with dose rate limits in Chapter 5 to establish cool time limits as a function of burnup and initial enrichment. Cool time limits are shown in Tables 5.6.1-10 for Maine Yankee fuel assemblies without installed control components, and in Table 5.6.1-12 for fuel assemblies with installed control components.

High burnup fuel (45,000 – 50,000 MWD/MTU) may be loaded as intact fuel provided that no more than 1% of the fuel rods in the assembly have a peak cladding oxide thickness greater than 80 microns, and no more than 3% of the fuel rods in the assembly have a peak oxide layer thickness greater than 70 microns. The high burnup fuel must be loaded as failed fuel (i.e., in a Maine Yankee fuel can), if these criteria are not met, or if the cladding oxide layer is detached or spalled from the cladding. Since the transportable storage canister is tested to be leak tight, no additional confinement analysis is required for the high burnup fuel.

4.5.1.2.1 Maximum Allowable Temperature and Decay Heat for 50,000 MWD/MTU Fuel

To evaluate higher burnup fuel, cladding oxidation layer thickness and fission gas release fractions are established. Maine Yankee reports that for high burnup fuel rods (i.e., rod peak burnup up to 55,000 MWD/MTU), ABB/Combustion Engineering Incorporated imposes a cladding oxide layer thickness of 120 microns as an operational limit and reports that the maximum gas release fraction (fuel pellet to rod plenum in intact fuel rods) is less than 3% [36]. Therefore, the allowable cladding temperature calculations employ a cladding oxide layer thickness of 0.012 cm (120 microns). This is conservative with respect to the 80 micron cladding oxide layer thickness considered for high burnup fuel that is loaded as intact fuel. A 12% release fraction, established for standard PWR fuel burned up to 45,000 MWD/MTU, is conservatively applied to higher burnup PWR fuel.

Using the evaluation method presented in Section 4.4.7 and a cladding oxidation layer thickness of 0.012 cm, the cladding stress levels for the 50,000 MWD/MTU burnup PWR assembly (maximum stress) are determined and listed in Table 4.5.1.2-1. The data is plotted against the generic allowable temperature curves in Figure 4.5.1.2-2. Included in Figure 4.5.1.2-2 are the 35,000 MWD/MTU to 45,000 MWD/MTU limit lines developed in Section 4.4.7. The intercept of the 50,000 MWD/MTU results in the limiting cladding temperatures shown in Table 4.5.1.2-2, which considers the 1% creep strain limit. The resulting maximum allowable heat load per canister for fuel assemblies with burnup of 50,000 MWD/MTU is listed in Table 4.5.1.2-3.

4.5.1.2.2 Preferential Loading with Hotter Fuel on the Periphery of the Basket

The design basis heat load for the UMS thermal analysis is 23 kW uniformly distributed throughout the basket (0.958 kW per assembly). This heat load applies to the basket structural components at any initial fuel loading time. Further reduction in heat load is required for the Maine Yankee fuel assemblies that fall outside the bounds of the requirement of maximum heat load as shown in Tables 4.4.7-8 and 4.5.1.2-3. These assemblies include:

1. Fuel assemblies (with specific burnup and cool time) that may exceed the maximum allowable decay heat dictated by their cladding temperature allowable (exceeding the limits as shown in Tables 4.4.7-8 and 4.5.1.2-3), if loaded uniformly (all 24 fuel assemblies with the same burnup and cool time, i.e., the same decay heat).
2. Fuel assemblies that are expected to exceed the design basis heat load of 0.958 kW per assembly (maximum heat per assembly less than 1.05 kW).

To ensure that these fuel assemblies do not exceed their allowable cladding temperatures, a loading pattern is considered that places higher heat load assemblies at the periphery of the basket (Positions "A" in Figure 4.5.1.2-1) and compensates by placing lower heat load assemblies in the basket interior positions (Positions "B" in Figure 4.5.1.2-1). There are 12 interior basket locations and 12 peripheral basket locations in the UMS PWR basket design. The maximum total basket heat loads indicated in Tables 4.4.7-8 and 4.5.1.2-3 are maintained for these peripheral loading scenarios.

Two preferential loading scenarios are evaluated. The first approach limits any assembly to the 0.958 kW design basis heat load limit (23 kW divided by 24 assemblies), while the second approach increases the per assembly heat load limit to 1.05 kW for assemblies in the basket peripheral locations. The split approach allows maximum flexibility at fuel loading.

In order to load the preferential pattern, the fuel cladding maximum temperature must be maintained below the allowable temperatures for peripheral and interior assemblies. The requirement of maximum total heat load per basket, as shown in Tables 4.4.7-8 and 4.5.1.2-3, must also be met.

4.5.1.2.2.1 Peripheral Assemblies Limited to a Decay Heat Load of 0.958 kW per Assembly

With a basket heat load of 23 kW, uniformly loaded, the maximum cladding temperature of a peripheral assembly location was determined to be 566°F (297°C) based on the thermal analysis using the three-dimensional canister model as presented in Section 4.4.1.2. While any basket location is restricted to a heat load of 0.958 kW, any non-uniform loading with a total basket heat load less than 23 kW will result in a peripheral assembly cladding temperature less than 297°C. This temperature is well below the lowest maximum allowable clad temperature of 313°C indicated in Table 4.5.1.2-2 (which was already reduced from the actual allowable of 322°C). Fuel assemblies at a maximum heat load of 0.958 kW may, therefore, be loaded into the peripheral basket location at any cool time, provided interior assemblies meet the restrictions outlined below.

Decay Heat Limit on Fuel Assemblies Loaded into Basket Interior Positions

Interior fuel assembly decay heat loads must be reduced from those in a uniform loading configuration, see Table 4.4.7-8 and Table 4.5.1.2-3, to allow loading of the higher heat load assemblies in the peripheral locations. A parametric study is performed using the

three-dimensional periodic model as described in Section 4.5.1.1 (Figure 4.5.1.1-2) to demonstrate that placing a higher heat load in the peripheral locations does not result in heating of the fuel assemblies in the interior locations beyond that found in the uniform heat loading case. The side surface of the model is assumed to have a uniform temperature of 350°F.

Two cases are considered (total heat load per cask = 20 kW for both cases):

1. Uniform loading: Heat load = 0.833 (20/24) kW per assembly for all 24 assemblies
2. Non-uniform loading:
Heat load = 0.958 (23/24) kW per assembly for 12 Peripheral assemblies
Heat load = 0.708 (17/24) kW per assembly for 12 Interior assemblies

The analysis results (maximum temperatures) are:

| | <u>Case 1</u> | <u>Case 2</u> |
|------------------------|-----------------------------|---------------------------------|
| | <u>Uniform Loading (°F)</u> | <u>Non-Uniform Loading (°F)</u> |
| Fuel (Location 1) | 675 | 648 |
| Fuel (Locations 2 & 4) | 632 | 611 |
| Fuel (Location 5) | 577 | 588 |
| Fuel (Locations 3 & 6) | 563 | 576 |
| Basket | 611 | 592 |

Locations are shown in Figure 4.5.1.2-1.

The maximum fuel cladding temperature for Case 2 (non-uniform loading pattern) is well below that for Case 1 (uniform loading pattern). The comparison shows that placing hotter fuel in the peripheral locations of the basket and cooler fuel in the interior locations (while maintaining the same total heat load per basket) reduces the maximum fuel cladding temperature (which occurs in the interior assembly), as well as the maximum basket temperature.

Because the basket interior temperatures decrease for non-uniform loading, it is conservative to determine the maximum allowable heat load for the interior assemblies based on the values (total allowed heat load) shown in Tables 4.4.7-8 and 4.5.1.2-3, and the heat load for the fuel assemblies in 12 peripheral locations (12 × 0.958 kW). For example, the 10-year cooled, 45,000 MWD/MTU fuel in a uniform loading pattern, is restricted to a basket average heat load of 19.5 kW per Table 4.4.7-8. Placing 12 fuel assemblies at 23/24 (0.958) kW into the basket periphery

requires the interior assemblies to be reduced to 0.667 kW per assembly to retain the 19.5 kW basket total heat load. Table 4.5.1.2-4 contains the matrix of maximum allowable heat loads per assembly as a function of burnup and cool time for interior assemblies for the configuration with the peripheral assemblies having a maximum heat load of 0.958 kW per assembly.

4.5.1.2.2.2 Peripheral Assemblies Limited to a Decay Heat Load of 1.05 kW per Assembly

The Maine Yankee fuel inventory includes fuel assemblies that will exceed the initial per-assembly heat load of 0.958 kW at a loading prior to August 2002. To enable loading of these assemblies into the storage cask, higher peripheral heat load is evaluated. The maximum heat load for peripheral assemblies is set at 1.05 kW.

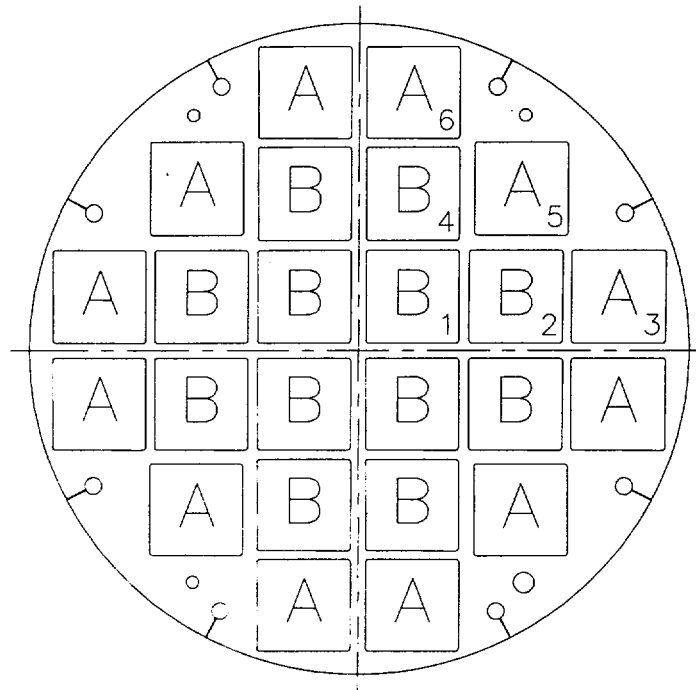
The maximum basket heat load for this configuration is restricted to 23 kW. Given the higher than design basis heat load in peripheral basket locations, an evaluation is performed to assure that maximum cladding allowable temperatures are not exceeded.

Based on the parametric study (uniform versus non-uniform analysis) of the 20 kW basket, a 15% redistribution of heat load resulted in a maximum increase of 13°F (576-563=13) in a peripheral basket location. Changing the basket peripheral location heat load from 0.958 kW maximum to 1.05 kW is a less than 10% redistribution for the 23 kW maximum basket heat load. The highest temperature of a peripheral basket location may, therefore, be estimated by adding 13°F to 566°F (maximum temperature in peripheral assemblies for the 23 kW basket). The 579°F (304°C) is less than the lowest maximum allowable cladding temperature of 313°C indicated in Table 4.5.1.2-2 (which was already reduced from the actual allowable of 322°C). Fuel assemblies at a maximum heat load of 1.05 kW may, therefore, be loaded into the peripheral basket location at any cool time, provided interior assemblies meet the restrictions outlined below.

Decay Heat Limit on Fuel Assemblies Loaded into Basket Interior Positions

Basket interior assemblies heat load limits are based on the same method used for the configuration with 0.958 kW assemblies in peripheral locations, with the exception that each peripheral fuel assembly is assigned a maximum decay heat of 1.05 kW. The higher peripheral heat load in turn will reduce the allowable heat load in the interior locations. Table 4.5.1.2-5 contains the maximum allowable decay heats for basket interior fuel assemblies with an assembly heat load of 1.05 kW for peripheral locations.

Figure 4.5.1.2-1 Canister Basket Preferential Loading Plan



“A” indicates peripheral locations.

“B” indicates interior locations.

Numbered locations indicate positions where maximum fuel temperatures are presented.

Figure 4.5.1.2-2 Maximum Allowable Cladding Temperature at Initial Storage versus Cladding Stress (50,000 MWD/MTU)

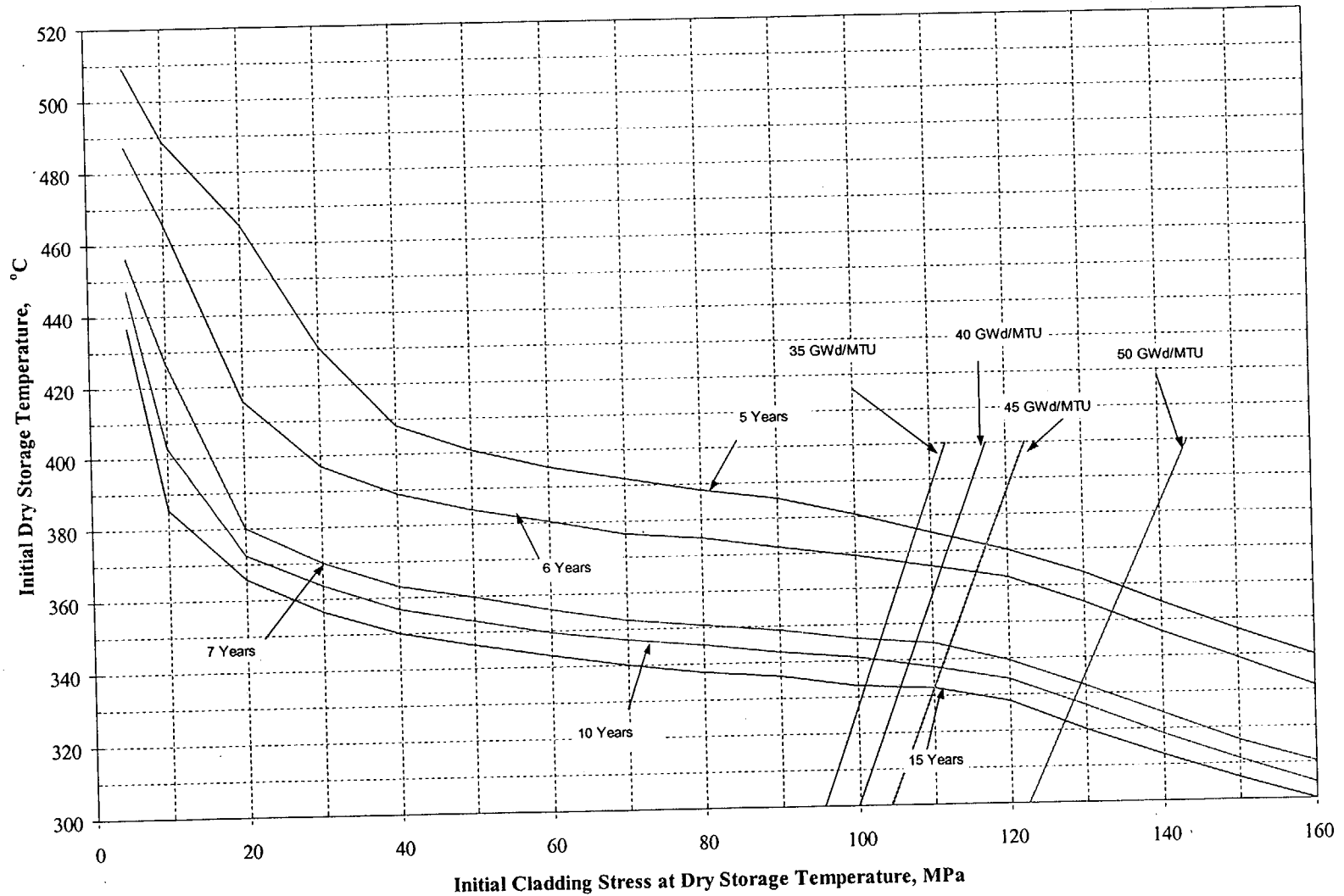


Table 4.5.1.2-1 Cladding Stress for 50,000 MWD/MTU Burnup Fuel

| | | |
|---------------------------------|--------------|--------------|
| Clad Maximum Temperature | 300°C | 400°C |
| Stress (MPa) | 122.3 | 143.9 |

Table 4.5.1.2-2 Maximum Allowable Cladding Temperature for 50,000 MWD/MTU Burnup Fuel

| Cool Time | Maximum Allowable Cladding Temperature | Bias-Adjusted Cladding Temperature |
|------------------|---|---|
| 5 yr | 359°C | 350°C |
| 6 yr | 352°C | 342°C |
| 7 yr | 333°C | 323°C |
| 10 yr | 328°C | 318°C |
| 15 yr | 322°C | 313°C |

Table 4.5.1.2-3 Maximum Allowable Canister Heat Load for 50,000 MWD/MTU Burnup Fuel

| Cool Time | Maximum Allowable Heat Load |
|------------------|------------------------------------|
| 5 yr | 22.1 kW |
| 6 yr | 21.2 kW |
| 7 yr | 19.5 kW |
| 10 yr | 19.1 kW |
| 15 yr | 18.7 kW |

Table 4.5.1.2-4 Heat Load for Interior Assemblies for the Configuration with 0.958 kW Assemblies in Peripheral Locations

| Heat Load Limit (kW)¹ | | | | |
|---|-------------------------|---------------|---------------|---------------|
| Interior Assembly | Burnup (MWD/MTU) | | | |
| | 35,000 | 40,000 | 45,000 | 50,000 |
| Cool Time (years) | --- | --- | --- | --- |
| 5 | 0.958 | 0.958 | 0.958 | 0.883 |
| 6 | 0.908 | 0.883 | 0.867 | 0.808 |
| 7 | 0.725 | 0.717 | 0.708 | 0.667 |
| 10 | 0.683 | 0.675 | 0.667 | 0.633 |
| 15 | 0.633 | 0.625 | 0.617 | 0.600 |

1. Decay heat per assembly, based on twelve (12) 0.958 kW assemblies in peripheral locations.

Table 4.5.1.2-5 Heat Load Limit for Interior Assemblies for the Configuration with 1.05 kW Assemblies in Peripheral Locations

| Heat Load Limit (kW)¹ | | | | |
|---|-------------------------|---------------|---------------|---------------|
| Interior Assembly | Burnup (MWD/MTU) | | | |
| | 35,000 | 40,000 | 45,000 | 50,000 |
| Cool Time (years) | --- | --- | --- | --- |
| 5 | 0.867 | 0.867 | 0.867 | 0.792 |
| 6 | 0.817 | 0.792 | 0.775 | 0.717 |
| 7 | 0.633 | 0.625 | 0.617 | 0.575 |
| 10 | 0.592 | 0.583 | 0.575 | 0.542 |
| 15 | 0.542 | 0.533 | 0.525 | 0.508 |

1. Decay heat per assembly, based on twelve (12) 1.05 kW assemblies in peripheral locations.

THIS PAGE INTENTIONALLY LEFT BLANK

4.6 References

1. Code of Federal Regulations, "Licensing Requirements for the Independent Storage of Spent Nuclear Fuel and High Level Radioactive Waste," Part 72, Title 10, January 1996.
2. PNL-4835, Johnson, A.B., and Gilbert, E.R., "Technical Basis for Storage of Zircaloy-Clad Fuel in Inert Gases," 1985.
3. PNL-4555, "Results of Simulated Abnormal Heating Events for Full-Length Nuclear Fuel Rods," Gwenther, R.J., Pacific Northwest Laboratories, 1983.
4. ACI-349-85, American Concrete Institute, "Code Requirement for Nuclear Safety Related Concrete Structures and Commentary."
5. PNL-6189, Levy, et al., Pacific Northwest Laboratory, "Recommended Temperature Limits for Dry Storage of Spent Light-Water Zircalloy Clad Fuel Rods in Inert Gas," May 1987.
6. ANSYS Revision 5.2 and ANSYS Revision 5.5, Computer Program, ANSYS, Inc., Houston, PA.
7. MIL-HDBK-5G, Military Handbook, "Metallic Materials and Elements for Aerospace Vehicle Structures," U.S. Department of Defense, November 1994.
8. Genden Engineering Services & Construction Company, NS-4-FR Fire Resistant Neutron and/or Gamma Shielding Material - Product Technical Data.
9. Baumeister T. and Mark, L.S., Standard Handbook for Mechanical Engineers, 7th Edition, New York, McGraw-Hill Book Co., 1967.
10. The American Society of Mechanical Engineers, "ASME Boiler and Pressure Vessel Code," 1995.
11. ARMCO Product Data Bulletin No. S-22, "17-4PH, Precipitation Hardening Stainless Steel," ARMCO, Inc., 1988.

12. The American Society of Mechanical Engineers, "ASME Boiler and Pressure Vessel Code, Code Cases - Boilers and Pressure Vessels," Code Case N-71-17, 1996.
13. The American Society of Mechanical Engineers, "ASME Boiler and Pressure Vessel Code, Section II, Part D - Properties," 1995.
14. Hanford Engineering Development Laboratory, "Nuclear Systems Materials Handbook," Volume 1, Design Data, Westinghouse Hanford Company, TID26666.
15. Bucholz, J.A., "Scoping Design Analyses for Optimized Shipping Casks Containing 1, 2-, 3-, 5-, 7-, or 10-Year-Old Spent Fuel, Oak Ridge National Library," ORNL/CSD/TM-149, 1983.
16. Ross R. B., "Metallic Specification Handbook," 4th Edition, London, Chapman and Hall, 1992.
17. Kreith, F., and Bohn, M. S., "Principles of Heat Transfer," 5th Edition, West Publishing Company, 1993.
18. Edwards, "TRUMP, A Computer Program for Transient and Steady State Temperature Distributions in Multidimensional Systems," Lawrence Radiation Laboratory, Livermore, Rept, UCLR-14754, Rev. 1, May 1968.
19. Kreith, F., "Principles of Heat Transfer," 3rd Edition, New York, Intext Educational Publishers.
20. Vargaftik, Natan B., et al., "Handbook of Thermal Conductivity of Liquids and Gases," CRC Press, October 1993.
21. Chapman, A.J., "Heat Transfer," 4th Edition, MacMillan Publishing Company, New York, 1987.

22. Hagrman, D.L., Reymann, G.A., "Matpro-Version 11 A Handbook of Material Properties for Use in the Analysis of Light Water Reactor Rod Behavior," Idaho Falls, ID, EG&G Idaho, Inc., 1979.
23. Rust, J.H., "Nuclear Power Plant Engineering," Atlanta, GA, S.W., Holland Company, 1979.
24. AAR BORAL Sheet Manufacturers Data, Sheet Product Performance Report 624, Brooks & Perkins Advanced Structures Company, 1983.
25. AAR Standard Specification Sheet for BORAL[™] Composite Sheet, Brooks & Perkins Advances Structures Company, BRJREVO-940107.
26. Fintel, M., "Handbook of Concrete Engineering," 2nd Edition, Van Nostrand Reinhold Co., New York.
27. ASTM C150-95a, American Society for Testing and Materials, "Standard Specification for Portland Cement."
28. Siegel, R., and Howell, J. R., "Thermal Radiation Heat Transfer," 3rd Edition, Hemisphere Publishing Co., 1992.
29. Incropera, E. P., and DeWitt, D. P., "Fundamentals of Heat and Mass Transfer," 4th Edition, 1996.
30. SAND90-2406, Sanders, T.L., et al., "A Method for Determining the Spent-Fuel Contribution to Transport Cask Containment Requirements," TTC-1019, UC-820, November 1992.
31. Olander, D. R., "Fundamental Aspects of Nuclear Reactors Fuel Elements," Technical Information Center (U. S. Department of Energy), 1985.
32. Kreith, F., "Principles of Heat Transfer," 2nd Edition, 1965.

33. PNL-6364, "Control of Degradation of Spent LWR Fuel During Dry Storage in an Inert Atmosphere," Pacific Northwest Laboratory, Richland, Washington, October 1987.
34. PNL-4835, "Technical Basis for Storage of Zircaloy-Cladding Spent Fuel in Inert Gas," September 1983.
35. Regulatory Guide 1.25, "Assumptions Used for Evaluating the Potential Radiological Consequences of a Fuel Handling Accident in the Fuel Handling and Storage Facility for Boiling and Pressurized Water Reactors (Safety Guide 25)," March 1972.
36. Pati, S.R., Garde, A. M., Clink, L.J., "Contribution of Pellet Rim Porosity to Low-Temperature Fission Gas Release at Extended Burnups," American Nuclear Society Topical Meeting on LWR Fuel Performance, April 17-20, 1988, Williamsburg, VA.
37. NET 152-03, "METAMIC Qualification Program for Nuclear Fuel Storage Applications – Final Test Results," Revision 0, Northeast Technology Corporation, September 2001.